



Master's thesis
Geoinformatics

QUIET PATHS FOR PEOPLE:
DEVELOPING ROUTING ANALYSIS AND WEB GIS APPLICATION

Joose Helle
2020

Supervisor:
Tuuli Toivonen

University of Helsinki
Faculty of Science
Department of Geosciences and Geography
PL 64 (Gustaf Hällströmin katu 2)
00014 University of Helsinki



Tiedekunta/Osasto Fakultet/Sektion – Faculty Faculty of science	Laitos/Institution– Department Department of Geosciences and Geography	
Tekijä/Författare – Author Joose Helle		
Työn nimi / Arbetets titel – Title Quiet paths for people: developing routing analysis and Web GIS application		
Oppaine /Läroämne – Subject Geoinformatics		
Työn laji/Arbetets art – Level Master's thesis	Aika/Datum – Month and year April 2020	Sivumäärä/ Sidoantal – Number of pages
Tiivistelmä/Referat – Abstract <p>It is likely that journey-time exposure to pollutants may compromise the positive health effects of active transport modes (e.g. walking and cycling). One of the pollutants caused by vehicular traffic is traffic noise, which is likely to cause various negative health effects such as increased stress levels and blood pressure. In prior studies, individuals' exposure to community noise has usually been assessed only with respect to home location, as required by national and international policies. However, these static exposure assessments most likely ignore a substantial share of individuals' total daily noise exposure that occurs while they are on the move.</p> <p>In this study, I developed a multifunctional routing application for 1) finding shortest paths, 2) assessing dynamic exposure to noise on the paths and 3) finding less noisy (i.e. quieter) paths for walking. The application uses street network data from OpenStreetMap and modelled traffic noise data of typical daytime traffic noise levels. The underlying least cost path (LCP) analysis employs a custom-designed environmental impedance function for noise and a set of (various) noise sensitivity coefficients. Hence, the application typically finds several alternative (quiet) paths for one pathfinding problem. I defined a set of indexes for quantifying and comparing dynamic (i.e. journey-time) exposure to high levels of noise. I applied the developed routing application in a case study of pedestrians' dynamic exposure to noise on commuting related walks in Helsinki. The walks were projected by carrying out an extensive public transport itinerary planning on census based commuting flow data. Statistical analysis was carried out to explore the average dynamic noise exposures at both municipality and neighborhood level. Also, achievable reductions in exposure to traffic noise by taking quieter paths were assessed with statistical means by a subset of 12180 commuting related walks (OD pairs).</p> <p>The results show significant spatial variation in average dynamic noise exposure between neighborhoods but also significant achievable reductions in noise exposure by quieter paths; depending on the situation, quieter paths provide 12–57 % mean reduction in exposure to noise levels higher than 65 dB and 1.6–9.6 dB mean reduction in mean dB (compared to the shortest paths). I published the quiet path routing application as a web-based quiet path routing API (application programming interface) and developed an accompanying quiet path route planner as a mobile-friendly interactive web map application. The online quiet path route planner demonstrates the applicability of the quiet path routing method in real-life situations and thus can help pedestrians to choose quieter paths. Since the quiet path routing API is open, anyone can query short and quiet paths equipped with attributes on journey-time exposure to noise.</p> <p>The results suggest that at least the following factors affect the achievable reduction in noise exposure on quiet paths: 1) exposure to noise on the shortest path, 2) length of the shortest path and 3) additional length of the quiet path. It is likely that the presence of alternative (quieter) paths limit the accuracy of indirect dynamic noise exposure assessments to some extent. Hence, the results of the case study may not provide reliable results on the true variation in opportunities for walking in quiet. When developing exposure-based routing methods further, attempts should be made to enable simultaneously considering multiple environmental exposures in order to optimize overall healthier paths. Finally, the real effect of such methods on peoples' health depends on what kind of user interface layers are built to make them accessible.</p>		
Avainsanat – Nyckelord – Keywords Dynamic exposure, traffic noise, environmental impedance, least-cost path analysis, Web GIS, Helsinki		
Säilytyspaikka – Förvaringsställe – Where deposited		
Muita tietoja – Övriga uppgifter – Additional information		



Tiedekunta/Osasto Fakultet/Sektion – Faculty Matemaattis-luonnontieteellinen tiedekunta	Laitos/Institution– Department Geotieteiden ja maantieteen laitos
Tekijä/Författare – Author Joose Helle	
Työn nimi / Arbetets titel – Title Dynaamisen melualttistuksen arvointi ja minimointi reitinetsinnän ja Web GIS:n keinoin	
Oppiaine /Läroämne – Subject Maantiede, geoinformatiikka	
Työn laji/Arbetets art – Level Pro gradu -tutkielma	Aika/Datum – Month and year Huhtikuu 2020
Tiivistelmä/Referat – Abstract	
Avainsanat – Nyckelord – Keywords	
Säilytyspaikka – Förvaringsställe – Where deposited	
Muita tietoja – Övriga uppgifter – Additional information	

TABLE OF CONTENTS

I.	INTRODUCTION	2
II.	BACKGROUND	5
2.1	Noise definition and measurement.....	5
2.2	Traffic noise and health.....	6
2.3	Traffic noise modeling	7
2.4	Concepts and approaches in assessing dynamic exposure.....	8
2.5	Graph theory and least cost path analysis	10
2.6	Exposure-based impedances in routing.....	12
2.7	Web GIS concepts and developments.....	14
III.	DATA & METHODS	18
3.1	Overview of the methods	18
3.2	Study area.....	18
3.3	Data	19
3.3.1	Modelled traffic noise data	20
3.3.2	OpenStreetMap data.....	25
3.3.3	Register based origin-destination (OD) commuting data	26
3.3.4	Online routing service of the local public transport authority	27
3.4	Technical framework and architecture.....	27
3.5	Quiet path routing method	28
3.5.1	Network acquisition and manipulation	29
3.5.2	Environmental impedance function	31
3.5.3	Quiet path routing application	34
3.5.4	Noise exposure assessment of short and quiet paths	37
3.6	Web-based quiet path route planner.....	39
3.7	Assessment of pedestrians' exposure to traffic noise at a neighborhood level.....	41
3.7.1	Overview of the analysis.....	41
3.7.2	Estimation of local walks by commutes	43

3.7.3 Least cost path calculations: short and quiet paths	48
3.7.4 Assessment of exposures to traffic noise on the paths.....	49
3.8 Assessment of achievable reductions in exposure to traffic noise	50
IV. RESULTS	52
4.1 Pedestrians' exposure to traffic noise	52
4.2 Spatial patterns in pedestrians' exposures to traffic noise	53
4.3 Quiet path routing API.....	60
4.4 Quiet path route planner.....	64
4.5 Achievable reductions in exposure to traffic noise.....	68
4.6 Sharing of the methods and results	73
V. DISCUSSION AND CONCLUSIONS	75
5.1 Technical assessment – quality of the paths	75
5.2 Indirect assessment of pedestrians' dynamic exposures to traffic noise can reveal unequal distribution of exposures to high noise levels.....	77
5.3 Significant but varying reductions in traffic noise exposure can be achieved by quiet path routing	78
5.4 The presence of alternative paths limits the accuracy of the indirect dynamic exposure assessment.....	79
5.5 Alternative quiet paths need to be calculated to suit different situations and people with varying preferences	81
5.6 Uncertainties in exposure-response relationships challenge the environmental impedance function	81
5.7 Exposure-based routing should be developed as a concept to consider multiple pollutants ...	83
5.8 Publishing a green path routing application online can facilitate citizens to choose healthier paths	85
VI. REFERENCES.....	88
ACKNOWLEDGEMENTS	94
APPENDICES	95

LIST OF FIGURES

Figure 1. Equal loudness contours as in ISO 226 (<i>Acoustics – normal equal-loudness contours. International Standard ISO 226</i>).....	5
Figure 2. Composed scatterplot between L_{den} and percentage of highly annoyed (HA%) for several studies on road traffic noise and annoyance by Guski et al. (2017).....	7
Figure 3. Dynamic exposure to traffic noise level on a path as distances (left) and durations (right) of different traffic noise levels.....	9
Figure 4. An illustration of the sequence of steps in finding least cost paths with Dijkstra's algorithm by Jasika et al. (2012).....	11
Figure 5. A figure by Veenendaal et al. (2017): “Interacting web services feeding into apps within application workflows.”	15
Figure 6. Illustration by Veenendaal et al. (2017): "Focus and trends in increasing web mapping functionality".	17
Figure 7. Illustration of the internal dependencies of the methods and outcomes of the study.....	18
Figure 8. The study area and its key transportation networks.....	19
Figure 9. Modelled daytime traffic noise levels (dB(A)) in Helsinki.....	23
Figure 10. Modelled daytime traffic noise levels (dB(A)) in Viikki.....	24
Figure 11. Modelled daytime traffic noise levels (dB(A)) in Kallio and Vallila (in Helsinki).....	25
Figure 12. Technical framework of the study: internal (blue) and external (grey) technical dependencies (* = Python library). The several external dependencies of the used Python libraries are not included in the graph.....	28
Figure 13. Workflow of street network graph acquisition and construction.....	30
Figure 14. Workflow of extracting exposures to traffic noise (contaminated distances) to the edges of the graph.	30
Figure 15. Noise cost coefficients for dB range 45–75 dB calculated with both equations presented in this chapter (Table 3).....	34
Figure 16. Workflow of calculating and adding noise sensitivity specific edge costs as new edge attributes.....	35
Figure 17. The sequence of high-level actions included in solving a regular pathfinding problem with quiet path routing application.	37
Figure 18. Technical architecture of the quiet path route planner web application.....	40
Figure 19. Workflow of the analysis for identifying origin – PT stop (or commuting destination) walks and estimating of their utilization rates based on commuter flows.	42
Figure 20. Workflow of the analysis for 1) calculating short and quiet paths by ODs of the local walks, 2) assessing exposures to traffic noise on the paths and 3) assessing achievable reductions in traffic noise exposure by taking quiet paths (see 3.8).....	43
Figure 21. Extent of the itinerary planning analysis by commuting flow data. The point symbols represent “central workplace locations” within each city district.	44
Figure 22. An example of local walks and their utilization rates from one origin as a result of the itinerary planning analysis. Most of the destinations of the walks are public transport stops.	46
Figure 23. Inclusion (%) of commutes per origin in the itinerary planning analysis for finding local walks to PT stops and commuting destinations.	47

Figure 24. Number of commutes vs. commutes included in the routing analysis (%) per origin.....	48
Figure 25. All shortest paths visualized with feature blending method: overlapping paths show darker on the map.....	49
Figure 26. Mean walking distances from homes to public transport (PT) stops. The averages are weighted with the estimated utilization rates of the walks based on the total flow of commutes using each origin – PT stop pair.....	55
Figure 27. Mean traffic noise level (dB(A)) on walks from homes to PT stops. The averages are weighted with the estimated utilization rates of the walks based on the total flow of commutes using each origin – PT stop pair.....	56
Figure 28. Mean exposures to +65 dB(A) traffic noise levels (m) on walks from homes to public transport (PT) stops. The averages are weighted with the estimated utilization rates of the walks based on the total flow of commutes using each origin – PT stop pair.....	57
Figure 29. Mean exposures to +70 dB traffic noise levels (m) on walks from homes to public transport (PT) stops. The averages are weighted with the estimated utilization rates of the walks based on the total flow of commutes using each origin – PT stop pair.....	58
Figure 30. Mean exposure to +65 dB(A) traffic noise levels (%) on walks from homes to public transport (PT) stops. The averages are weighted with the estimated utilization rates of the walks based on the total flow of commutes using each origin – PT stop pair.....	59
Figure 31. Mean exposure to +70 dB(A) traffic noise levels (%) on walks from homes to public transport (PT) stops. The averages are weighted with the estimated utilization rates of the walks based on the total flow of commutes using each origin – PT stop pair.....	60
Figure 32. A typical sequence of actions included in solving one pathfinding problem from the perspective of the route planner application (green) and user (blue).	66
Figure 33. The user interface of the quiet path route planner when showing two alternative paths (one shortest path and one quiet path).	67
Figure 34. The user interface of the quiet path route planner when showing several alternative paths (one shortest path and six quiet paths). In the third picture, longest paths are being filtered by a user-defined length threshold.	67
Figure 35. “Add to home screen” -functionality of the web application; the quiet path route planner can be "installed" on user's phone to work similarly as installed apps (without web browser and address bar).	68
Figure 36. Regression analysis between the reductions in traffic noise exposures on quiet paths and the initial traffic noise indexes. The analysis covers shortest paths in the length range of 300 to 600 m and the respective quiet paths. The red lines represent the regression lines of the regression analysis and the green lines show the theoretical maximum reductions in the noise exposure indexes (-100 %).	70
Figure 37. Regression analysis between the reductions in traffic noise exposures on quiet paths and the initial traffic noise indexes. The analysis covers shortest paths in the length range of 700 to 1300 m and the respective quiet paths. The red lines represent the regression lines of the regression analysis and the green lines show the theoretical maximum reductions in the noise exposure indexes (-100 %).	71

LIST OF TABLES

Table 1. Data that were used in the study.	20
Table 2. Query strings for street network data downloads to be used with Overpass API and OSMnx python library.	26
Table 3. Noise cost coefficients for dB range from 45 dB to 75 dB calculated with both equations presented in this chapter (3 & 4).	33
Table 4. The noise exposure indexes that were defined for measuring dynamic traffic noise exposure and reduction in noise exposure on quiet paths.	39
Table 5. Parameters used in routing with Digitransit routing API.....	45
Table 6. Descriptive statistics of the length of the shortest paths to PT stops and commuting destinations (n=31291).	48
Table 7. Descriptive statistics of exposure to traffic noise on the first walks of public transport itineraries to workplaces and on direct walks to nearby workplaces (n=30160).	52
Table 8. Descriptive statistics of exposure to traffic noise on the first walks of public transport itineraries to workplaces (direct walks to nearby workplaces are filtered out, n=17891).	53
Table 9. Descriptions of the path properties returned by the quiet path routing API.	61
Table 10. A FeatureCollection of two paths returned from the quiet path routing API.	63
Table 11. Minor features and functionalities of the route planner UI that aim to improve the overall user experience of the application.....	64
Table 12. Descriptive statistics of the achievable reductions in noise exposure index ER_{+65dB} on different subsets of the paths. The subsets were defined by 1) the length of the shortest path, 2) the length difference of the quiet path and 3) the initial ER_{+65dB} ($n_{300-600m} = 4338$, $n_{700-1300m} = 7842$).....	72
Table 13. Descriptive statistics of the achievable reductions in noise exposure index dB_{mean} on different subsets of the paths. The subsets were defined by 1) the length of the shortest path, 2) the length difference of the quiet path and 3) the initial dB_{mean} ($n_{300-600m} = 4103$, $n_{700-1300m} = 6925$).....	73
Table 14. Differences in path lengths between the calculated shortest paths and the reference paths (n=31228)..	76
Table 15. Statistics of offsets (distances) between the origin and destination points of the paths and the origin and destination points of the reference paths.....	77

ABBREVIATIONS

API	Application Programming Interface
A-weighting	A method for modelling perceived loudness of sounds of different frequencies
CNOSSOS-EU	Common Noise Assessment Methods in Europe (framework)
dB(A)	A-weighted sound pressure level in decibels
EIF	Environmental Impedance Function
ERR	Exposure-response Relationship
GeoJSON	A geospatial adaptation of the JSON format
GIS	Geographic Information System
GPS	Global Positioning System
HOPE	Healthy Outdoor Premises for Everyone (EU project)
HRT	Helsinki Region Transport (HSL)
HTML	Hypertext Markup Language
JS	JavaScript (programming language)
JSON	JavaScript Object Notation format
L _{Aeq}	A-weighted Equivalent Continuous Sound Pressure Level
LCP	Least Cost Path
L _{den}	Day Evening Night Sound Level
OD	Origin-Destination
OSM	OpenStreetMap
PT	Public Transport
REST	Representational State Transfer
RESTful API	See REST & API
SPA	Single-page (web) Application
SPL	Sound Pressure Level
UI	User Interface
WGS84	World Geodetic System

I. INTRODUCTION

Active transport modes are getting increasing attention among policy makers and urban planners. The term active transport usually refers to walking and cycling but also to other active transport modes such as E-scooters and even city rowboats that are emerging in urban context. Undoubtedly, walking remains the most popular mode of active transport since it doesn't require any accessories and it is essential part of all itineraries made by public transport.

Significant health and environmental benefits have been anticipated and identified from shifting to active transport modes from use of cars (Pucher & Buehler, 2010; Rabl & de Nazelle, 2012); increasing popularity of active transport modes can reduce traffic related pollution and support better health for individuals due to the physical activity. Hence, cities often have a strong willingness to facilitate and promote active transport modes for urban mobility. In encouraging people to choose active transport modes, it is essential for the cities to provide sufficient infrastructure and suitable environments to make using them practical and pleasant.

Multiple factors affect the ease with which active transport is applicable in different urban environments. While infrastructure for cycling is predominantly defined by the more or less exclusive network of cycleways and bike lanes, the one for walking (footpaths, sidewalks etc.), in the other hand, is denser and more evenly distributed. However, not only the physical properties of networks define their applicability and desirability for active transport modes (i.e. walkability or bikeability), but also multiple more ambiguous factors need to be considered (Maghelal & Capp, 2011). These include variables such as safety, presence and types buildings, openness of spaces, proximity to opportunities, quietness, air quality and green spaces – all perceived differently by different individuals.

Many of the factors limiting walkability and other active transport modes are caused by (or at least related to) other, “non-human”, users of the urban space. Evidently, one of the most significant of these is vehicular traffic and the related infrastructures. Vehicular traffic affects walkability and bikeability by establishing large and typically unpleasant built structures to urban spaces. These structures often act as barriers fragmenting the networks that support active transport modes and thus reduce the opportunities for e.g. walking and cycling.

Moreover, vehicular traffic consumes the opportunities for active transport with at least two “invisible” ways. Firstly, since most of it is powered by gasoline engines, it has a negative impact on air quality due to the exhaust gases. According to many studies, individuals’ exposure to the urban

air pollutions caused by vehicular traffic can cause or worsen many lung diseases such as asthma or even cancer. Secondly, varying levels of noise are caused by both the engines and the wheels of the vehicles. According to several studies, individuals' exposure to traffic noise is likely to cause negative health effects such as increased stress levels and problems related to blood circulation (Babisch et al., 2005; Ising et al., 1980; Passchier-Vermeer W & Passchier W F, 2000). The list of potential negative health effects of traffic noise is longer but lacking strong enough scientific evidence. Many of the potential health effects are not immediate but can accumulate over time. Therefore, assessing children's health effects from exposure to noise is particularly important. Due to simultaneously increasing traffic flows and numbers of daily commuters, the negative effects of traffic noise on public health are likely to get amplified in the fast urbanizing world (Passchier-Vermeer W & Passchier W F, 2000).

In this study, the comprehensive definition of walkability, nor bikeability, is not tried to be addressed *per se*. Instead, from the perspective of walkability (or bikeability), this study can be seen as an attempt to capture one narrow but important component of it. Assessing exposure to environmental pollutants have the potential to offer relevant spatial information of routes and areas of low utility for active transport modes. Also, it is important to study the risks for negative health effects associated with active transport modes and potential spatial (in)equality in them.

Methodologically, this study aims to develop a conceptual and technical framework for assessing dynamic (i.e. journey-time) exposure to environmental pollutants using traffic noise as an example. Despite that the methods focus on assessing exposures to traffic noise, they should be applicable, with appropriate adjustments, in assessing also other environmental exposures. Opportunities for applying the developed methods in general environmental exposure analysis and exposure-based routing are discussed further in chapter (5.7). It is anticipated, yet not demonstrated in the study, that traffic noise levels may spatially covary with also other negative impacts of traffic such as air pollution and presence of large unwalkable and unpleasant infrastructures.

Given this context, the aims of the study were defined as follows:

- 1) Develop a routing method that can both assess dynamic (i.e. journey-time) exposure to traffic noise and optimize quieter paths
- 2) Discover spatial patterns and possible (in)equality in pedestrians' dynamic exposure to traffic noise in Helsinki
- 3) Assess achievable reductions in dynamic exposure to traffic noise by using the "quiet path routing" method in Helsinki

- 4) Develop a mobile-friendly web-based route planner application on the quiet path routing method

By these aims, the study intends to facilitate both 1) citizens to choose healthier (quieter) walking routes for their daily walks and 2) city planners to discover areas of problematic walking conditions with respect to traffic noise. The first can be seen as a short-term and latter as a long-term solution in mitigating the negative effects of traffic noise exposure on individuals' health.

II. BACKGROUND

2.1 Noise definition and measurement

Noise can be defined simply as unpleasant sound. Other defining expressions such as unwanted, loud and disruptive reflect the subjective nature of the concept of noise. The lack of explicit definition derives from *noise* being indistinguishable from *sound* by its physical properties; both are fundamentally just vibrations in the air (or other transmission medium). Regardless, the concept of noise is critical in assessing health effects from exposure to high or unpleasant sounds.

A common measure of noise has been sound pressure level (SPL) which is measured in decibels. The decibel (dB) is a logarithmic unit and works well in measuring audible differences in sound levels. However, since human ear is unequally sensitive to sounds of different frequencies, SPL does not reflect the perceived loudness well as such. Thus, so-called A-weighting is often used to balance out these unequal (perceived) responses to different frequencies. A-weighting method utilizes standardized equal loudness contours, where loudness-SPL (phon-dB) relationships are modelled for a range of frequencies starting at different SPLs (Figure 1).

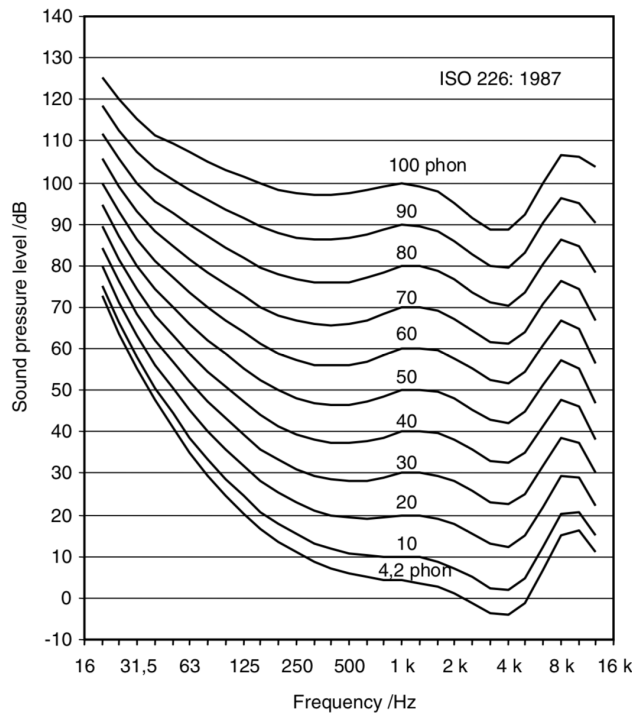


Figure 1. Equal loudness contours as in ISO 226 (*Acoustics – normal equal-loudness contours. International Standard ISO 226*).

2.2 Traffic noise and health

In urban areas, vehicular traffic is usually one of the major sources of community noise. Level of noise is affected by at least the flow and speed of the traffic and the type of the vehicles and road surface. Increased but varying traffic noise levels are typical to highways and other major roads.

A variety of metrics have been developed to measure level of traffic noise. The metrics aim to reflect the perceived loudness but given the time-varying nature of traffic noise, this gets rather challenging. Different vehicles and road surfaces cause noise of different frequencies and tones, resulting differences in perceived loudness due to human ears varying sensitivity to different frequencies. A widely used approach to measure and compare traffic noise levels is to use the A-weighted sound pressure level averaged at certain time frames of the day. According to Torija & Flindell (2015), A-weighting may be particularly suitable for modeling the loudness of traffic noise due to the appropriate weighting of the low-frequency sounds. The environmental noise guidelines by WHO Europe (2018) as well as scientific traffic noise research commonly utilize metrics that are based on averaged “equivalent continuous sound pressure levels” for different times of the day (e.g. L_{day} , $L_{evening}$ and L_{night}). One of the standard metrics for community noise levels considers day, evening and night-time noise levels together (L_{den}) and features additional weightings for evening and night-time noise levels (WHO Europe, 2018). These metrics are heavily compressed, and thus lose information about the fluctuations of SPL in time. Nevertheless, uniform metrics are needed in order to efficiently compare different noise environments in space and time.

Several studies have aimed to evaluate the relationship between noise level and annoyance by statistical means. A common approach has been assessing and comparing the percentages of highly annoyed people (HA%) to average noise level (e.g. L_{den} or L_{Aeq}). An important feature of these assessments is that they consider exposures to noise only with respect to home locations. Guski et al. (2017) reviewed many of the studies and plotted the found HA% values against SPL (L_{den}) (Figure 2). Both somewhat linear and non-linear relationships can be seen in the scatterplot, indicating an unclear and case-specific statistical relationship between static noise exposure and annoyance.

According to two literature reviews on traffic noise and annoyance (e.g. Brown & Van Kamp, 2017; Guski et al., 2017) and a report on those reviews by WHO Europe (WHO Europe, 2018), prolonged exposure to noise levels above 53 dB can cause negative health effects and should therefore be avoided. Accurate assessment of different health effects from traffic noise exposure has been challenging due to different temporal realizations of the effects and overlapping exposure-response - relationships of multiple pollutants (Passchier-Vermeer W & Passchier W F, 2000); it is likely that

some of the health effects are developed over years or decades of cumulative exposure while some are perceived and realized in the present time. Accordingly, the potential longer-term effects from exposure to traffic noise include e.g. respiratory infections, cardiovascular disease and stress (Recio et al., 2016; Van Kempen et al., 2018) whereas the short-term effects can be e.g. annoyance or stress. Moreover, the net health effect from and perception of noise is affected by various “nonacoustic factors” such as gender, age, education and subjective noise sensitivity (WHO Europe, 2018: 14).

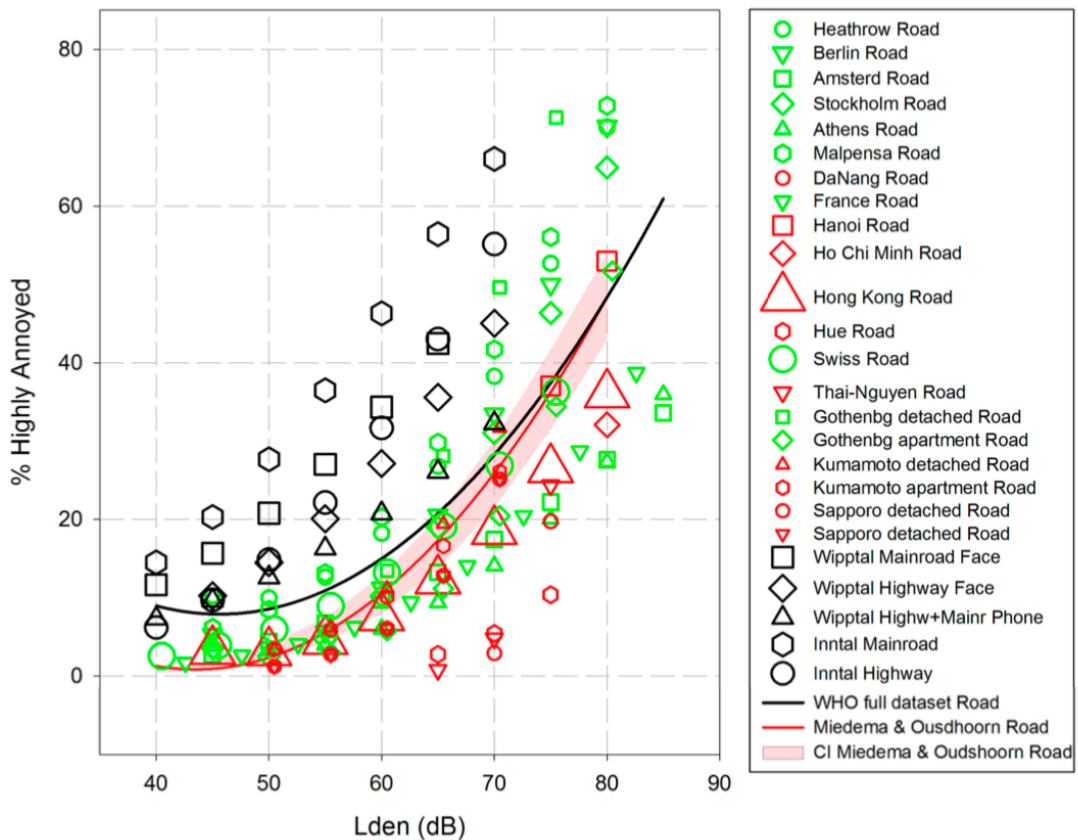


Figure 2. Composed scatterplot between L_{den} and percentage of highly annoyed (HA%) for several studies on road traffic noise and annoyance by Guski et al. (2017).

2.3 Traffic noise modeling

While air pollution is often challenging to quantify, measure and model (and tends to be rather dynamic with respect to weather conditions), then traffic noise can be measured and modelled in a more straightforward manner. Vehicular traffic noise levels have been spatially modelled in many cities with fairly high spatial resolution - not only due to the developing technical possibilities and national legislation, but also as required by the environmental policies of the EU (e.g. *Directive 2002/49/EC*, 2002).

Advanced software is nowadays available to perform ever more complex noise modelling. Noise models are usually established by either national or international policies. In the Nordics, a commonly used noise model is Nord2000 (Jonasson & Storeheier, 2001). Also the EU has recently established a noise modeling framework “Common noise assessment methods in Europe” (CNOSSOS-EU) (Kephhalopoulos et al., 2012) that is being employed at EU’s environmental policies and assessments.

Many environmental features can be included in the noise models in calculating modelled noise surfaces. Typically, two kinds of input data are needed to run the models: 1) spatial data of the noise sources and 2) spatial data on features that affect the pathways and absorption of noise. Noise sources usually cover measured or modelled data on vehicular traffic flow, rail traffic and air traffic whereas the latter category includes features such as 3D surface model of the landscape, buildings, noise barriers and weather conditions.

2.4 Concepts and approaches in assessing dynamic exposure

In this chapter, literature on dynamic exposure either to air pollution or traffic noise are reviewed, since only few studies have focused solely on noise exposure and the concepts and spatial analysis methods for assessing dynamic exposures to different pollutants have been more or less analogous.

According to several authors (e.g. Rabl & de Nazelle, 2012; Reynolds et al., 2010; Tainio et al., 2016), negative health impacts of vehicular traffic can compromise the potential health benefits of walking. Thus, means for assessing pedestrians’ exposure to the pollutants produced by traffic are required in estimating the net health effect. The concept “journey-time exposure” has been used in a few studies (e.g. Davies & Whyatt, 2009; Gulliver & Briggs, 2005), emphasizing the relative importance of dynamic exposure as a component in individual’s total daily exposure. Journey-time exposure occurs in space and time, where both location of the individual and environmental conditions are dynamic. These considerations introduce a conceptual and technical challenge in implementing assessments for journey-time exposure: the used data needs to have both high spatial and temporal resolution. In the later parts of the thesis, the concept *dynamic exposure* is used interchangeably with the concept *journey-time exposure*.

Exposure to a pollutant is commonly measured simply as either duration or distance of exposure to certain concentrations or levels of the pollutant (e.g. Figure 3). A commonly used index of exposure to a pollutant can be calculated simply by multiplying a set of travel times by the respective levels or concentrations of the chosen pollutant (e.g. Hasenfratz et al., 2015). Specific to studies on exposure to air pollution, one of the metrics have been (estimated) total inhaled doses of different pollutants.

Depending on the study setting, dynamic exposures can finally be aggregated by predefined thresholds for concentration (or level) or spatially by a set of area, street or trajectory features.

In the studies where pedestrians' exposure to pollutants was assessed on modelled trajectories, distance and duration of exposure were often considered proportional and hence used interchangeably (Gulliver & Briggs, 2005). Another type of spatial approximation of dynamic exposures to noise was demonstrated by Sheng & Tang (2011); instead of assessing dynamic exposure by measured or modelled trajectories, they analyzed relative significances and lengths of sidewalks and respective traffic noise levels.

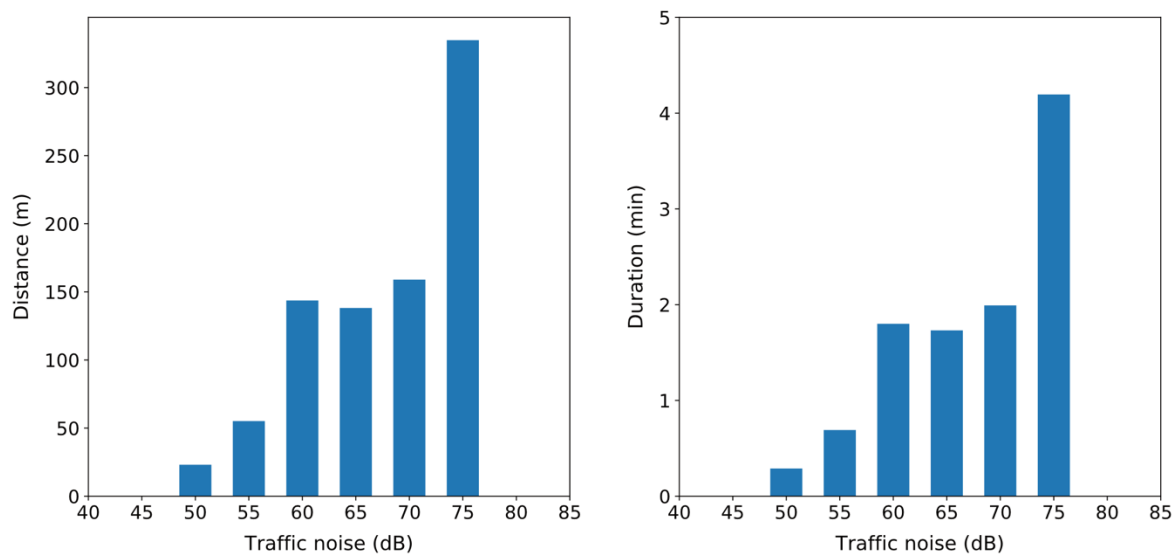


Figure 3. Dynamic exposure to traffic noise level on a path as distances (left) and durations (right) of different traffic noise levels.

Based on the literature review of this study, at least three common approaches for assessing pedestrians' or cyclists' dynamic exposure to pollution exist:

- 1) Direct way: using measurement instruments (e.g. air quality or volume sensor) attached to members of a study group and tracking them temporally and spatially with GPS (e.g. Apparicio et al., 2016; Cole-Hunter et al., 2012).
- 2) Indirect way: using measured and modelled pollutant surfaces and spatial analysis to assess exposure to pollution on e.g. GPS-tracked routes of people (Whyatt et al., 2007).
- 3) Indirect way: using measured and modelled pollutant surfaces and spatial analysis to assess exposure to pollution on modelled routes of people by e.g. OD data.

However, due to varying urban contexts and availability of technology and data in different studies, the methodologies and study questions have been rather case specific. Hence, along with the three approaches listed above, many alternative or mixed methodologies have been used to in assessing dynamic exposure. Different approaches are suitable for different spatial and temporal scales. While the entirely direct way (1) can provide accurate data on dynamic exposure for a small subset of the population, then spatial exposure analysis by modelled routes and pollutant surfaces (2 & 3) can reveal broader patterns in individuals' exposures. The latter approach is more appropriate in studying population or district level health effects from exposure to pollutants but relies on the knowledge of composition of individual's dynamic exposure gained via direct measurements.

GIS, as a technical framework, has been widely utilized in processing and analyzing data in indirect dynamic exposure analysis. Its advantage is clearly the ability to spatially and temporally compare data on both pollutants and individuals' movements. A common step for many dynamic exposure assessments has been the spatial join between pollutant surfaces and GPS-trajectories or modelled routes of people. It is a critical step in determining the dynamic exposure as durations or distances of different concentrations (or levels) of pollutants. Technicalities of the spatial join vary depending on the schema and type (e.g. raster or vector) of the pollutant data, route data, used software and possibly programming environment.

Furthermore, methods for dynamic exposure assessments can empower exposure-based routing. In the following two chapters, approaches and methods for minimizing dynamic exposures through routing analysis are reviewed.

2.5 Graph theory and least cost path analysis

Graph is a data structure that can model connected phenomena or set of objects such as social network, decision tree (abstract phenomena) and transport network (physical phenomena). Essentially, graphs consist of nodes and edges that represent connections and features in the modelled network. Edges are connections between nodes and thus allow "travelling" from one point (node) to another, given that the required connections between the two nodes exist in the graph. Depending on the type of the graph, between any two nodes, one or more edges can exist, and the edges may or may not be traversable to both directions.

One of the widely adapted applications of graphs is modeling and analyzing street networks. In the typical abstraction, intersections are modelled as nodes and streets as edges. Both features can have arbitrary number of attributes describing their physical properties. Numerical edge attributes enable

routing analysis within the modelled street network. A common application of graph theory is the least cost path (LCP) analysis, which aims to find the path of least total cost by a given edge attribute between any two (connected) nodes in a graph. If the length of edges is used as the cost attribute (i.e. weight), least cost path becomes the same as the shortest path. However, as any numerical non-negative edge attribute can be used as the cost, a variety of routing problems can be addressed by solving adapted LCP problems.

Several algorithms exist for least cost path routing, one of the most well-known being Dijkstra's algorithm. According to Noto & Sato (2000), the other two key methods for solving the simple least cost path problem are the A* algorithm (1) and genetic algorithms (2). Dijkstra's algorithm finds the very least cost paths between two nodes in a graph by first finding the least cost paths from an origin node to all other nodes of the graph, as illustrated by Jasika et al. (2012) in Figure 4. If the shortest path is needed for only one origin-destination (OD) pair, pathfinding is stopped once the least cost path to the destination node is included in the cumulative set of all known least cost paths.

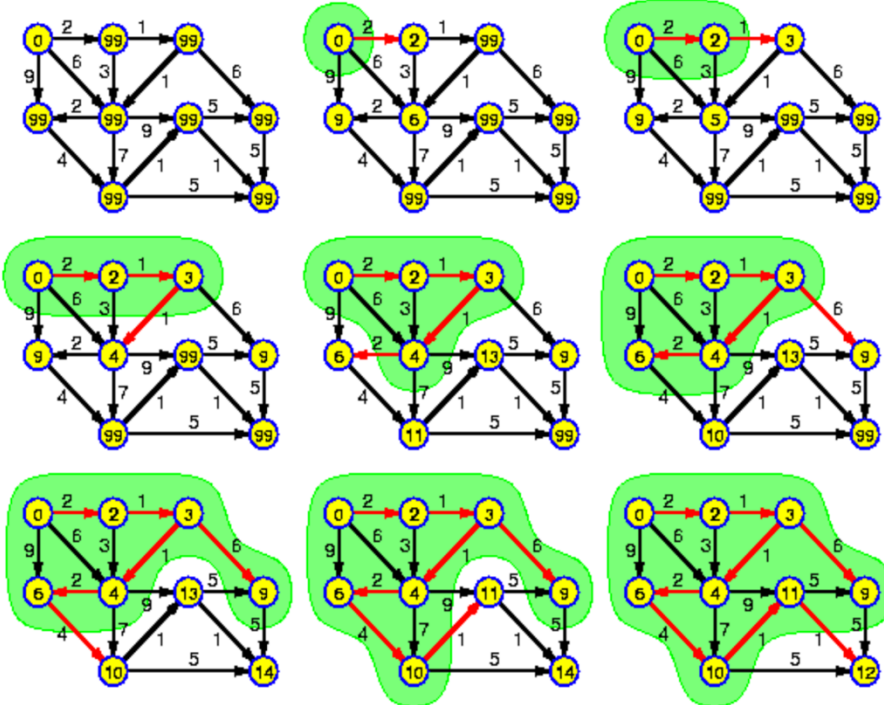


Figure 4. An illustration of the sequence of steps in finding least cost paths with Dijkstra's algorithm by Jasika et al. (2012).

When size of the graph grows, the original form of Dijkstra's algorithm becomes computationally increasingly demanding. Thus, many studies have focused on optimizing the least cost path analysis itself by developing advanced algorithms (e.g. Ahuja et al., 1990; Goldberg & Harrelson, 2005; Noto

& Sato, 2000). A commonly pursued objective in enhancing least cost path finding has been reducing the total number of shortest paths that need to be known before reaching the desired path (OD pair). Alongside other types of advanced pathfinding algorithms, this has resulted in faster ways of using Dijkstra's algorithm. One of the latter is A* algorithm, that introduces euclidean bounds around the origin and destination nodes and selects only a subset of the nodes to be visited. As Noto and Sato (2000) put it: “[A* algorithm] eliminates fruitless searches by considering the distance to the destination”.

2.6 Exposure-based impedances in routing

In accessibility research, travel time is often used as one of the key metrics of accessibility. Likewise, in also routing analysis, travel time seems to be one of the most often optimized variables. However, also other types of costs have been incorporated in routing analysis when using special criteria for pathfinding. Adjusted LCP analysis can be used to solve a variety of pathfinding problems, including finding least exposure paths. Several vivid names have been introduced to describe and promote different types of least-exposure paths. These names include e.g. green, healthy, happy, sustainable, safe and quiet paths (e.g. Hatzopoulou et al., 2013; Quercia, 2015; Quercia et al., 2014). In the context of this study, the concept quiet path is used to refer to routes of less noise exposure.

In route planners for walking and cycling, environmental exposure-based costs have been introduced in LCP analysis in order to find more pleasant and healthier routes for active transport. Both raster (surface) and graph -based routing methods have been used in exposure-based routing. In urban contexts, many of the studies have utilized graph-based methods since graphs apply well in modeling urban street networks (see chapter 2.5). Many studies have demonstrated how graph-based LCP analysis can be used to minimize exposure to pollutants (e.g. Alam et al., 2018; Hasenfratz et al., 2015; Hertel et al., 2008; Sharker et al., 2012; Su et al., 2010).

Based on the discovered literature, raster-based LCP analysis methods (in exposure-based routing) were applied only in a few studies. For example, Davies & Whyatt (2009) used air pollution surfaces (PM_{10}) and spatial data on traversable and non-traversable features of the study area to find least-exposure paths with common raster-based LCP functions. The decision to use raster-based method enabled them to incorporate continuous areas (e.g. parks) in the routing analysis. Their method worked well for a relatively small study area but required careful data preparations to mask out all unwalkable features.

Incorporating dynamic exposures in LCP analysis has commonly required defining a custom cost function for calculating adjusted costs (i.e. impedances) by the exposures. For example, (Ribeiro & Mendes, 2013) used the concepts “contamination of distances” and “environmental impedance function” (EIF) to model exposure-based impedance from noise and air pollution (PM_{10}). They assigned noise-based costs to edges of a graph according to contaminated distances of different noise levels, using predefined thresholds (dB) to decide whether a noise cost should be assigned or not. A commonly used way to balance between exposure-based impedances and travel-time has been to include distance as a base-cost in the EIF. In many studies, distance and travel time were considered as proportional, limiting complexity of the EIF. If exposures to multiple pollutants need to be integrated in a single EIF, or their relative weights in the cost function need to be adjusted (with respect to distance or to one another), EIF can also include additional cost coefficients. The idea of integrating multiple environmental exposures in a composite EIF is discussed further in chapter 5.7.

Despite the common goal of the exposure based EIFs presented in different studies, namely reducing dynamic exposure to pollutants, the composition of the cost functions has varied considerably between studies. This suggests that minimizing environmental exposures through routing analysis is more emerging than already well-established area of research. Many of the demonstrated methodologies have been influenced by different constraints on data availability but also by varying and subjective perceptions of impedances of different pollutants. Given this scientific background, a custom EIF for traffic noise was designed also in this study (see 3.5.1) and can be considered as one of the main outcomes.

Many of the previously developed exposure-based routing methods (and applications) focus on dynamic exposure to air pollution. Finding least cost paths with respect to exposures to e.g. $PM_{2.5}$ or PM_{10} particles has been demonstrated or at least addressed in several studies (e.g. Davies & Whyatt, 2009; Hertel et al., 2008; Ribeiro & Mendes, 2013). In these studies, considerable decreases (%) in the total exposure to the pollutants were found on the exposure-optimized paths, indicating a potential for green path route planners. Common to most of the prior studies on exposure-based routing, the alternative routes are presented with comprehensive statistics allowing comparison of differences in dynamic exposure, route length and travel time.

Some of the exposure-based LCP methods were developed further as web-based route planner services (e.g. Hasenfratz et al., 2015; Hatzopoulou et al., 2013; Su et al., 2010). In these services, special attention has been paid on the visualization of the different route alternatives as well as presenting respective differences in exposures to pollutants and travel times. However, no visual

representations of dynamic exposures to pollutants on the alternative routes were seen in the published route planners at the time of writing this thesis. Instead, the properties of the routes (e.g. exposures, travel time and distance) were often presented only numerically. To the author's knowledge, this is one of the identified shortcomings of the currently available (exposure-based) route planners and thus one of the motivations for creating a novel green path route planner application; how to better communicate journey-time exposure of different routes also visually to the user?

In the prior studies, publishing an exposure-based routing application as an online service has also required optimizing the efficiency of the LCP analysis to support responsive enough user experience. Hasenfratz et al. (2015) demonstrated how using static pollution maps and loading the whole LCP analysis application into the memory of a smartphone can provide very fast responses to user's actions. On the other hand, for example Su et al. (2010) implemented their route planner as a service based web application, where a distinct user interface application communicates with a exposure-based LCP service via asynchronous requests, leaving the user interface active even at times when routes are being calculated. By reviewing the discovered literature on exposure-based route planners, the latter approach was found somewhat more utilized than building standalone mobile or desktop applications (such as the one by Hasenfratz et al. (2015)). A variety of viable technical implementations for such services seem to be available due to the increased opportunities that modern Web GIS technologies enable (see 2.7).

2.7 Web GIS concepts and developments

In this chapter, some concepts and developments of modern Web GIS are reviewed. In order to ensure that state of the art technologies are used in the technical implementation of the quiet path route planner, the focus is on the latest technological advancements that can empower highly interactive web map applications.

According to Agrawal & Gupta (2017) and Veenendaal et al. (2017), recent developments in Web GIS technologies and in their applications have happened in the context of emerging paradigms in common web technologies and increasing numbers of users. Alongside the growing number of web users, also the ways using web services have changed. Increasing number of web users prefer mobile over desktop (Meeker & Wu, 2013, 2018), which has created new demand and opportunities for mobile-friendly web map applications (Veenendaal et al., 2017). In other words, it has been acknowledged that mobile users are the primary user group of many, if not most, new web applications. This shift has facilitated the adaptation of mobile-first principle and Responsive Web

Design (RWD) in web development; the content and user interfaces (UIs) of modern web applications have been designed to look good on screens of all sizes (RWD), starting from the very smallest ones (mobile-first).

Emerging service-oriented architectures (SOA) have allowed distributing the most expensive data processing and analysis operations in dedicated machines. The concept has also been applied in Web GIS applications, enabling uninterrupted user interfaces and fast geospatial processing and analysis. Another benefit from SOA is scalability of web applications to support high but changing numbers of concurrent users. These developments can be seen as an adoption of a larger scale paradigm shift from independent applications to service-oriented architectures in Web GIS (Agrawal & Gupta, 2017). As per Lu (2005), “The service-oriented architecture is a very promising architecture for practical implementation of the next generation geographical information systems”. Development of SOA-based Web GIS solutions have been facilitated by the emergence of cloud-computing platforms. These services allow running GIS applications in appropriate infrastructure, either in hosted servers or using a serverless architecture. Then, distributed GIS services and data sources can be utilized via application programming interfaces (APIs) in similar manner as other web services. Complex GIS systems can be composed from a desired set of separate services and data sources, as illustrated by Veenendaal et al. (2017) in Figure 5.

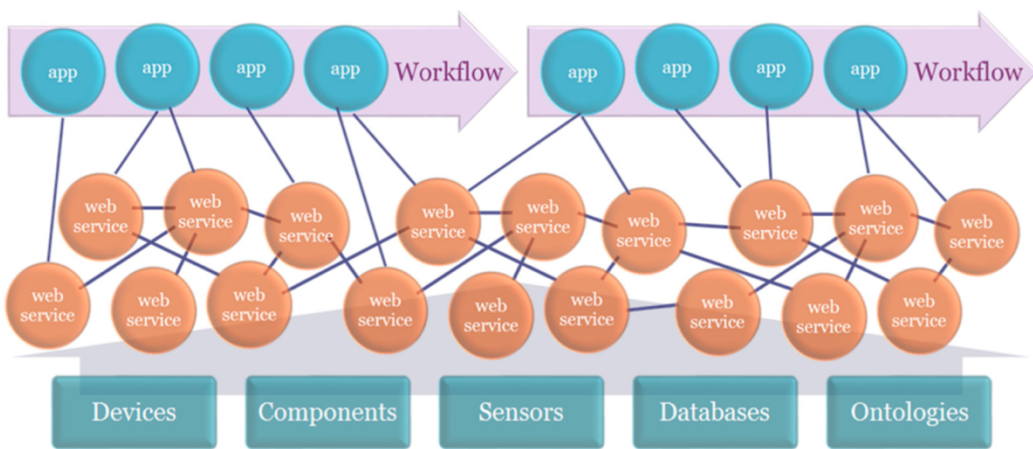


Figure 5. A figure by Veenendaal et al. (2017): “Interacting web services feeding into apps within application workflows.”

The advantages of SOA for Web GIS systems also includes the ability to utilize services provided by public authorities and governments. Virtually any service that can be accessed through APIs can be integrated into Web GIS system using SOA. Integration of geospatial services has been facilitated with standardized geographical data formats and protocols such as web map service (WMS) and web

feature service (WFS). Encouraged by SOA, the user interface of a Web GIS system can communicate with the supporting GIS services asynchronously (e.g. Neis & Zipf, 2017; Su et al., 2010), leaving the user interface layer always reactive to user's actions. This is a major difference (and improvement) compared to e.g. traditional desktop GIS software, which still often struggle to provide smooth user experience while executing geospatial analysis.

Some of the advancements in Web GIS technologies are enabled by the increased computational capabilities of users' devices and servers. Today, web browsers of personal computers and smart phones have access to increased computing power and graphics processing capabilities. Thus, modern web browsers enable running ever more vivid and interactive web map applications and also executing simple geospatial analysis right in the user's device (i.e. "client-side"). The limitations for running Web GIS applications in the browser are ever less set by the capabilities of the users' devices but then more by the available software that can utilize them.

Another aspect that has facilitated the advancing of Web GIS is the development of open source data formats and code for geospatial analysis and web-based visualizations (e.g. web map libraries, spatial databases and libraries for geospatial analysis). Many of these formats and software (e.g. Leaflet; OpenLayers & PostGIS) are actively developed by open source communities and some of them also financially supported by authorities of private companies.

A critical component of a Web GIS system is its user interface, which often is a web map application - if excluding pure Web GIS *services* such as geocoding and routing APIs. Many web map libraries are available for building customized interactive web map applications. They are usually implemented with JavaScript (JS) programming language as that is one of the few programming languages that is natively supported by most web browsers. While most web maps used to be (and probably still are) based on tiled raster maps (often called as basemap), some novel web map technologies have been introduced (Gaffuri, 2012; Lienert et al., 2012). The latest major revision of HTML (hypertext markup language), HTML5, added prominent capabilities for drawing increasingly rich and interactive vector-based visualizations. It has been demonstrated that HTML5-enabled technologies can be used in implementing web map applications with vivid vector graphics (e.g. Boulos et al., 2010; Farkas, 2019; Qiu & Chen, 2018). Also, HTML5 reduces the need for additional plugins (e.g. Adobe Flash Player) when dealing with interactive graphics. For example, one of the promising (HTML5-enabled) technologies for vector-based interactive web mapping, among other use cases, is WebGL. For example, one of the web map libraries that heavily utilize WebGL is Mapbox GL JS.

Apart from the technical advancements of the components of Web GIS, the broader picture of contemporary Web GIS has been studied with respect to various parallel developments, trends and opportunities. Veenendaal et al. (2017) illustrated this larger conceptual and technical framework (around Web GIS) with a pyramid of labelled Data, Information, Knowledge, Intelligence and Wisdom (DIKIW) (Figure 6). According to the review by Veenendaal et al. (2017), the advanced technical frameworks within and around Web GIS can facilitate providing users with both more personal and richer geospatial information.

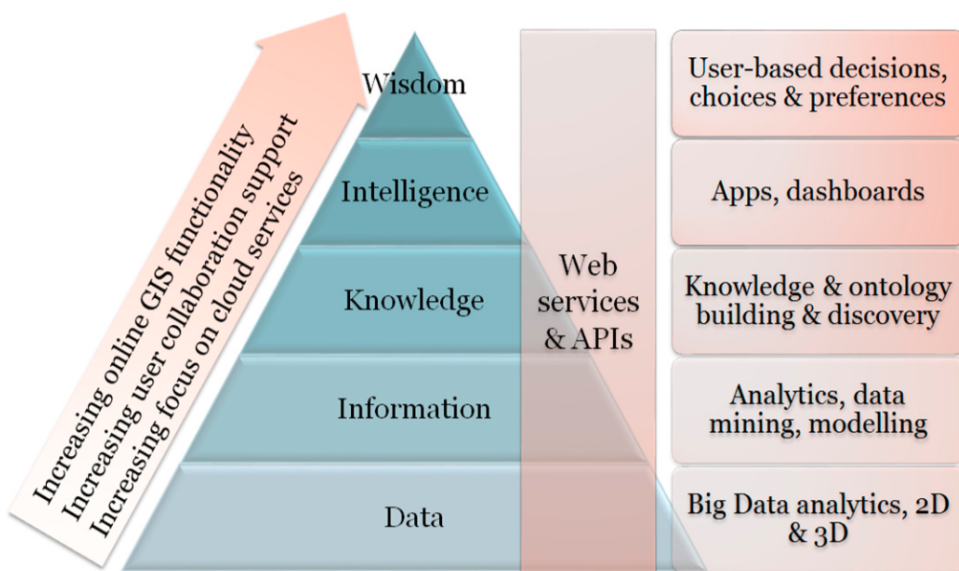


Figure 6. Illustration by Veenendaal et al. (2017): "Focus and trends in increasing web mapping functionality".

III. DATA & METHODS

3.1 Overview of the methods

Overview of the methods and their internal dependencies is illustrated in Figure 7. As shown in the figure, the three outcomes of the thesis depend on the routing application that optimizes both shortest and quiet paths. Assessments of pedestrians' exposure to traffic noise (1) and potential to reduce exposure to traffic noise (2) are linked to each other, as the achievable reductions are calculated using the same set of origin-destination walks determined in the first assessment. The web-based quiet path route planner (3) is a detached outcome from the first two and has additional dependencies to several Web GIS technologies.

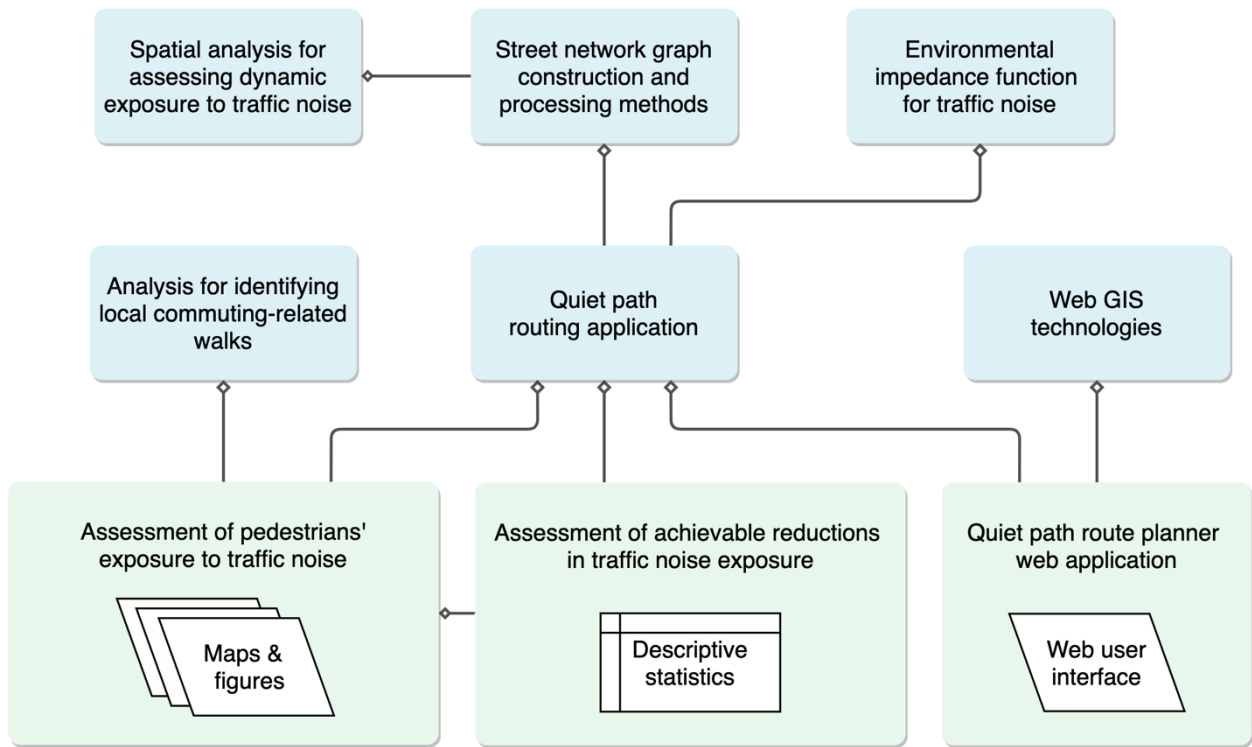


Figure 7. Illustration of the internal dependencies of the methods and outcomes of the study.

3.2 Study area

The study area of this work is Helsinki, as defined by the extent of the modelled traffic noise zones in Helsinki (Figure 8). Some of the islands in the very southern Helsinki were excluded from the study area as the traffic noise data does not cover them and they feature only restricted street

networks. Despite defining a study area, the concepts and methods developed in the study were designed to be applicable also in different areas by reasonable effort.

Helsinki is the capital of Finland and also one of the most important workplace hubs of the country. Its 653 835 inhabitants and 397 346 workplaces (Statistics Finland, 2020) make it a vibrant city with high flows of daily commuters. Most of the trips in Helsinki are made by walking, cycling or with public transport organized by Helsinki Region Transport (City of Helsinki, 2020).

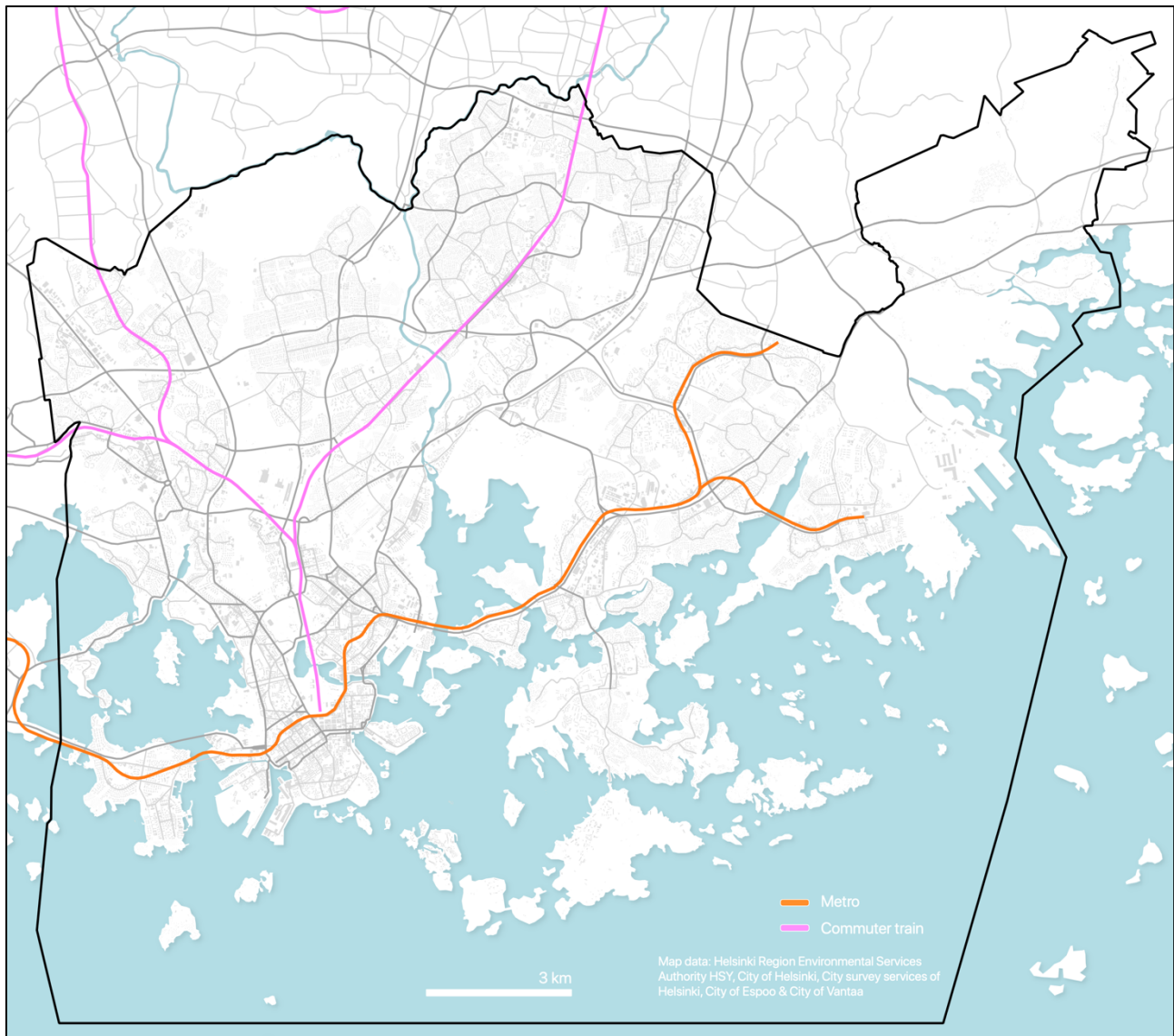


Figure 8. The study area and its key transportation networks.

3.3 Data

Several datasets were used in the study (Table 1). The developed routing application required only two input data, street network data from OpenStreetMap (1) and modelled traffic noise zones (2), of

which both were available as open data. On the other hand, the assessment of pedestrians' exposure to traffic noise required a set of additional datasets of which the census-based commuting flow data was not openly available.

Table 1. Data that were used in the study.

Name	Source	Description	Use in the study	Open data
Traffic noise zones in Helsinki 2017	Urban Environment Division of city of Helsinki (Helsingin kaupunkiympäristön toimiala)	Modelled traffic noise surfaces by different noise sources, e.g. A-weighted equivalent continuous sound pressure levels from traffic noise (L_{Aeq}).	Dynamic exposures to noise pollution are assessed by the noise zones of this data.	Yes
250m statistical grid	Statistics Finland	250m * 250m polygon grid layer that is linked to YKR-commuting data.	Grid cells are used as origins and destinations in the analysis of pedestrians' dynamic exposure to traffic noise and in visualization of the results.	No
YKR-commuting data	Finnish Environment Institute (SYKE) / Statistics Finland	T06_tma_e_TOL2008_2016_hel – census-based commuting flows between 250m statistical grid cells. One row in the data reports the total number of commutes between a pair of grid cells.	Commuting-related walks are modelled by planning public transport itineraries for the commuting flows.	No
City districts in the Helsinki Metropolitan Area	Helsinki Region Environmental Services Authority HSY	City districts as polygons.	Centers of the city districts are used as destinations for distant workplaces in the itinerary planning analysis.	Yes
OpenStreetMap	© OpenStreetMap contributors	All walkable highways and paths as features of the street network.	A street network graph suitable for routing is constructed from the data.	Yes
Digitransit Routing API	Helsinki Region Transport (HRT)	A routing service for planning public transport itineraries via an application programming interface (API).	Itinerary planning for commuting flows was carried out using the routing API.	Yes

3.3.1 Modelled traffic noise data

Dynamic exposures to traffic noise were assessed with respect to modeled traffic noise zones for Helsinki (*City of Helsinki: strategic noise mapping*, 2017). The noise modelling was carried out with

a special software for the purpose (Datakustik CadnaA 2017) by Sito Oy as a commission from the city of Helsinki (*City of Helsinki: strategic noise mapping*, 2017). As per the documentation of the data, a wide range of factors affecting the ways and levels of noise were taken into account in the modelling. For example, these included noise source data of modelled traffic flows and speeds on different roads, the three-dimensional surface model of the city, buildings, sound barriers and acoustic properties of different surfaces (*City of Helsinki: strategic noise mapping*, 2017).

It should be noted that the decision to use noise data of only noise source in the dynamic exposure assessment is arguably in line with the *Environmental noise guidelines for the European Region* (Kephalopoulos et al., 2012). The guidelines and the supplementary literature state that the thresholds for harmful noise levels vary between different noise sources. Also, the mitigation actions for dealing with different types of community noises vary, making the results of separate exposure assessments more valuable for planning purposes. In this study, the main focus is on dynamic exposure to vehicular traffic noise, excluding exposure to noise from rail and air traffic and industrial sites. Despite that this approach may be appropriate for the dynamic noise exposure assessment, the noise exposure-based routing application could benefit from integration of also other noise sources in the routing analysis. The prospects for integrating multiple environmental exposures (including different noise sources) in exposure-based routing are discussed further in chapter 5.7.

Prior to pre-processing the noise surface data, two parallel noise surface layers for vehicular traffic were inspected, one produced with CNOSSOS-EU modelling (Jarno Kokkonen et al., 2016; Kephalopoulos et al., 2012) and the other with joint-Nordic traffic noise estimation model (Jonasson & Storeheier, 2001; Nielsen, 1997). The latter was chosen for the study since its modeling height of 2 meters was closer to the typical walking altitude of pedestrians than the 4 meters from the ground used in CNOSSOS-EU model. However, since CNOSSOS-EU model has been described to have higher level of detail in both noise source and noise diffusion modeling (*City of Helsinki: strategic noise mapping*, 2017), choosing it could have been justified as well. Nonetheless, a visual comparison of the two noise layers did not reveal major differences between the two.

The noise surface data contained a few alternative noise indexes. For this study, A-weighted equivalent continuous sound pressure level (L_{Aeq}) for daytime (7am –22pm) was chosen as the primary noise index (layer: *2017_alue_01_tielikenne_L_Aeq_paiva*). A-weighting is used to consider the human ear's sensitivity to sounds of different frequencies. Then equivalent continuous sound pressure level is an averaging method for calculating a single sound pressure level from a time-varying sound pressure level during a defined time period (see chapters 2.1–2.3 for more

information). As per Guski et al. (2017) and Van Kempen et al. (2018), both of these metrics (A-weighting and equivalent continuous sound pressure level) have been widely utilized in the studies on traffic noise and annoyance.

The data included modelled traffic noise surfaces attached with attribute data on the minimum and maximum traffic noise levels (L_{Aeq}) as per a pre-defined set of 5-decibel ranges. The modelled traffic noise levels ranged from 45 dB(A) to 80 dB(A). Three map visualizations of the noise surfaces were made to illustrate the high spatial precision of the modelling (Figure 9, Figure 10 & Figure 11). For example, the effect of buildings as effective noise barriers can be seen when comparing the noise surfaces between Figure 10 and Figure 11; in the first map the +60 dB(A) noise surfaces spread hundreds of meters from the highways whereas in the latter they are more restricted between the buildings.

Only small amount of pre-processing was needed prior to utilizing the noise surface data in the other phases of study. A few topological errors were found in the data (revealed first in the assessment of pedestrians' dynamic exposure to traffic noise and then in the validation of the spatial join); in some cases, two or more noise surfaces intersected with each other, resulting areas with multiple (alternative) noise index values. These topological anomalies were not fixed, but instead considered when spatially joining the noise values to street network data. When two or more competing noise values were found in the spatial join, only the maximum value was extracted (see chapter 3.5.2). This practice was validated through a visual inspection of the noise surface data: the surfaces representing higher noise levels appeared considerably more logically with respect to the presumed noise sources than the intersecting (underlying) ones of lower noise levels.

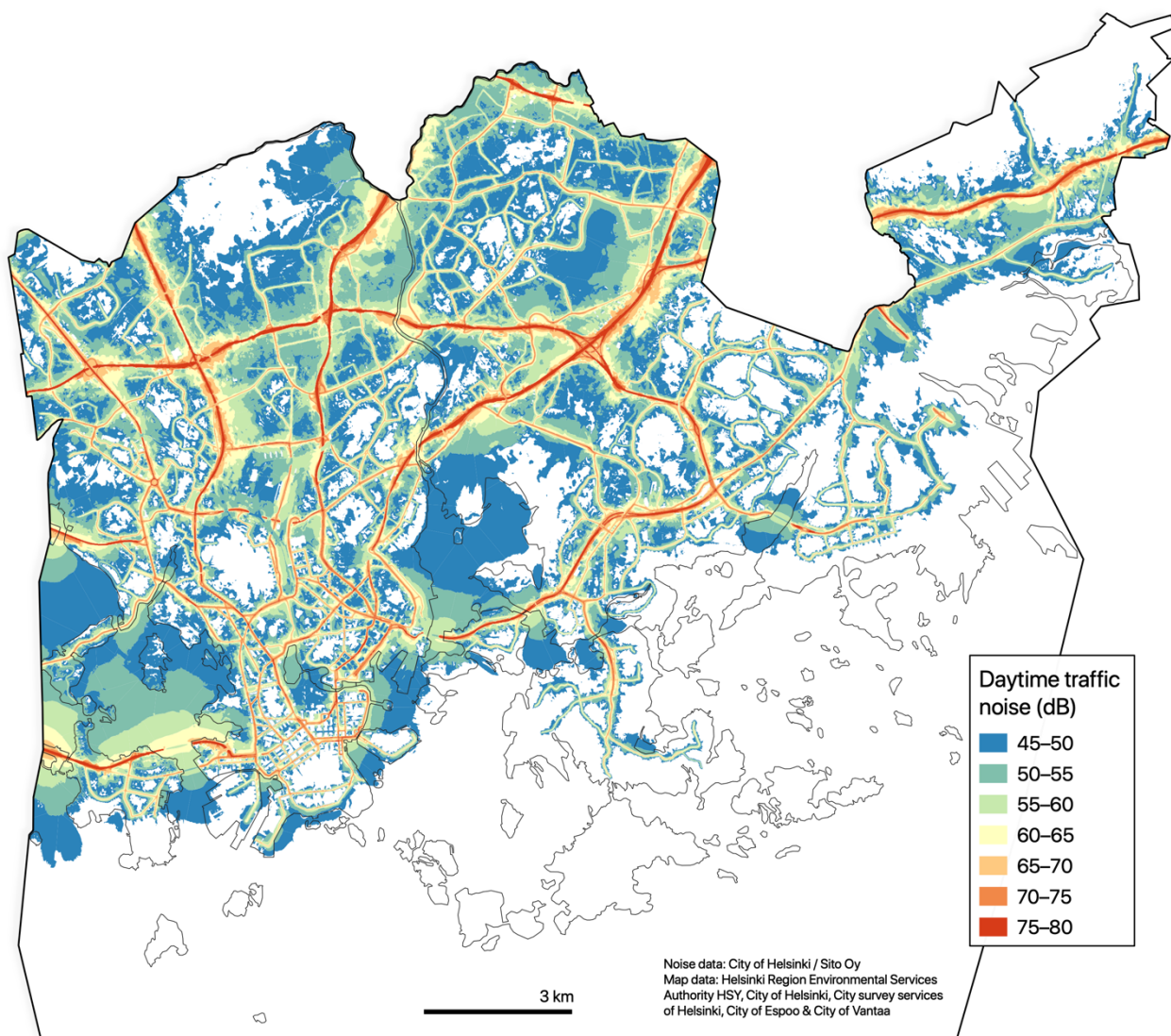


Figure 9. Modelled daytime traffic noise levels (dB(A)) in Helsinki.

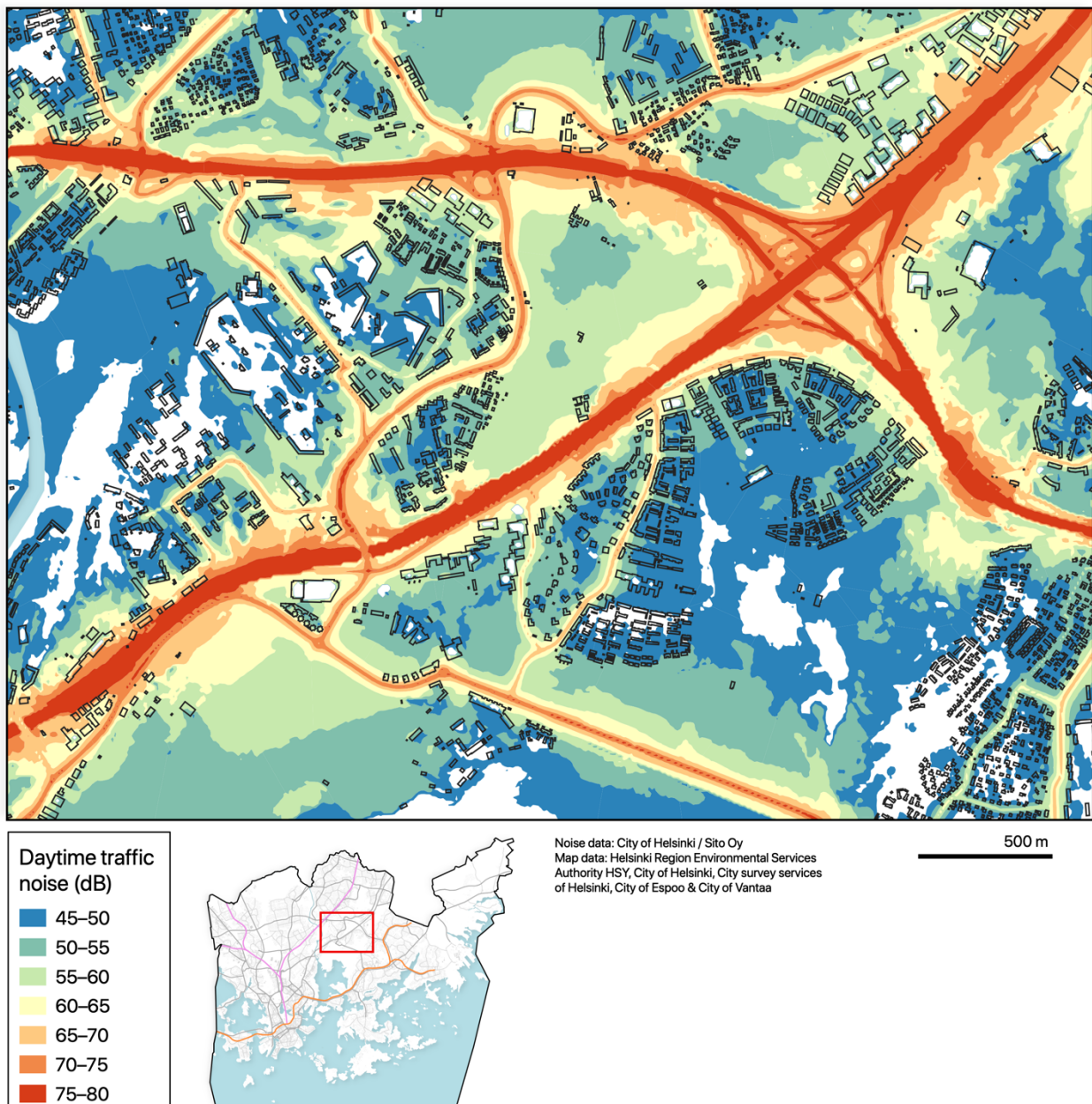


Figure 10. Modelled daytime traffic noise levels (dB(A)) in Viikki.

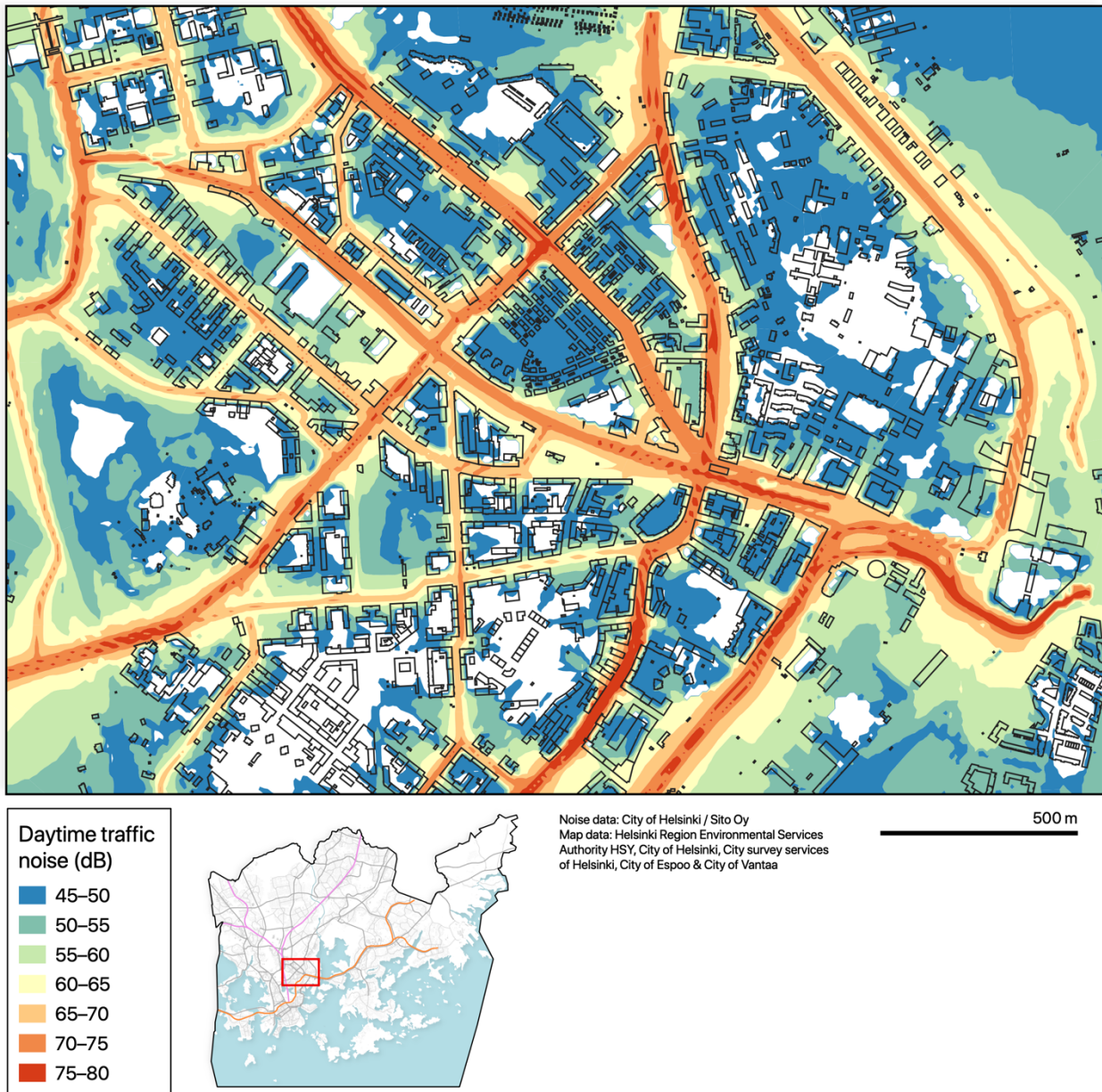


Figure 11. Modelled daytime traffic noise levels (dB(A)) in Kallio and Vallila (in Helsinki).

3.3.2 OpenStreetMap data

A large dataset of street network features was downloaded from OpenStreetMap (OSM) for walkable street network graph construction. The data was queried from Overpass API (2019) which allowed using a custom query string to request only the appropriate features based on their attributes. The python library OSMnx (Boeing, 2017) provided a practical way for accessing the API and using a customized query string. The query string was based on the default query string of OSMnx for walkable street features and adjusted to exclude several unwalkable features (Table 2).

Yet, some unwalkable street features were needed to be filtered out from the graph only after creating it due to limitations in the querying capabilities of OSMnx. Hence, a subsequent download of unwalkable street network data was required.

Choosing OSM data as the basis of the walkable street network graph can be justified with at least three arguments. As demonstrated by a number of studies, e.g. Zielstra & Hochmair (2011, 2012), OSM often contains a comprehensive set of walkable street features of major cities, since the data is updated by active local OSM communities (1). The street network data used in the official route planner application of Helsinki Region Transport (HSL) authority is solely based on OSM data. Therefore, OSM of the area is kept up to date by also professional mappers (2). Moreover, the use of OSM data allows easier adopting of the methodology in other study settings and areas (3).

Table 2. Query strings for street network data downloads to be used with Overpass API and OSMnx python library.

Graph description	Query string
Walkable street network graph	<code>["area"!~"yes"]["highway"!~"trunk_link motor proposed construction abandoned platform raceway"]["foot"!~"no"]["service"!~"private"]["access"!~"private"]</code>
Additional graph of unwalkable street segments (e.g. service tunnels)	<code>["area"!~"yes"]["highway"!~"trunk_link motor proposed construction abandoned platform raceway"]["foot"!~"no"]["service"!~"private"]["access"!~"private"]["highway"~"service"]["layer"~-1 -2 -3 -4 -5 -6 -7"]</code>

3.3.3 Register based origin-destination (OD) commuting data

Census-based commuting data (T06_tma_e_TOL2008_2016_hel) was acquired for the study to enable public transport itinerary planning from homes to workplaces. The planned itineraries were needed for the assessment of pedestrians' exposure to traffic noise. The commuting data was produced by Statistics Finland and provided by the Finnish Environment Institute. In the data, commutes are reported by aggregated origin-destination (OD) flows between 250 m statistical grid cells covering the whole country. Essentially, a commuting flow for one OD (cell) pair is reported with one row in the data. The only pre-processing that was done for the data was extracting commuting flows that originated in the study area.

3.3.4 Online routing service of the local public transport authority

The online route planner service of Helsinki Region Transport (HSL) authority was utilized in planning public transport itineraries for the commutes. The service was accessed via its application programming interface (API) to allow efficient and reproducible itinerary planning. The planned itineraries were needed in two phases of the study: 1) in finding local (commuting-related) walks for the assessment of pedestrians' exposure to traffic noise and 2) in assessing the quality of the shortest paths calculated with the quiet path routing method in comparison to the reference paths (returned from the API).

3.4 Technical framework and architecture

The technical framework of the study is composed of several internal and external dependencies (Figure 12). Majority of the data analysis and the quiet path routing method were implemented in Python programming language. Thus, the main external dependencies of the study cover several Python libraries that were used in processing and analyzing statistical, geospatial and graph data (e.g. Pandas, GeoPandas, NetworkX and OSMnx). The used libraries and packages have also their own external dependencies which are now shown in the figure.

Modular design was favored in developing the methods as a Python project. This meant establishing common utilities to be used in different phases of the analysis as well as by the quiet path routing application. Functions were distributed into separate Python modules with distinct responsibilities to make finding and using them practical. A single Conda-environment was created to provide all Python libraries needed in the study, including the ones for the server-based quiet path routing application. The detailed technical description of the Python environment is attached as Appendix 1.

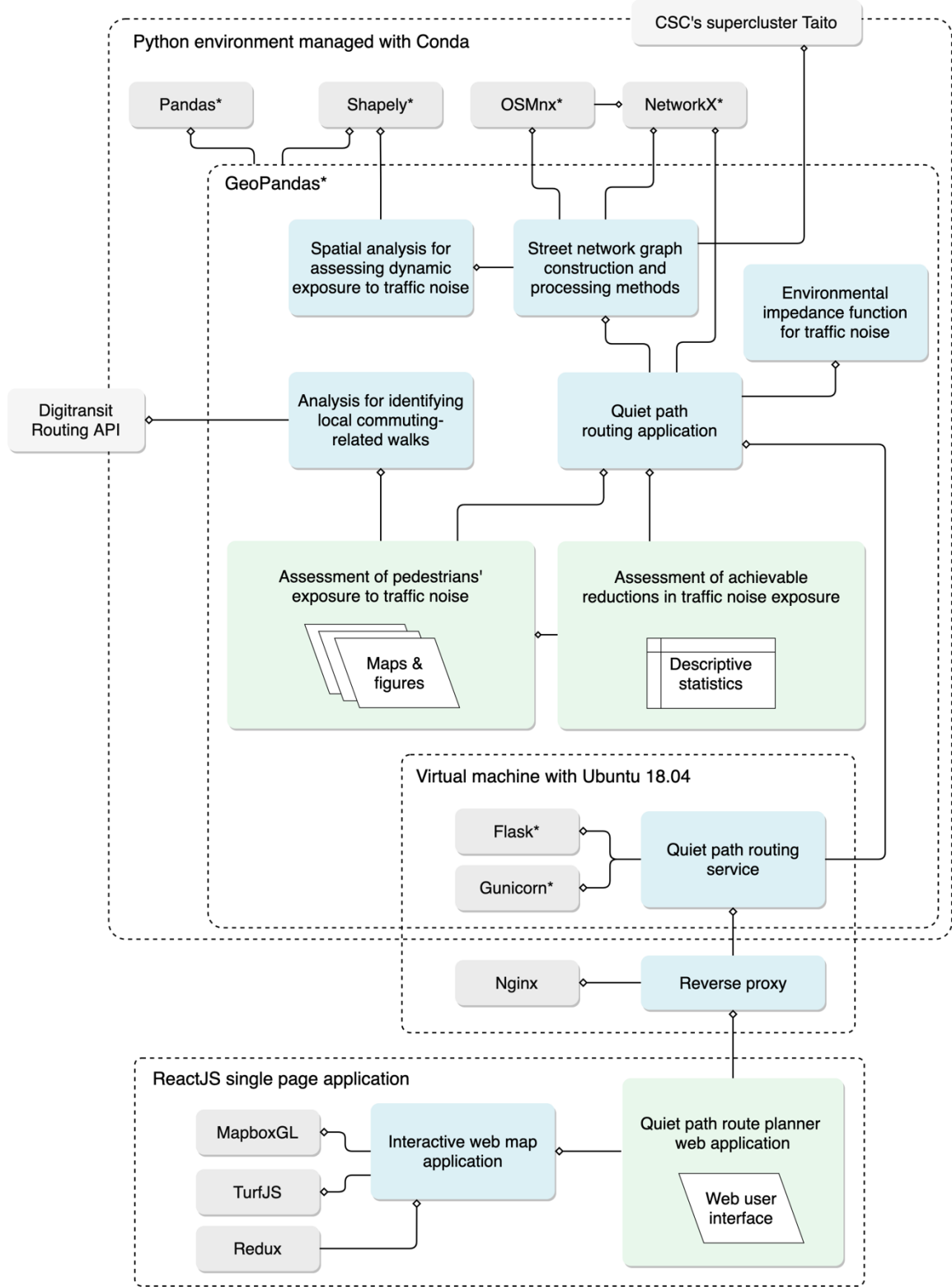


Figure 12. Technical framework of the study: internal (blue) and external (grey) technical dependencies (* = Python library). The several external dependencies of the used Python libraries are not included in the graph.

3.5 Quiet path routing method

3.5.1 Network acquisition and manipulation

The following three steps were included in acquiring and processing street network data to a graph suitable for noise exposure -based routing analysis:

- 1) Walkable street network data acquisition and graph construction (Figure 13).
- 2) Determining contaminated distances with different noise levels: spatially joining noise surface data to edges (Figure 14).
- 3) Calculating noise exposure -based costs to the graph with an environmental impedance function for noise (see chapters 3.5.2 & 2.5.3 and Figure 16).

The Python library OSMnx was used to download walkable street network data from OSM and to build a graph from it in NetworkX format (as described in chapter 3.3.2). OSMnx was also used to convert the directed graph to an undirected one, as street segments can be traversed to both directions by walking. Undirected graphs also require less computing power and memory for processing. After initial graph construction, straight line geometries were added to edges that were missing them, based on locations of the origin and destination nodes of the edges.

A temporary graph of unwalkable edges (e.g. service tunnels) was constructed in similar manner as the main graph but by using an edited query string (Table 2). The unwalkable edges were matched with the edges of the main graph by both *osm_id* and geometrical overlay analysis. Both matching methods were needed since *osm_id* is not guaranteed to be unique in all cases. The edges that were matched and identified as unwalkable were then removed from the graph. Finally, it was made sure that no inaccessible edges or nodes were left in the graph as subgraphs (due to lost connections between nodes).

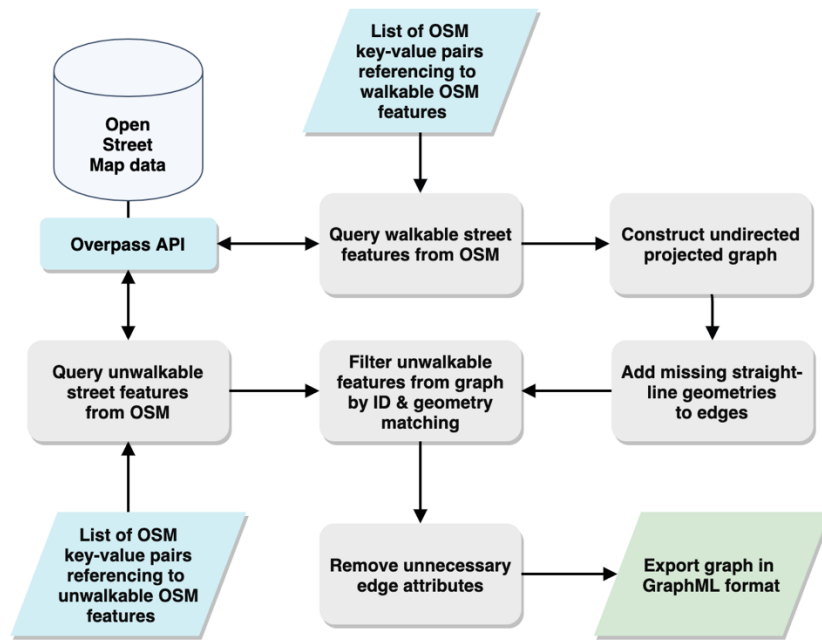


Figure 13. Workflow of street network graph acquisition and construction.

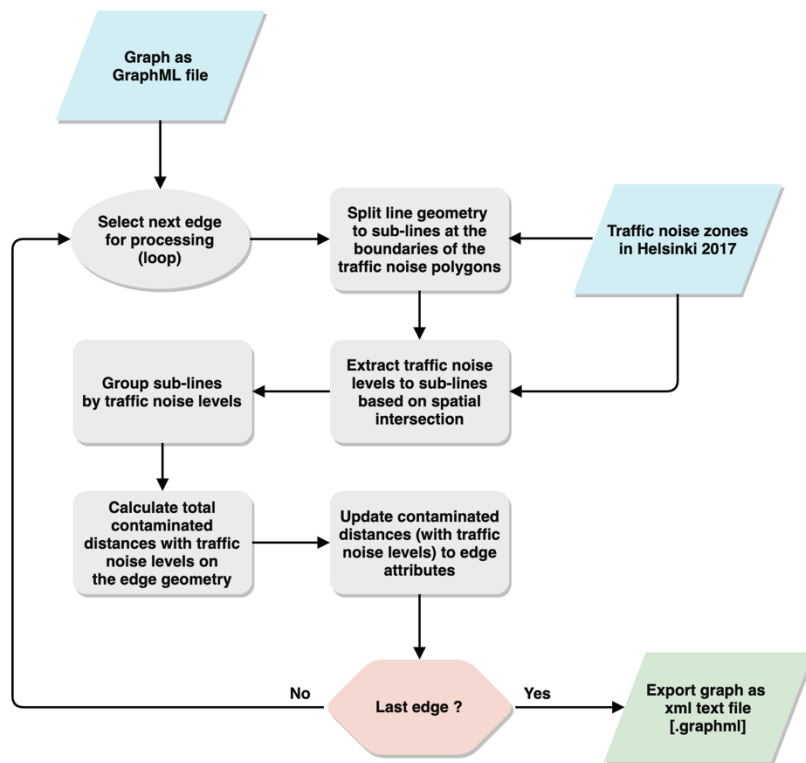


Figure 14. Workflow of extracting exposures to traffic noise (contaminated distances) to the edges of the graph.

A lossless spatial join of noise data (L_{Aeq}) to the edges of the graph was carried in three phases (Figure 14). First, the edge geometries were split at the boundaries of the traffic noise surfaces by intersection analysis. Second, underlying traffic noise data was extracted to the split edge geometries by their center point using vector-based point sampling in GeoPandas. Third, the split edges were aggregated by their original edge IDs and contaminated distances with different noise levels were added up for each edge. The result of the spatial join was validated by checking that the sum of the contaminated distances to different noise levels never exceeded the total length of the edge. This validation revealed the few topological inconsistencies in the noise surface data (see 3.3.1) and was fixed by only considering the maximum noise value when multiple values were sampled by a simple sampling point.

Due to the high number of edges (180647), a challenge of the spatial join was its high demand for computing power and high memory consumption. Hence, the first iteration of the analysis was run in CSC's (IT Center for Science Ltd.) supercluster Taito, where 20 processing cores and plenty of memory were reserved for the run. However, the Python implementation of the spatial join could be further optimized which allowed running it also on a normal desktop computer. The more efficient analysis included 1) using spatial indexing and GeoDataFrames, 2) organizing the edges as lists of edges (i.e. edge-chunks) and 3) processing the edge-chunks in parallel. The standard multiprocessing library of Python was used in the parallel processing. These means gave a significant performance boost compared to using the standard list iteration of Python and executing the spatial join one edge at a time.

3.5.2 Environmental impedance function

An environmental impedance function (EIF) for noise was designed to enable exposure -based routing analysis. The equation for calculating composite edge costs from length and dynamic noise exposure was defined as:

$$C_e = d_e + C_{en} \quad (1)$$

where C_e is the total composite cost of the edge; d_e is the length of the edge (i.e. base cost) and C_{en} is an additional noise exposure -based cost (by an EIF). In later parts of the thesis, the noise exposure -based cost is referred to as noise cost. The concept of contamination of distances (Ribeiro & Mendes, 2013) was applied in calculating the noise costs. However, instead of using a few fixed thresholds

(dB) in assigning the costs (as in Ribeiro & Mendes, 2013), the following EIF was developed to calculate them on a continuous scale:

$$C_{en} = \sum_{i=dB_{min}}^{dB_{max}} d_{dB_i} \times a_{dB_i} \times s \quad (2)$$

where dB_i refers to a 5 dB range from dB_i to $dB_i + 5$ dB (e.g. dB_{55} refers to the dB-range of 55 dB to 60 dB), d_{dB_i} is the total contaminated distance (m) with the dB-range dB_i (e.g. 14 m of dB_{55}) on the edge geometry, a_{dB_i} is a dB-specific noise cost coefficient and s is an arbitrary noise sensitivity coefficient (e.g. on range of 0.1 to 40).

Arguably, the critical, yet conceptually most challenging, component of the EIF is the dB-specific noise cost coefficient (a_{dB_i}). Ideally, the noise cost coefficient should reflect the perceived loudness and annoyance of a given L_{Aeq} . According to Guski et al. (2017), assessing exposure to A-weighted equivalent continuous sound level (e.g. L_{Aeq}) has been the standard metric in the studies on static noise exposure and annoyance. However, based on their review, no widely accepted linear or non-linear relationship seem to exist between A-weighted sound pressure level (SPL) and perceived loudness (or particularly annoyance), regardless of the several sound attempts to find one (e.g. Miedema & Oudshoorn, 2001). Furthermore, as the reviewed papers focus on static exposure (e.g. L_{Aeq} at home location), the applicability of their findings in assessing annoyance of dynamic traffic noise exposure is somewhat limited. Given this uncertainty on modelling loudness or annoyance by L_{Aeq} , two alternative functions were created for calculating the noise cost coefficients. First of the functions (3) assumes a linear relationship between loudness and L_{Aeq} and sets the noise costs on a (linear) range of 0.0 to 1.0 with respective L_{Aeq} (dB) range of 40 dB to 75 dB:

$$a_{dB_i} = \frac{dB_i - 40 \text{ dB}}{75 \text{ dB} - 40 \text{ dB}} \quad (3)$$

The second function (4) introduces a power law between loudness and sound pressure level based on what Parmanen (2007: 60) reformatted from widely used Stevens' power law (Stevens, 1960):

$$a_{dB_i} = 10^{\frac{0.3 * dB_i}{10}} \quad (4)$$

where dB_i is the lower limit of a 5-dB interval and the minimum dB_i is 40 dB. Despite having its basis in noise research, the applicability of the Stevens' power law is probably limited in this context since it was not originally designed to work with averaged A-weighted sound pressure levels (but with simple intensity metrics). The respective noise cost coefficients by both functions for dB_i values from 45 dB to 75 dB are presented in Table 3 and in Figure 15.

Equation 4 was selected for calculating the noise cost coefficients. The power law doubles the cost (loudness) roughly at every 10-dB increase, hence giving significantly higher costs to the highest noise levels. This could be seen as a desired feature of the function, as the highest noise levels (> 65 dB) are considered as most harmful to people. The power function may also be partially supported by interpretation of the nonlinear HA%/ L_{den} curves displayed in Figure 2 by Guski et al. (2017): a majority of the annoyance/SPL curves took the form "J" instead of a straight line, suggesting that an increase in SPL at higher noise level may have an amplified effect on the perceived annoyance compared to an equivalent increase in SPL at lower noise levels.

However, when both functions for noise cost coefficient were tested in developing the quiet path routing application, almost identical quiet paths options were found in most cases. It may be that the sensitivity index and the overall availability of alternative paths (between origin and destination) override the effect of the small differences in noise costs between the two noise cost functions. Uncertainties in noise-annoyance-loudness -relationships are considered further in chapter 5.6.

Table 3. Noise cost coefficients for dB range from 45 dB to 75 dB calculated with both equations presented in this chapter (3 & 4).

Traffic noise level (dB)	Noise cost coefficient (a_{dB_i})
	$\frac{dB_i - 40 \text{ dB}}{75 \text{ dB} - 40 \text{ dB}}$ (Eq. 3)
45–50	0.14
50–55	0.29
55–60	0.43
60–65	0.57
65–70	0.71
70–75	0.86
75–80	1.00
	$10^{\frac{0.3 * dB_i}{10}} / 100$ (Eq. 4)

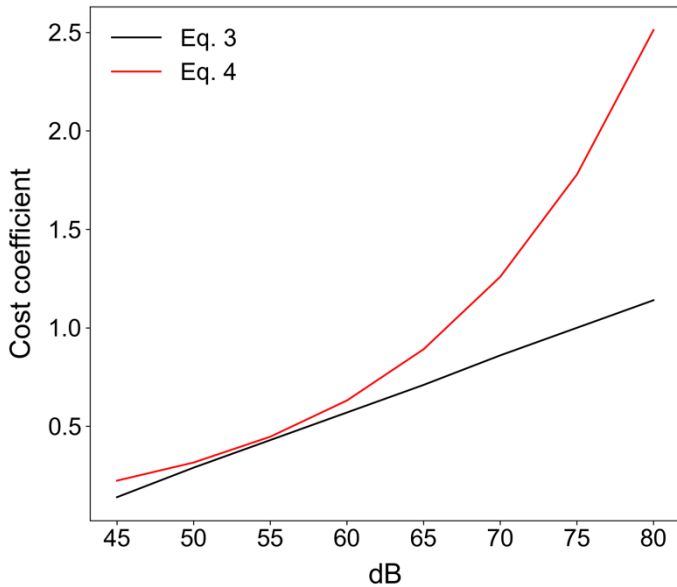


Figure 15. Noise cost coefficients for dB range 45–75 dB calculated with both equations presented in this chapter (Table 3).

3.5.3 Quiet path routing application

In this chapter, operation and main functions of the quiet path routing application are described. The developed application features three key capabilities: it optimizes shortest paths (1), it optimizes quiet paths (2) and it assesses dynamic exposure to noise on the paths (3). The operation of the application is delineated by explaining the sequence of actions that are executed during:

1. Starting the application (1–2)
2. Creating origin and destination nodes in the graph for one OD pair (3–7)
3. Solving a single short and quiet path routing problem (8–12)
4. Filtering out duplicate paths by length and geometry (13–14)

The application first loads a processed graph from a GraphML file to a NetworkX graph object (1) and then calculates noise exposure -based costs to edges attributes (2). The environmental impedance function for noise (see 3.5.2) is applied in calculating the noise costs from contaminated distances with different noise levels (Figure 16). Parallel noise costs are calculated by different noise sensitivity indexes. The final set of noise sensitivity coefficients that were selected for the quiet path routing application was defined as [0.1, 0.15, 0.25, 0.35, 0.5, 1, 1.5, 2, 4, 6, 10, 20, 40]. This set was found to provide an appropriate balance between performance and path variability. In most cases, multiple identical or nearly identical quiet paths were found, indicating that adding more sensitivity coefficients would not have resulted in finding more unique alternative (quiet) paths.

Calculation of the noise costs is not computationally very demanding and could hence be set to run at runtime (initialization) of the application as opposed to loading the costs from a static graph file. This setup facilitated testing of different variants of the environmental impedance function and noise sensitivity coefficients.

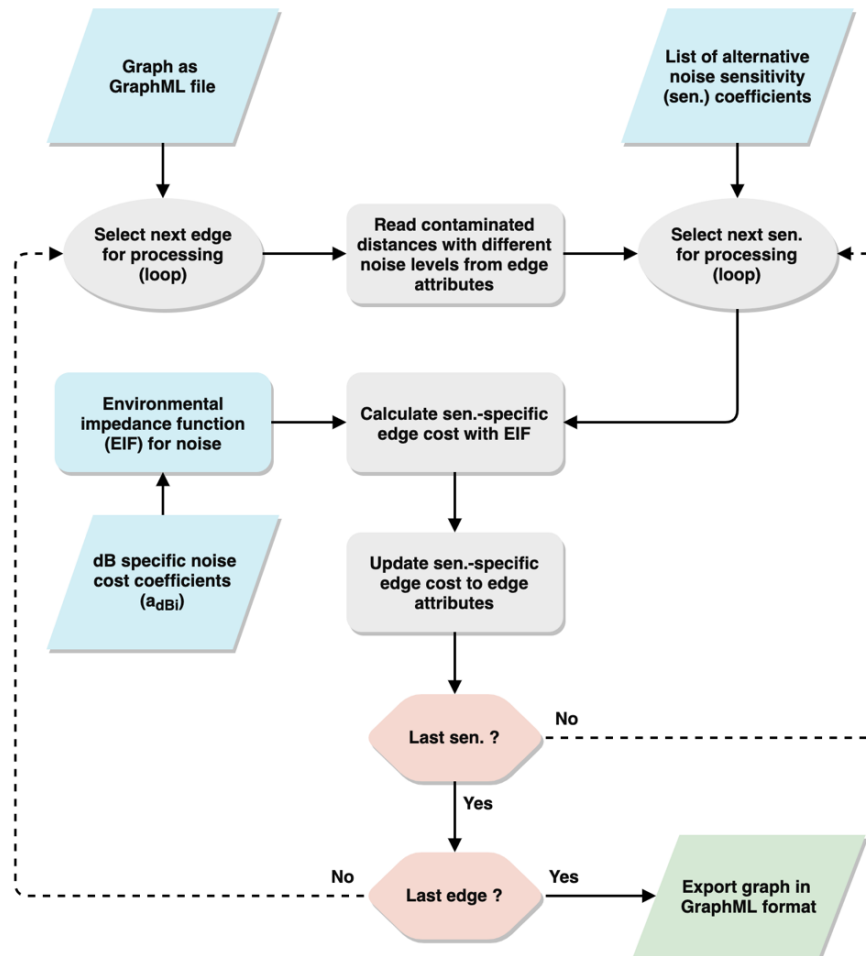


Figure 16. Workflow of calculating and adding noise sensitivity specific edge costs as new edge attributes.

To enable finding origin and destination nodes for a given OD pair fast, geometries of nodes and edges of the graph are collected to GeoPandas GeoDataFrames. The spatial indexes of the GeoDataFrames are used to quickly narrow down the candidates for nearest edge and node at a given location. Subsequently, the very nearest features are determined by using the geometrical distance functions from the Shapely package (3).

In most cases, the distance to the nearest edge is smaller than to the nearest node. Then, a new node needs to be created to the graph at the nearest point on the nearest edge (4). Subsequently, two linking edges need to be created to the graph to connect the newly created node to the origin and destination nodes of the nearest edge (5). Again, geometrical functions from the Shapely package are used in splitting the edge at the nearest point. Contaminated distances with different noise levels are then estimated for the linking edges as fractions of the contaminated distances of the nearest edge, by the ratio of the length of the linking edge to the length of the nearest edge (6). Then, noise costs (by different noise sensitivity coefficients) are calculated and updated to the edge attributes of the linking edges, allowing them to be used in the LCP analysis in the same way as all other edges (7).

The complete sequence of higher-level actions included in solving one quiet path routing problem is illustrated in Figure 17. As illustrated, after creating new nodes for origin and destination, LCP analysis is carried out to find the shortest and a set of quiet paths for the given OD. First, the shortest path is calculated by using length as the cost variable (8). Then, a set of quiet paths are calculated by the noise costs that were calculated to the graph when the application was started (9), resulting a collection of paths represented by sequences of node IDs. At this stage, the number of paths is equal to the number of noise sensitivity indexes. Then, the respective edges of the paths are fetched from the graph object by the sequences of node IDs (10). Subsequently, attributes of the edges are aggregated for each path. The line geometry of each path is constructed from the separate line geometries of its edges (11). Also, total lengths and contaminated distances with different noise levels and statistics on dynamic noise exposure (see chapter 3.5.4) are calculated from the aggregated edge attributes (12).

Finally, paths having unique geometry are filtered out from the full set of (quiet) paths. The filtering is done in two phases. First, the paths having exactly same length are filtered out (13). Then, a simple overlay analysis is performed to filter out paths with nearly identical geometries (14). For one path at a time, all paths that fall completely within a 30 m radius (buffer) around the path are collected. The collected paths must also have a length difference of less than 30 m. Then, the best path of the collection is determined by the normalized noise exposure index (see 3.5.4). Only the best path of the collection is retained, and others are discarded. Iterating the filtering results a set of fewer but geometrically more unique paths. One of the desired effects of this filtering step is to discard one of the two paths that use the same road but different sidewalks by it. Another one is to discard the path that uses the center line of a road if there is an alternative path using an adjacent sidewalk. The shortest path is also included in this filtering process, and hence may get “replaced” with a nearly identical quiet path.

Once the paths are fully processed, they are returned either as a GeoPandas GeoDataFrame or GeoJSON. The first format was used in the assessment of pedestrians' exposure to traffic noise and the second one in used in the web-based quiet path application programming interface (i.e. quiet path routing API). The attributes and schema of the short and quiet paths are described further in the next chapter (3.5.4) and in the documentation of the quiet path API (see 3.4).

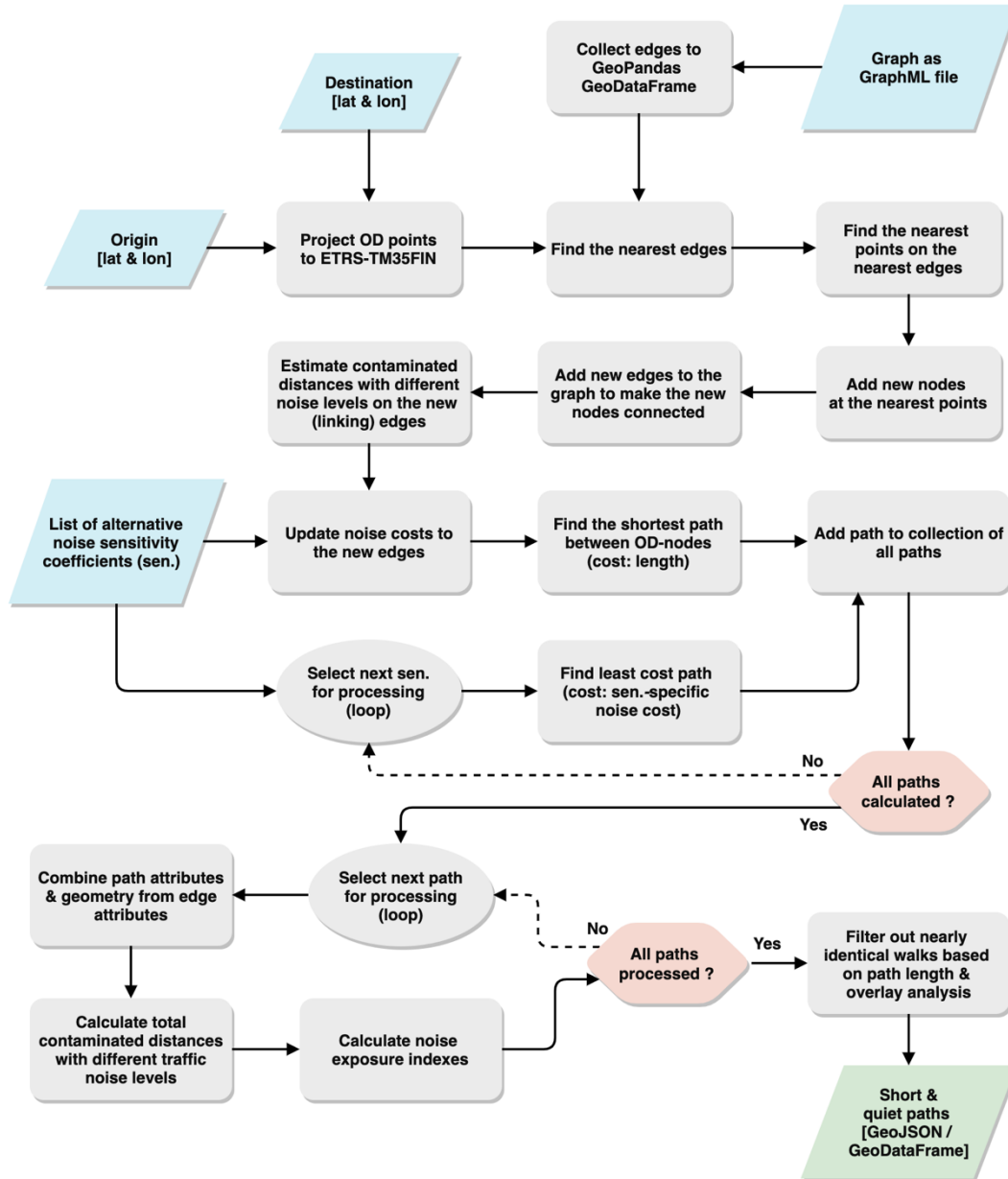


Figure 17. The sequence of high-level actions included in solving a regular pathfinding problem with quiet path routing application.

3.5.4 Noise exposure assessment of short and quiet paths

A set of metrics and indexes was developed for assessing dynamic exposure to traffic noise on short and quiet paths (

Table 4). The indexes defined in this chapter play a key role in comparing alternative quiet and short paths both in the web-based quiet path route planner and in the analysis of pedestrians' opportunities to reduce exposure to traffic noise (i.e. achievable reductions in traffic noise exposure). The challenge in developing such indexes was compressing the information from contaminated distances with different traffic noise levels (ED_{dB_i}) to simple but descriptive indexes of traffic noise exposure.

The simplest of the indexes (ED_{+dB_i} - Equation (6) describes the total cumulative contaminated distance (i.e. distance of exposure) with noise levels higher than a fixed threshold, for example the exposure to noise levels higher than 65 dB. Then, the ratio of ED_{+dB_i} to the total length of a path can be calculated as a *dB-specific noise exposure ratio* (ER_{+dB_i} - Equation (7)). This index can already be used to compare paths of different lengths, as it is distance normalized. The mean noise level (dB_{mean}) is calculated simply by adding up the products of contaminated distances and the respective noise levels and dividing the sum with the total length of the path (Equation (8)).

The environmental impedance function for noise (4) was applied to calculate a general *noise exposure index* (EI - Equation (9)). EI aims to model the total noise-related environmental impedance of a path. Only a simple form of the EIF was needed here, excluding the base-cost (length) and the noise sensitivity coefficient ($s = 1$). Also, a distance normalized version of the index was defined as *distance normalized noise exposure index* (EI_n - Equation (11)). It varies from 0.0 to 1.0, as it is calculated by dividing the noise exposure index of a path with the theoretical maximum noise exposure index of a path with equal length. Furthermore, the difference in EI can be calculated for a quiet path compared to the shortest path, to measure reduction in EI (Equation 10).

Table 4. The noise exposure indexes that were defined for measuring dynamic traffic noise exposure and reduction in noise exposure on quiet paths.

Metric	Equation	Description
Contaminated distance with noise level dB_i (m)	$ED_{dB_i} = d_{dB_i}$	(5) The total (cumulative) exposure to noise level dB_i on the path
Total contaminated distance with noise levels higher than dB_i (m)	$ED_{+dB_i} = \sum_{i=+dB_i}^{dB_{max}} ED_{dB_i}$	(6)
Percentage of total contaminated distance with noise levels higher than dB_i of the total path length (%)	$ER_{+dB_i} = \frac{\sum_{i=+dB_i}^{dB_{max}} ED_{dB_i}}{d} * 100$	(7)
Mean dB on the path	$dB_{mean} = \frac{\sum_{i=dB_{min}}^{dB_{max}} ED_{dB_i} * dB_i}{d}$	(8)
Noise exposure index (i.e. total noise-based environmental impedance)	$EI = \sum_{i=dB_{min}}^{dB_{max}} ED_{dB_i} \times a_{dB_i}$	(9) Similar to environmental impedance function (2) but without noise sensitivity coefficient ($s = 1$)
Reduction in noise exposure index (%)	$EI_{diff} = \frac{\Delta EI}{EI_s} * 100 = \frac{EI_q - EI_s}{EI_s} * 100$	(10) Reduction (%) in noise exposure index between short and quiet path
Distance normalized noise exposure index (index)	$EI_n = \frac{EI}{EI_{max}} = \frac{EI}{a_{max} * d} = \frac{EI}{a_{75dB} * d}$	(11) EI of the path normalized by dividing it with maximum theoretical EI for a path of same distance

$dB_i = 5$ dB range with dB_i as the lower value (e.g. 55 dB refers to noise range of 55–60 dB)

ED_{dB_i} = total contaminated distance with noise level of dB_i (e.g. 14 m of 55–60 dB noise)

a_{dB_i} = dB-specific noise cost coefficient (as in Equation 4)

3.6 Web-based quiet path route planner

A web-based quiet path route planner was developed as a proof of concept to demonstrate the potential utility of the quiet path routing method in practical situations. Also, it accelerated developing

and adjusting the quiet path routing method, as different variants of the street network graph and environmental impedance function could be easily tested.

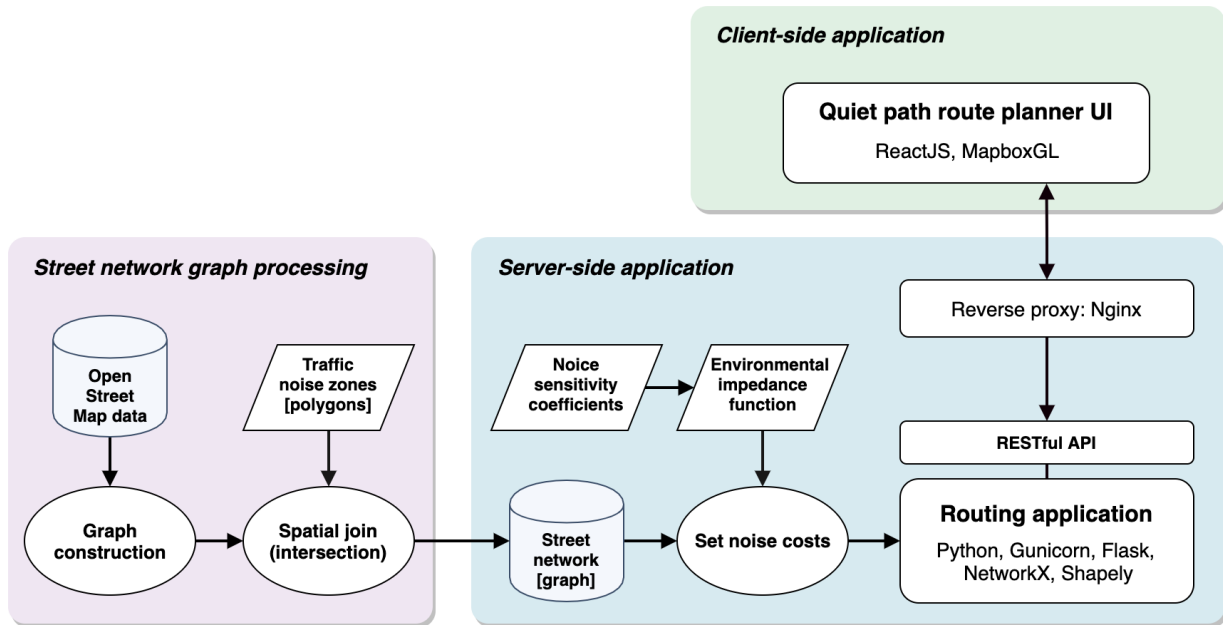


Figure 18. Technical architecture of the quiet path route planner web application.

The technical implementation of the quiet path route planner is composed of three components (Figure 18): graph processing for quiet path routing (1), server-side quiet path routing application (2) and client-side route planner user interface (3). The interface between the graph processing scripts and the routing application is a GraphML file. The client-side web application communicates with the routing application via a RESTful API exposed by the server application. The capabilities of the quiet path routing API are documented in more detail in the chapter 4.3.

A virtual machine was acquired for hosting the quiet path routing application as a stateless web service. The machine was provided by CSC (CSC - IT Center for Science Ltd.) with Ubuntu 18.04 operating system preinstalled. Again, a desired Python environment was installed with Conda package manager to match the development environment of the application. In addition to the normal scientific and geospatial Python libraries, the library Flask was installed to enable accessing the functionality of the routing application with RESTful web requests. Since Flask is not recommended for production environments, the library Gunicorn was configured to run the Python-Flask application in more efficient and secure manner. Practically, this meant running several instances of the application in parallel to be able to quickly handle many simultaneous routing requests. The web server application Nginx was installed and configured as a reverse proxy to handle all incoming and

outcoming connections to the machine. Finally, the server-side quiet path routing application (wrapped with Gunicorn) was configured as a system service and started.

An interactive web map application was developed to serve as the user interface for the quiet path routing service. It was implemented with ReactJS as a single page application (SPA). Mapbox GL JS was chosen as the web mapping library due to its great support for visualizing vector data interactively. Mapbox Studio was used to design a custom, light-colored, basemap to allow visualizing multiple paths with varying colors clearly on top of it. ReactJS SPA, as a technical framework, enabled building highly customized and reactive web map application for the purpose. Communication between the web map application and the routing service was implemented with asynchronous requests; after the routing request is sent from the client, a callback function (at the client) is invoked once the paths are returned from the routing service. The design and features of the user interface are presented in more detail in the results chapter (see 4.3 & 4.4).

During the making of this thesis, components of the web-based quiet path routing application, particularly the user interface, were developed iteratively based on the comments and suggestions from a small group of test users. Closer to the end of the thesis project, the focus in developing the routing application was guided also by the EU project Healthy Outdoor Premises for Everyone (HOPE). Thus, the support for assessing and minimizing exposure to also real-time air pollution was implemented in the routing application. Also, to enable significantly faster routing analysis for longer O-D distances, the routing analysis was converted to utilize graph library igraph (Csardi & Nepusz, 2006) instead of NetworkX. The links to the source-codes and further documentation of both versions of the routing application are presented in the results chapter (see 4.3, 4.4 & 4.6).

3.7 Assessment of pedestrians' exposure to traffic noise at a neighborhood level

3.7.1 Overview of the analysis

Pedestrians' dynamic exposure to traffic noise was assessed indirectly on a large-scale analysis. The assessment was composed of two parts:

- 1) Identification of origin (i.e. home) – PT stop (or commuting destination) walks and estimation of their utilization rates (Figure 19, chapter 3.7.2).
- 2) Assessment of pedestrians' exposure to traffic noise on the walks from origins to local PT stops or commuting destinations (Figure 20, chapters 3.7.3 & 3.7.4).

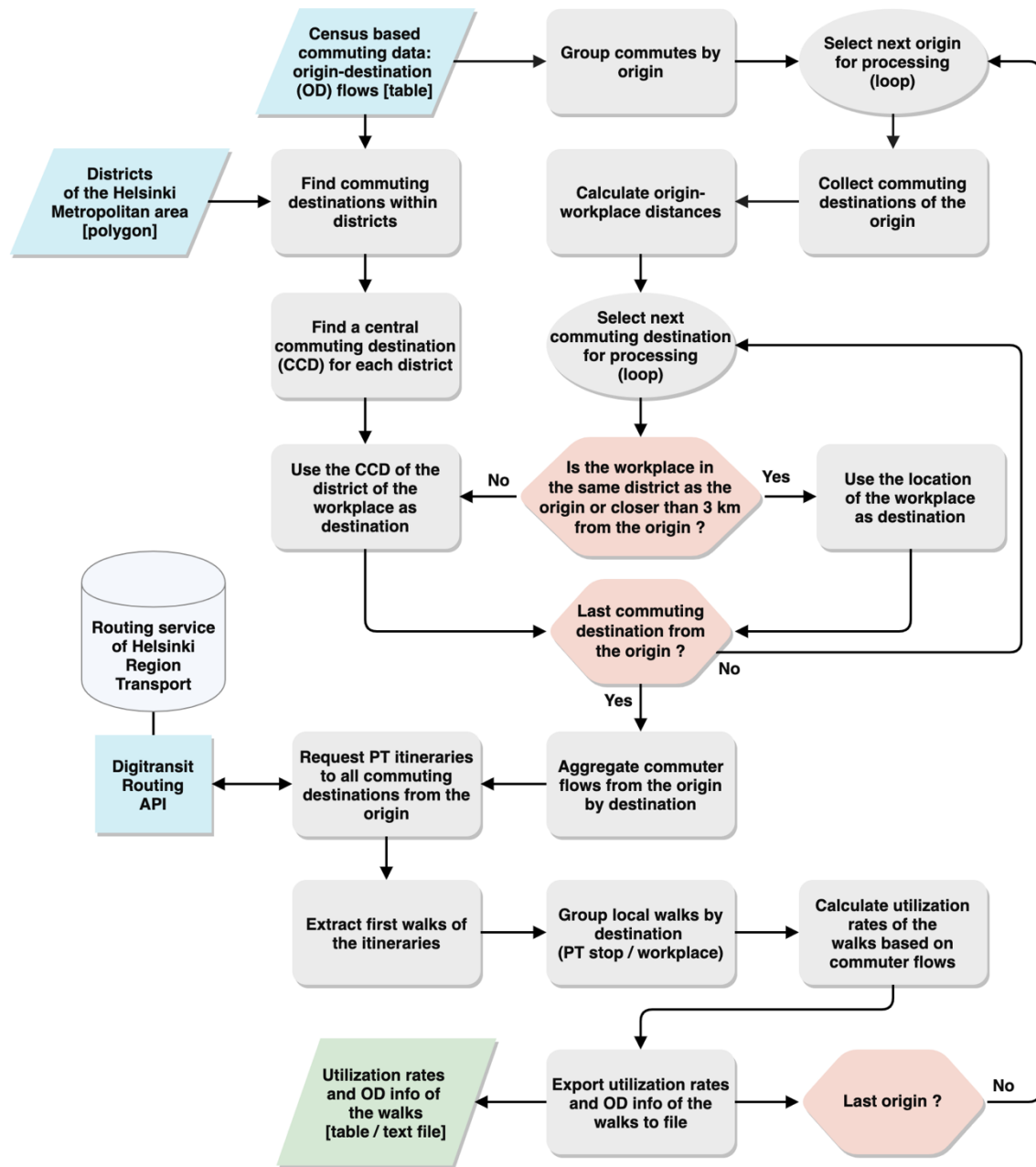


Figure 19. Workflow of the analysis for identifying origin – PT stop (or commuting destination) walks and estimating of their utilization rates based on commuter flows.

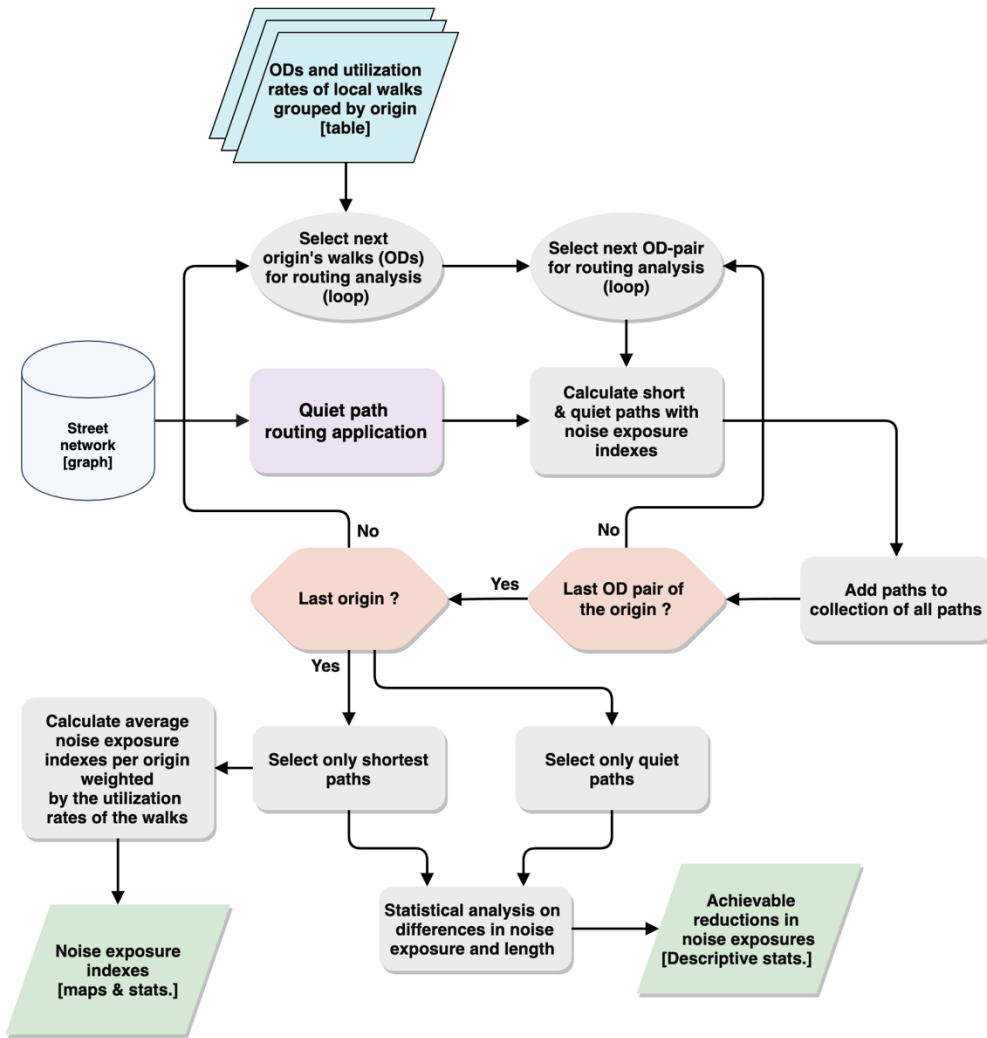


Figure 20. Workflow of the analysis for 1) calculating short and quiet paths by ODs of the local walks, 2) assessing exposures to traffic noise on the paths and 3) assessing achievable reductions in traffic noise exposure by taking quiet paths (see 3.8).

3.7.2 Estimation of local walks by commutes

In the following chapters, the word origin is used to refer to origins of commutes (i.e. home locations). Before the analysis, all commuting flows with origin in Helsinki were extracted from the YKR commuting data. Then, local walks to public transport stops (PT stops) or commuting destinations were identified as a result of an extensive routing analysis (Figure 19).

In this chapter, the necessary steps that were required for determining commuting destinations from one origin are described. The iteration of the full analysis is illustrated in Figure 19. The real commuting destinations (by the commuting data) were selected as destinations for all workplaces closer than 3 km from the origin. In order to limit the number of routing requests to Digitransit API,

distant commuting destinations (farther than 3 km from the origin) were aggregated by city districts. The centers of the districts were then used as the commuting destinations for the distant workplaces (Figure 21). The following sequence of GIS analysis was used to adjust the center of each district to better represent a “central workplace location” and to ensure that it is located in an accessible part of the street network:

- 1) Create a convex hull polygon by the commuting destinations of the district.
- 2) Calculate a center of gravity for the convex hull polygon.
- 3) Calculate distances from the commuting destinations (of the district) to the center of gravity.
- 4) Select the “central workplace location” as the commuting destination closest to the center of gravity.

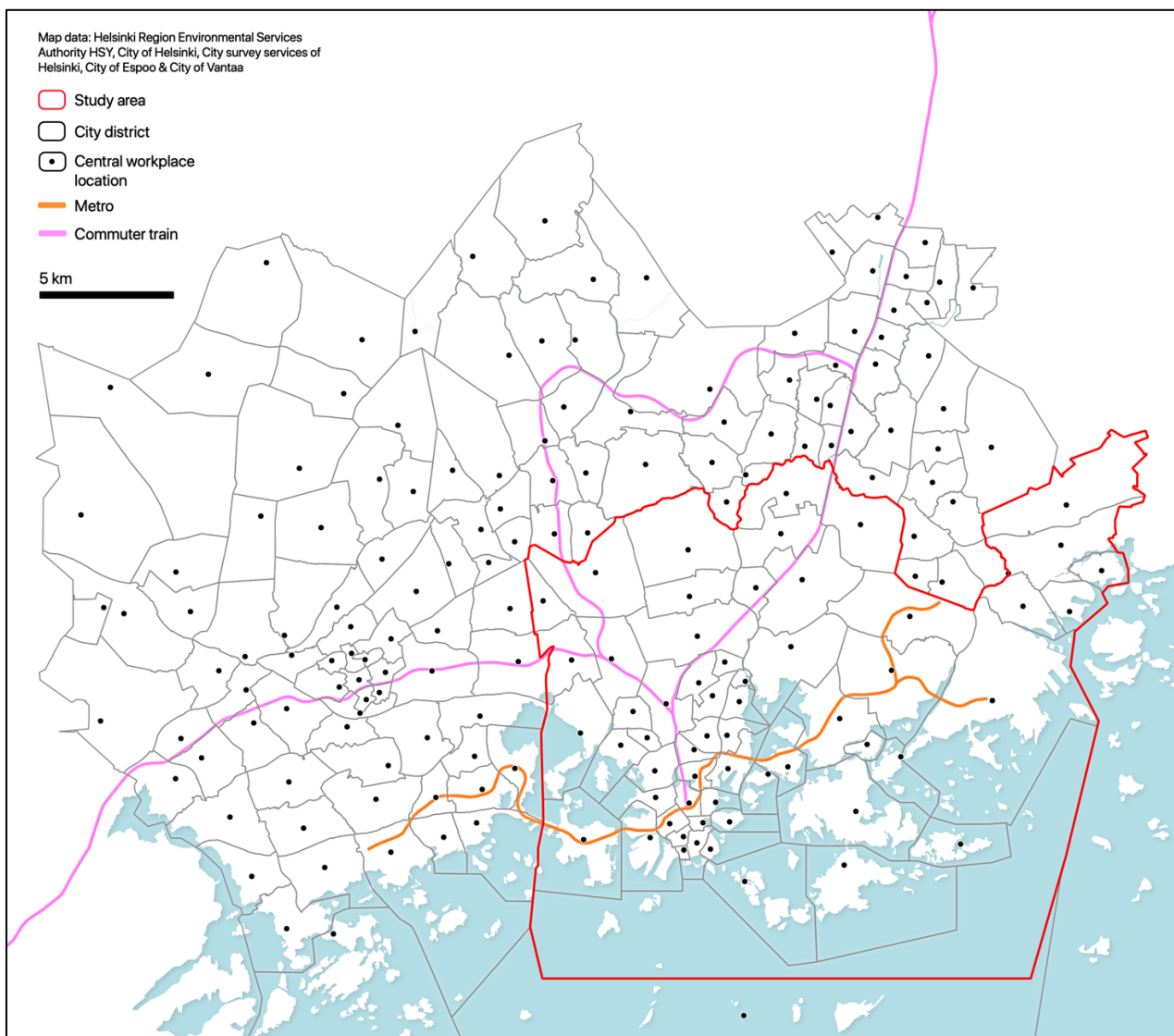


Figure 21. Extent of the itinerary planning analysis by commuting flow data. The point symbols represent “central workplace locations” within each city district.

For each origin-destination pair (commuting flow), three public transport itineraries were requested from Digitransit routing API. The open routing API is provided by the local public transport authority Helsinki Region Transport (HRT/HSL). In the routing requests, walking speed was set as 70 m/min (as in Jäppinen et al., 2013; Toivonen et al., 2014). Default values were used for other routing parameters to match typical user preferences (Table 5). In cases where the routing request did not result any itineraries, origin or target location was slightly adjusted in order to reach the underlying street network.

The resulting itineraries were aggregated by origin. The first walks of the itineraries were extracted and grouped by their destinations. Walks of two kinds were found: 1) walks from origins to PT stops and 2) direct walks from origins to commuting destinations. The walks from each origin were aggregated by their destination and combined utilization rates of the aggregated walks were calculated (Figure 22).

Table 5. Parameters used in routing with Digitransit routing API.

Parameter	Value
Origin	Center of the YKR grid cell
Destination	Destination of the commute
Date	Monday 8:30 am, 05/27/2019
Walking speed	70 m/min
Means of transport used	All except city bikes
Transfer safety margin	0 min
Number of itineraries to suggest	3

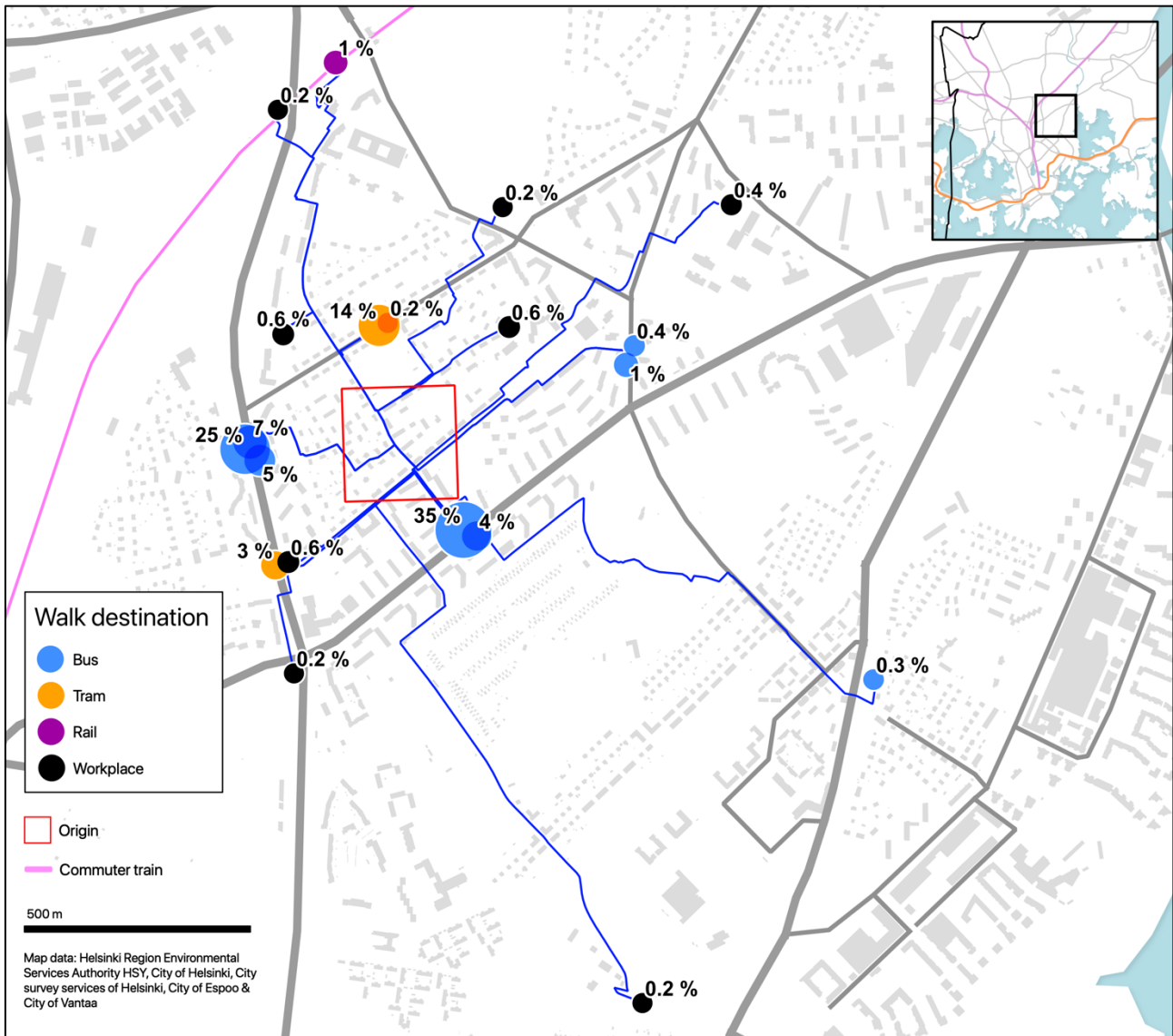


Figure 22. An example of local walks and their utilization rates from one origin as a result of the itinerary planning analysis. Most of the destinations of the walks are public transport stops.

In order to validate the results of the itinerary planning analysis, sums of the utilization rates of the walks were compared to the total flow of commutes from each origin by the original commuting flow data. Of the total number of commutes originating in the study area (296470), 83 % were included in the analysis. The mean inclusion of commutes per origin was 81% with a standard deviation of 14 %. The analysis performed well at most central and residential areas, but considerable share of the commutes from several remote and coastal areas were excluded, as illustrated in Figure 23. Comparing the number of commutes against the inclusion of the commutes (in the analysis) by origin revealed that the lower inclusion of commutes occurred mainly at origins with fewer commutes (Figure 24). Moreover, by further exploring the commuting statistics at origin-level, it was found that

of the origins with less than 50 % inclusion of commutes (in the analysis), none had more than 12 commutes in total.

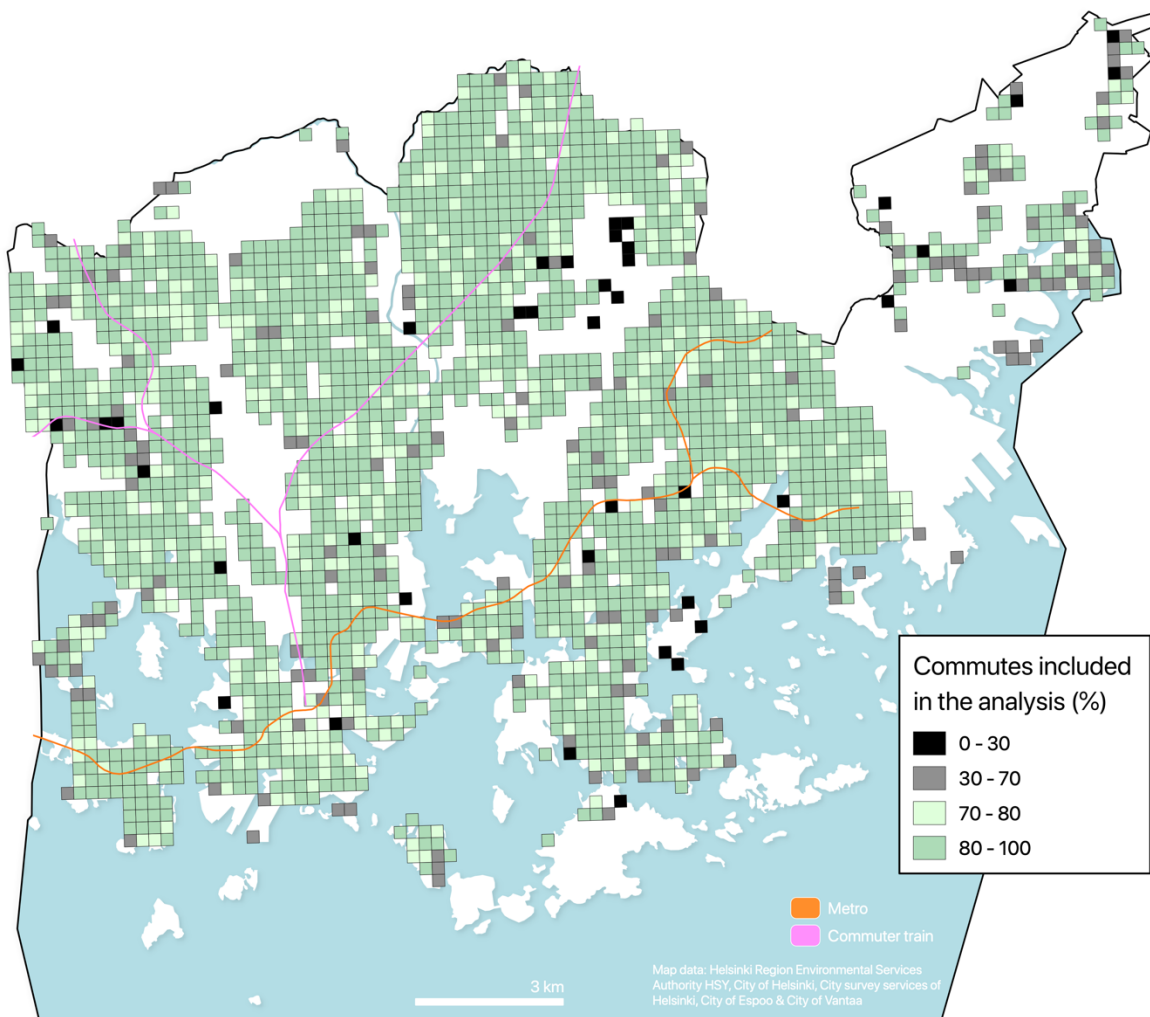


Figure 23. Inclusion (%) of commutes per origin in the itinerary planning analysis for finding local walks to PT stops and commuting destinations.

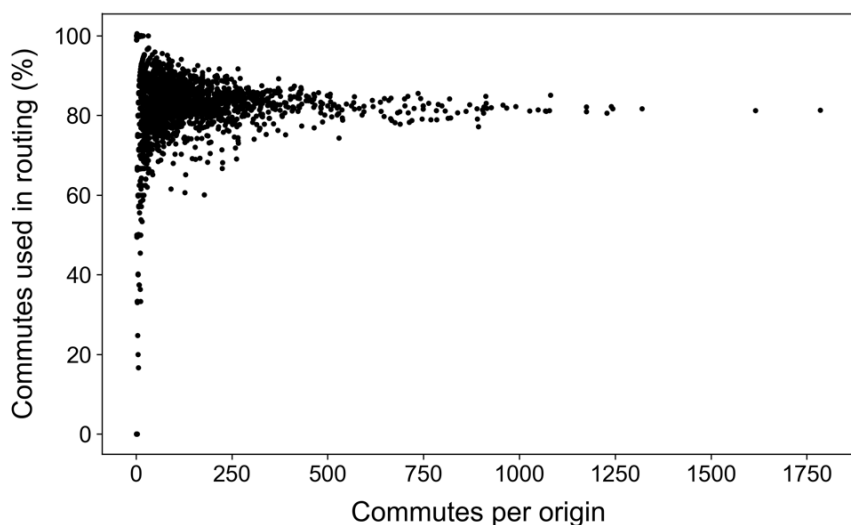


Figure 24. Number of commutes vs. commutes included in the routing analysis (%) per origin.

3.7.3 Least cost path calculations: short and quiet paths

Using the ODs of the local walks determined in the previous phases of the analysis, short and a set of quiet paths were routed for all walks with the quiet path routing application (see 3.5) developed in the study (Figure 20). The utilization rate of each walk was inherited as attribute information to the respective short and quiet paths. Once all paths were routed, descriptive statistics of the lengths of the shortest paths were calculated (Table 6). Figure 25 illustrates the spatial variation in the volume of the shortest paths.

Table 6. Descriptive statistics of the length of the shortest paths to PT stops and commuting destinations (n=31291).

Path length (m)	Mean	Median	SD	p10	p25	p75	p90
All (n=31291)	491	408	338	136	234	670	964
To PT stops (n=18716)	472	397	318	132	230	649	924
To workplaces (n=12575)	883	771	486	333	453	1209	1582

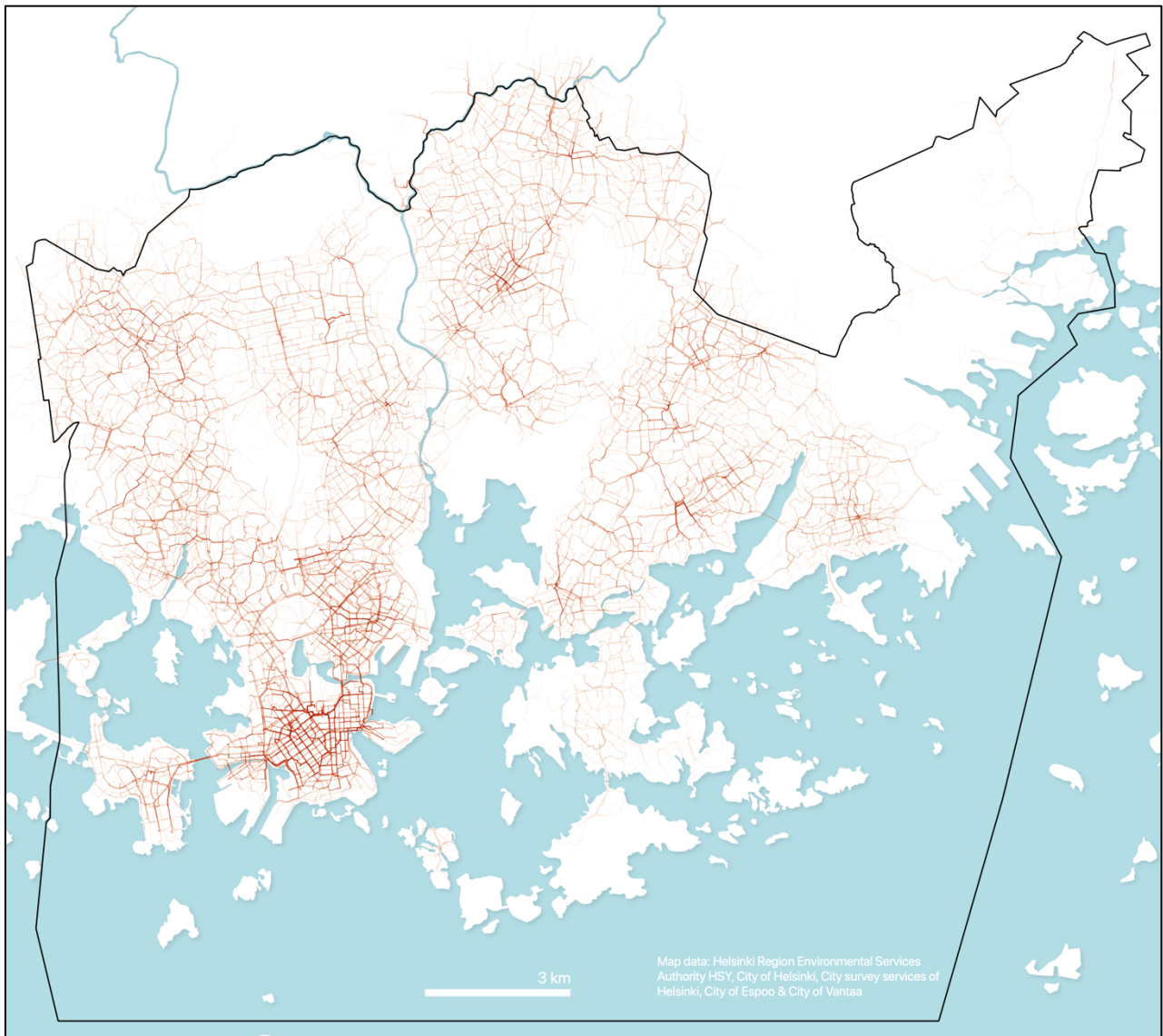


Figure 25. All shortest paths visualized with feature blending method: overlapping paths show darker on the map.

3.7.4 Assessment of exposures to traffic noise on the paths

As dynamic noise exposure assessment was already a built-in feature of the quiet path routing application, no separate analysis for determining exposures to traffic noise on the paths was needed. Yet, descriptive statistics for the noise exposure attributes (Table 4) of the paths were calculated and weighted by the utilization rates of the walks. The descriptive statistics were calculated separately for all paths and for a subset of only origin–PT stop paths (excluding origin – commuting destination paths).

Also, origin-level statistics of noise exposure indexes were calculated to enable exploring possible spatial patterns in the dynamic noise exposures. In this analysis, only the origin–PT stop paths were

included, to focus the assessment on the most local walks of the origins. Paths that were not completely inside the extent of the noise surface data were also filtered out in the analysis. The total utilization rates of the paths that were included in the analysis were added up per origin, to assess the statistical significance of the results (per origin). Again, the descriptive statistics were weighted by the utilization rates of the walks. Therefore, the (weighted) mean noise exposure index can indicate the expected noise exposure on a random walk from each origin.

3.8 Assessment of achievable reductions in exposure to traffic noise

Both shortest and quiet paths were calculated for 31291 commuting-related walks with the quiet path routing application (see 3.7). After filtering out paths that were outside the extent of the traffic noise data and a few other problematic paths, the achievable reductions in noise exposure were assessed for 12180 OD pairs having the shortest path in the length range from 300 to 1300 m. The achievable reductions in exposures were calculated per OD pair, by comparing different noise exposure indexes of the quiet paths to the corresponding indexes of the shortest path. The achieved reductions in noise exposures were evaluated with respect to the following properties of the paths:

- 1) Distance between origin and destination (O-D distance)
- 2) Noise exposure indexes of the shortest path
- 3) Length difference between quiet and shortest path

Two subsets of the paths (grouped by OD) were selected to assess the effect of the length of the shortest path (O-D distance) in the achievable reductions in noise exposure. Paths in the length range from 300 to 600 m were added to the first set (“short paths”) and paths in the length range from 700 to 1300 m to the second set (“longer paths”).

The reductions in noise exposures were measured against a set of thresholds for maximum length differences. The noise exposure indexes of each shortest path were compared to the noise exposure indexes of the corresponding quiet paths with maximum length difference of 100, 200 and 300 meters (respectively). Accordingly, for each OD pair, three metrics of achievable reductions in noise exposure indexes were calculated, one for each length difference threshold. Subsequently, descriptive statistics were calculated for all (achievable) reductions in noise exposure indexes by the maximum length difference thresholds (100, 200 and 300 meters). In addition, scatterplots of (achievable) reductions in exposures and length differences were made to explore the relationship between length difference and achievable reductions in noise exposures. Also, numbers of the quiet paths were

compared to the lengths of the shortest paths with scatterplots and boxplots - it was anticipated that more quiet path alternatives are found for longer shortest paths.

Another aggregation of the paths was done by selecting several subsets of the OD-level statistics by the exposure indexes of the shortest paths. Thus, the magnitude of the achievable reductions in noise exposures could be assessed also with respect to the initial noise exposures of the walks (by the shortest paths). Moreover, a simple linear regression analysis was carried out between the reductions in the exposure indexes and the initial values of the indexes (on the shortest paths). It was anticipated that for a higher noise exposure on a shortest path, also higher achievable reductions would be achievable on the respective quiet paths.

IV. RESULTS

4.1 Pedestrians' exposure to traffic noise

Table 7 and Table 8 represent both average exposures and variance in exposures to traffic noise on home – PT stop walks and on home–workplace walks, considering only the shortest paths. In Table 8, exposures on direct walks to workplaces are excluded from the statistics. The noise exposures on the paths were assessed by several noise exposure indexes (see 3.5.4). The noise level thresholds 60 dB, 65 dB and 70 dB were selected for the threshold-based indexes in order to assess exposures to the highest traffic noise levels. The statistics are weighted by the modelled utilization rates of the walks and hence better represent average exposures to traffic noise. The paths included in Table 8 were shorter, on average, than the ones in Table 7, as per the descriptive statistics of path lengths presented in Table 6 (see 3.7.3). Accordingly, the unnormalized noise exposure indexes show higher values (on average) for the longer paths (Table 7).

The average exposures to the highest noise levels are smaller compared to the exposures to the lower noise levels (e.g. ED_{+65dB} vs. ED_{+60dB}). On average, almost half (46 %) of the total distance of the walks is exposed to traffic noise levels higher than 60 dB (Table 7). Reduced, yet still remarkably high, average exposures were found for noise levels higher than 60 dB (e.g. 30 % mean ER_{+65dB}). However, high standard deviations of the exposure indexes indicate highly unequal exposures to traffic noise between different walks. For both EI, ED and ER indexes, excluding the highest noise level threshold (70 dB), the standard deviations of the indexes are of the same magnitude as their means (i.e. relatively high). The average traffic noise level on all walks is 58 dB but it varies considerably from quiet to noisy (SD = 7 dB).

Table 7. Descriptive statistics of exposure to traffic noise on the first walks of public transport itineraries to workplaces and on direct walks to nearby workplaces (n=30160).

Variable	Mean	Median	SD	p10	p25	p75	p90
EI	255	193	226	47	100	340	543
EI _n	0.31	0.29	0.17	0.1	0.19	0.41	0.52
dB _{mean}	58	58	7	48	52	63	67
ED _{+60dB} (m)	214	144	219	13	64	295	510
ED _{+65dB} (m)	137	75	178	0	21	179	352

ED _{+70dB} (m)	52	7	101	0	0	63	146
ER _{+60dB} (%)	47	42	33	4	19	74	100
ER _{+65dB} (%)	30	21	30	0	5	47	79
ER _{+70dB} (%)	11	2	20	0	0	14	36

Table 8. Descriptive statistics of exposure to traffic noise on the first walks of public transport itineraries to workplaces (direct walks to nearby workplaces are filtered out, n=17891).

Variable	Mean	Median	SD	p10	p25	p75	p90
EI	245	189	210	47	98	329	518
EI _n	0.31	0.29	0.17	0.1	0.19	0.41	0.52
dB _{mean}	58	58	7	48	52	63	67
ED _{+60dB} (m)	206	141	207	15	64	288	480
ED _{+65dB} (m)	131	74	166	0	21	173	335
ED _{+70dB} (m)	49	7	94	0	0	62	139
ER _{+60dB} (%)	47	42	33	5	19	75	100
ER _{+65dB} (%)	30	21	30	0	5	47	79
ER _{+70dB} (%)	11	2	20	0	0	14	36

4.2 Spatial patterns in pedestrians' exposures to traffic noise

Direct walks to workplaces were excluded in the spatial analysis of pedestrians' exposure to traffic noise. Therefore, the results represent average noise exposures on the most local walks from each origin. Figure 26 represents spatial variation in the mean walking distance from origin to (local) PT stops. Figure 27 represents mean traffic noise level (dB_{mean}) on the walks from each origin (for origin-level STD of dB_{mean}, see Appendix 4). Figure 28 and Figure 29 represent mean exposures (m) to traffic noise levels exceeding 65 dB(A) and 70 dB(A) thresholds (ED_{+65dB} & ED_{+70dB}). Respectively, Figure 30 and Figure 31 represent mean relative exposures (%) to traffic noise levels exceeding the thresholds as proportions of the total lengths of the paths (ER_{+65dB} and ER_{+70dB}). Choropleth maps of noise exposure index (EI) and normalized noise exposure index (EI_n) are attached only as Appendix

2 and Appendix 3, as they are conceptually more difficult but show mainly similar spatial patterns as ED and ER.

The choropleth maps represent mean traffic noise exposure indexes at origin-level, weighted with the estimated utilization rates of the walks. Thus, the concepts: 1) *average local walk*, 2) *typical local walk* and 3) *expected local walk* can be applied in interpreting the results. The three concepts aim to consider the spatial and statistical nature of the choropleth maps; as the indexes are weighted with the utilization rates of the walks, they can estimate the expected traffic noise exposure on an average (commuting-related) walk from each origin.

Some spatial patterns in the noise exposure indexes are visible on the maps. Exposure to the highest noise levels by dB_{mean} occur often on the walks from the origins near the major roads in the city. Similarly, the highest mean $\text{ED}_{+65\text{dB}}$, $\text{ED}_{+70\text{dB}}$, $\text{ER}_{+65\text{dB}}$ and $\text{ER}_{+70\text{dB}}$ appear often near the major roads of the city, but with considerable spatial variation. Some correlation between the average walking distances from the origins and the respective $\text{ED}_{+65\text{dB}}$ and $\text{ED}_{+70\text{dB}}$ indexes can be seen by visual comparison of the maps (Figure 26; Figure 28 & Figure 29). Exposures to the very highest noise levels are distributed unequally in the study area. For some neighborhoods (e.g. Itä-Pakila, Kruunuhaka and Koskela), the indexes $\text{ED}_{+65\text{dB}}$ and $\text{ED}_{+70\text{dB}}$ are considerably higher than the average of all walks (see Table 8). Despite that these indexes are likely to covary with the mean walking distances (as mentioned above), also the relative traffic noise indexes $\text{ER}_{+65\text{dB}}$ and $\text{ER}_{+70\text{dB}}$ show higher values in the same areas. For a substantial share of the areas (including the previously mentioned), the mean traffic noise level of the average walk is higher than 65 dB(A). Considering these findings, the results indicate that major dynamic exposures to unhealthy traffic noise levels are relatively common in the study area.

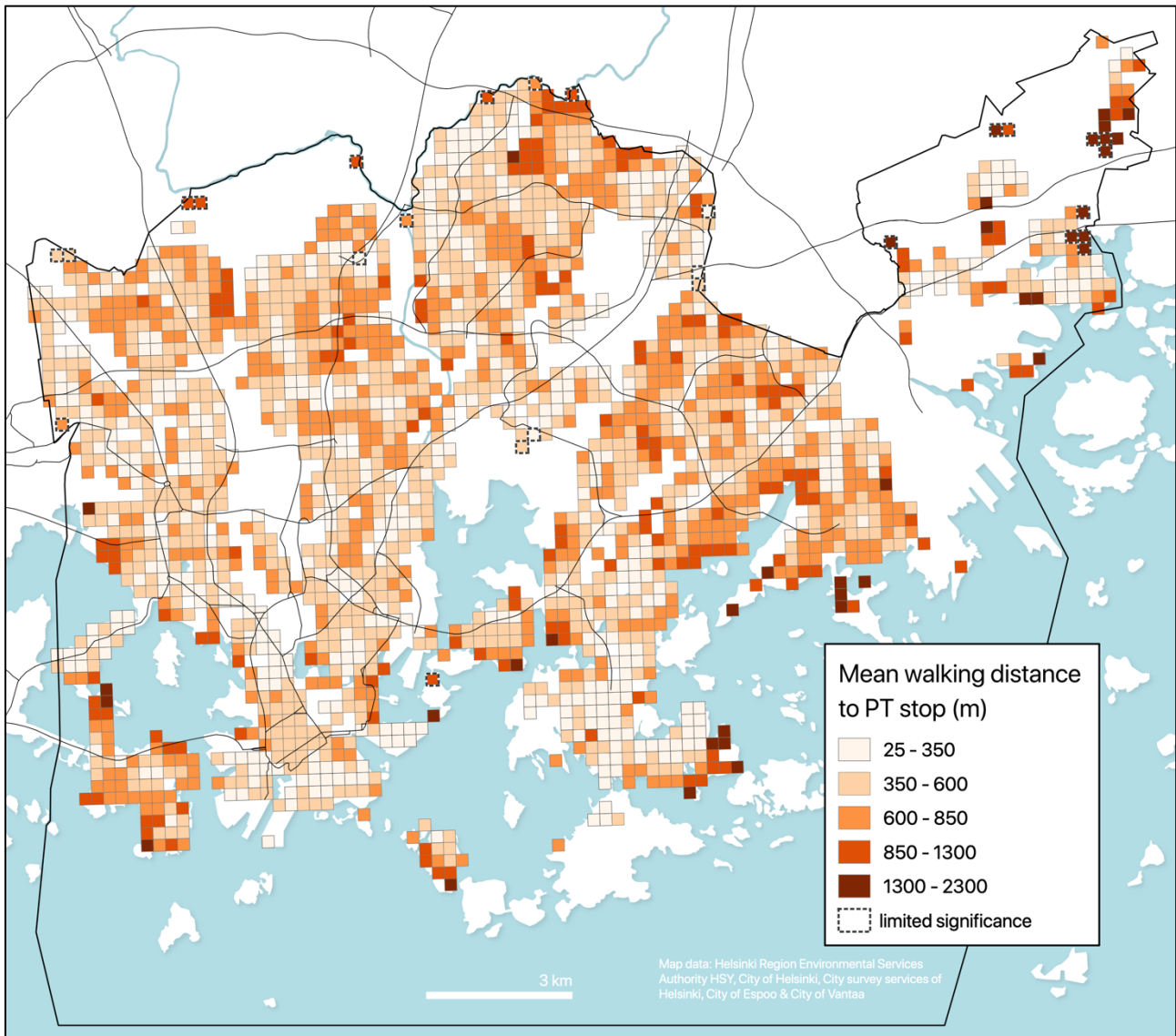


Figure 26. Mean walking distances from homes to public transport (PT) stops. The averages are weighted with the estimated utilization rates of the walks based on the total flow of commutes using each origin – PT stop pair.

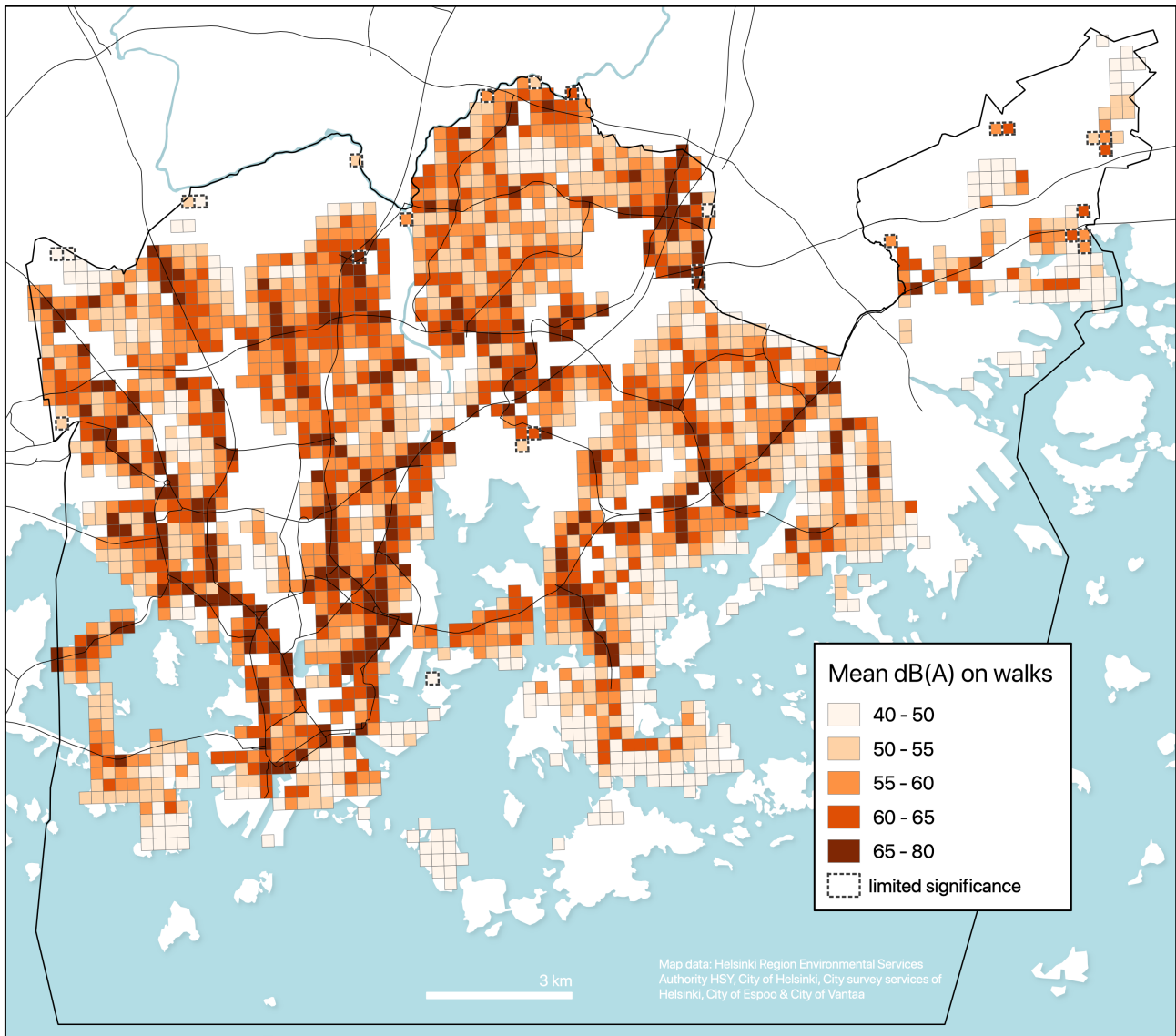


Figure 27. Mean traffic noise level (dB(A)) on walks from homes to PT stops. The averages are weighted with the estimated utilization rates of the walks based on the total flow of commutes using each origin – PT stop pair.

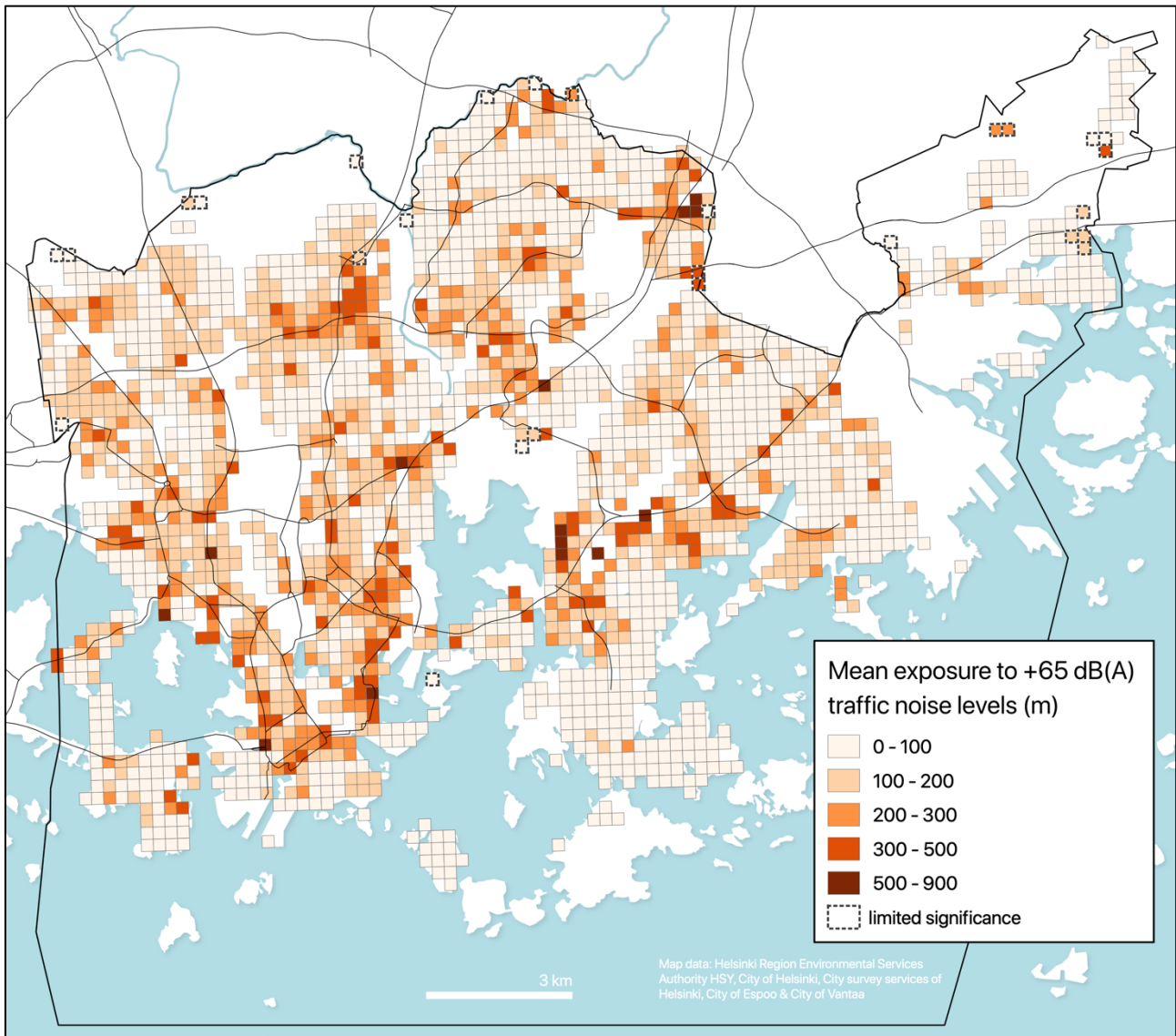


Figure 28. Mean exposures to +65 dB(A) traffic noise levels (m) on walks from homes to public transport (PT) stops. The averages are weighted with the estimated utilization rates of the walks based on the total flow of commutes using each origin – PT stop pair.

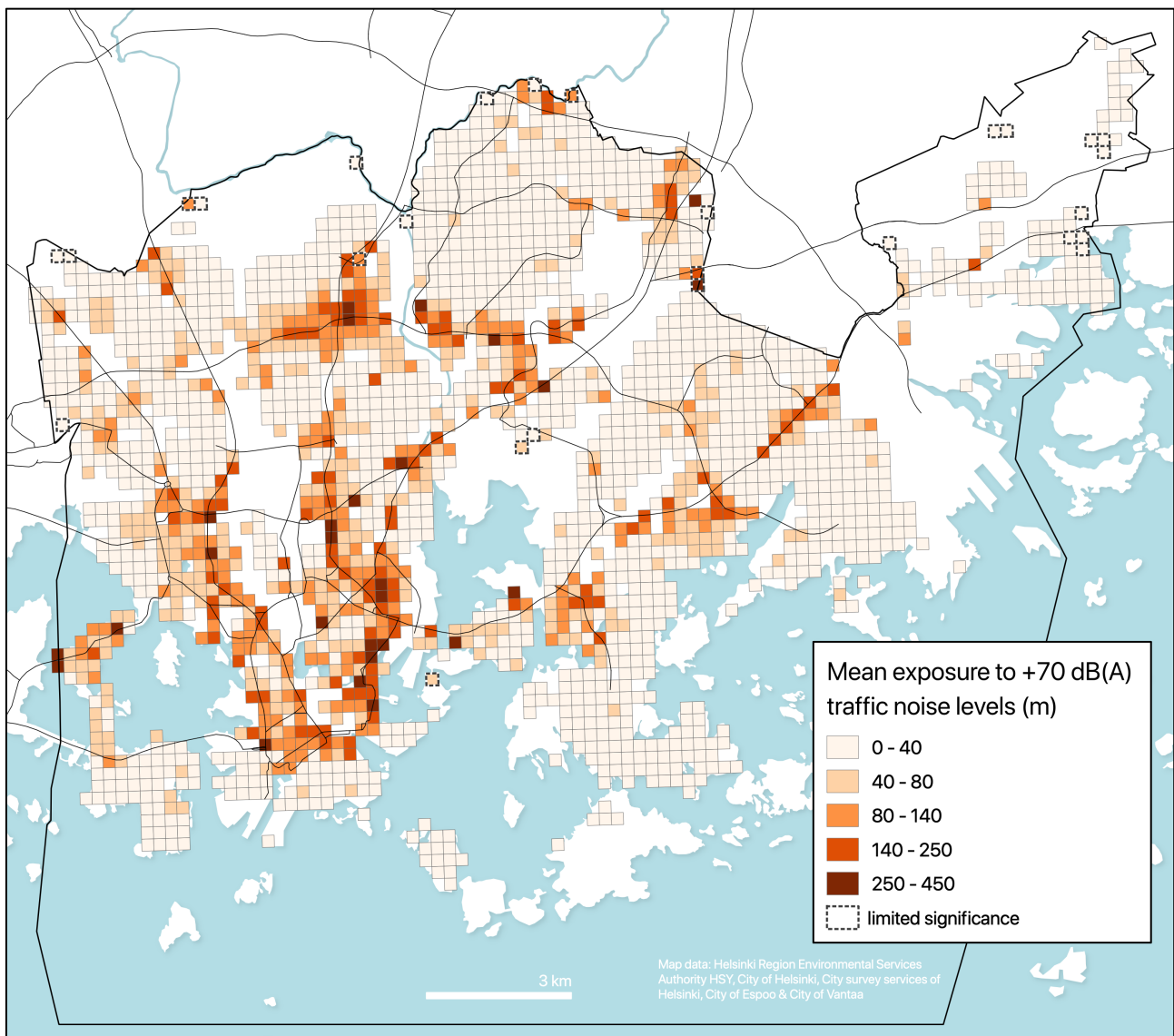


Figure 29. Mean exposures to +70 dB traffic noise levels (m) on walks from homes to public transport (PT) stops. The averages are weighted with the estimated utilization rates of the walks based on the total flow of commutes using each origin – PT stop pair.

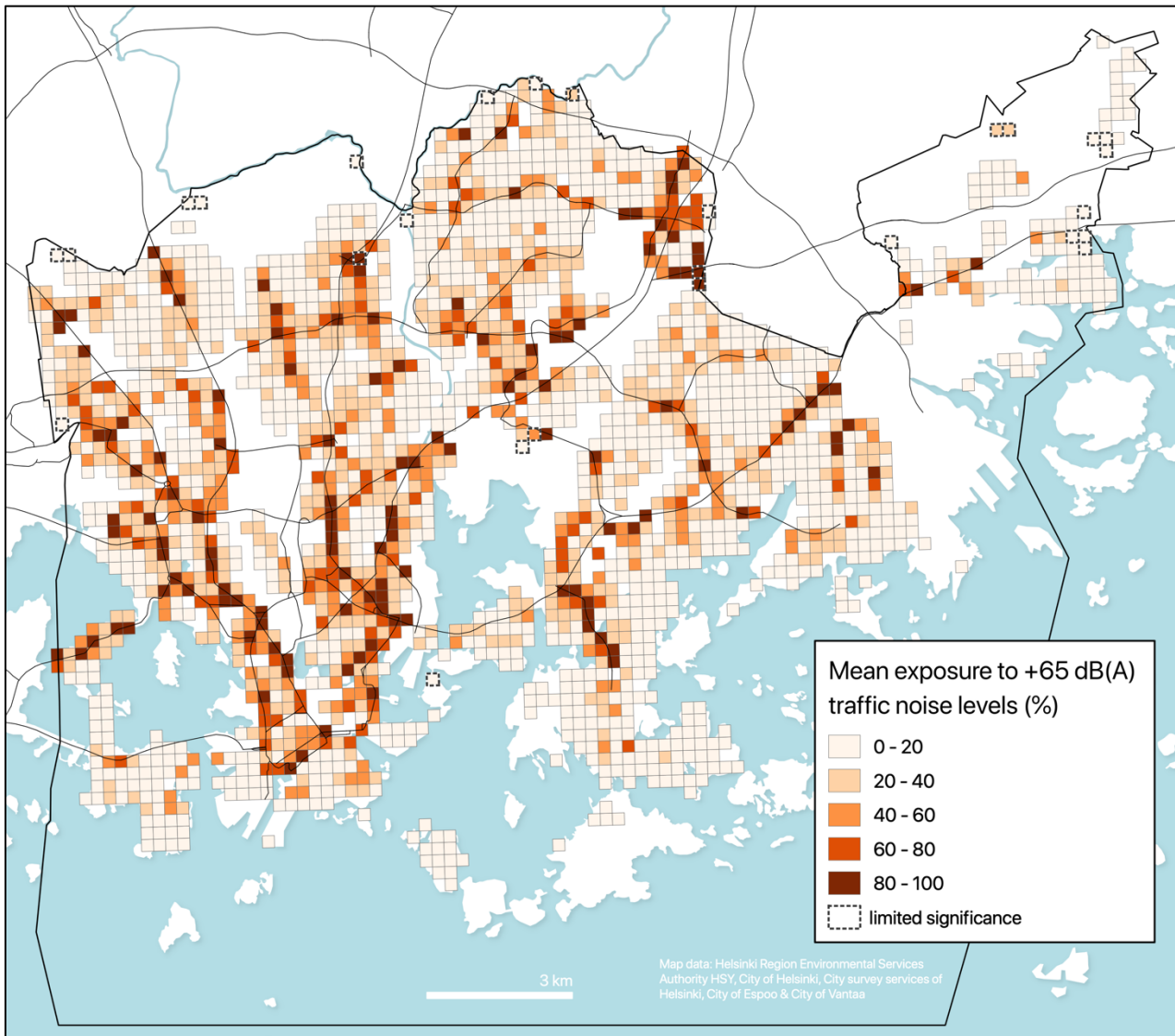


Figure 30. Mean exposure to +65 dB(A) traffic noise levels (%) on walks from homes to public transport (PT) stops. The averages are weighted with the estimated utilization rates of the walks based on the total flow of commutes using each origin – PT stop pair.

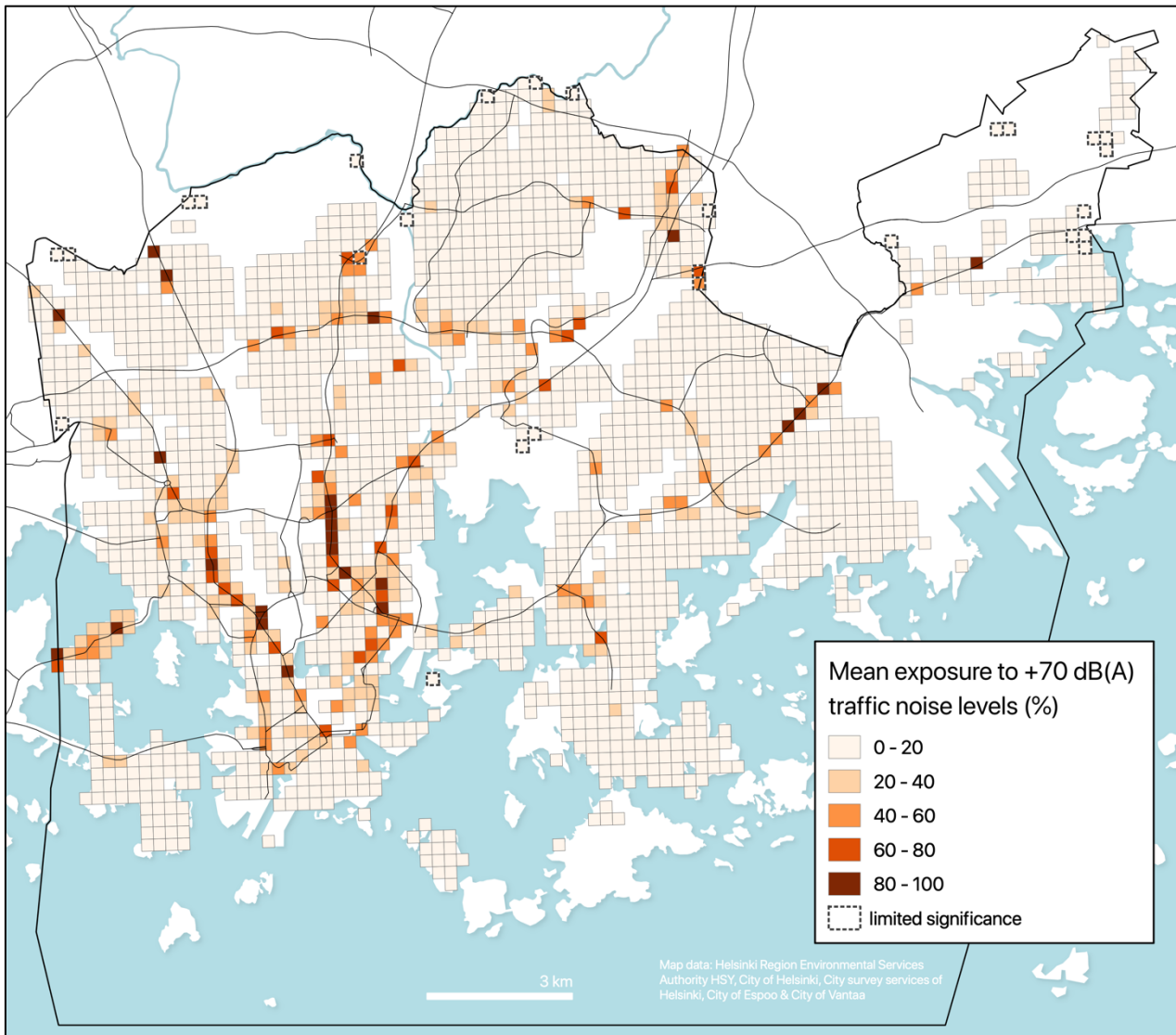


Figure 31. Mean exposure to +70 dB(A) traffic noise levels (%) on walks from homes to public transport (PT) stops. The averages are weighted with the estimated utilization rates of the walks based on the total flow of commutes using each origin – PT stop pair.

4.3 Quiet path routing API

At the time of writing this thesis, the web-based quiet path route planner service (3.6) is accessible via the quiet path routing API at www.greenpaths.fi/. The API is open and thus accepts requests over https from any client. The specific path for requesting quiet paths is www.greenpaths.fi/quietpaths/{origin}/{destination}. This endpoint expects the origin and destination in decimal coordinates in WGS84 coordinate system. For example, a valid request to the API is: greenpaths.fi/quietpaths/60.20772,24.96716/60.2037,24.9653.

The API responds to requests simply by returning either a collection of paths in the GeoJSON FeatureCollection format or a descriptive error message. The collection includes both shortest path and a set of quiet paths (if any were found). GeoJSON is a standard format for representing geographical features and their non-spatial attributes. It is an adaptation of the JavaScript Object Notation (JSON) format and can thus be easily used in a variety of data-interchange applications.

The returned short and quiet paths are equipped with several attributes on noise exposure and length (Table 9). Some of the attributes describe difference in noise exposure compared to the shortest path and thus have non-null values only for quiet paths. An example of a FeatureCollection of two paths is presented in

Table 10. Since the paths are given in a standard GeoJSON format, they can be easily viewed by common web mapping libraries and most desktop GIS applications (e.g. QGIS). More detailed documentation of the quiet path routing API can be viewed at:

https://github.com/DigitalGeographyLab/hope-green-path-server/blob/develop/docs/green_paths_api.md

Table 9. Descriptions of the path properties returned by the quiet path routing API.

Property	Type	Nullable	Description
type	string	no	Type of the path: either “short” or “quiet”.
id	string	no	Unique name of the path (e.g. “short” or “qp_0.2”). For quiet paths, the name is formatted as “qp_xx”, where xx is replaced with the noise sensitivity coefficient of the path.
length	number	no	Length of the path in meters.
cost_coeff	number	no	Noise sensitivity coefficient with which the quiet path was calculated.
len_diff	number	no	Difference in path length compared to the shortest path in meters.
len_diff_rat	number	yes	Difference in path length compared to the shortest path in percentages.
missing_noises	boolean	no	A boolean variable indicating whether noise data was available for all edges of the path (experimental attribute).
mdB	number	no	dB_{mean}
mdB_diff	number	yes	Difference in dB_{mean} compared to the shortest path.
nei	number	no	Noise exposure index (EI).
nei_norm	number	no	Distance-normalized noise exposure index (EI_n).
nei_diff	number	yes	Difference in noise exposure index (EI_{diff}) compared to the shortest path.
nei_diff_rat	number	yes	Difference in noise exposure index (EI_{diff}) as percentages compared to the shortest path.
noises	object	no	A dictionary containing contaminated distances with different noise levels. Keys of the dictionary represent noise levels (dB) and values distances in meters.

noise_range_exps	object	no	Exposures (m) to noise level ranges where noise levels exceeding 70 dB and lower than 50 dB are aggregated (separately). Keys represent noise levels and values distances (m).
noise_pcts	object	no	Relative exposures (%) to different noise level ranges (noise_range_exps). Keys represent noise levels and values shares.
noises_diff	object	yes	Exposures to different noise levels. Keys represent noise levels and values distances (m).
path_score	number	yes	Ratio of difference in noise exposure index to difference in length compared to the shortest path - i.e. reduction in noise exposure index per each additional meter walked.

The quiet path routing API allows anyone to query short and quiet paths in Helsinki and assess dynamic exposure to noise on the paths. Therefore, the routing API can facilitate both scientific dynamic noise exposure assessments and building route planner applications for people (both demonstrated in this study). However, due to the limited computing power of the current server setup, the recommended way to route large amounts of paths is to run a self-hosted instance of the quiet path routing application, as instructed in the documentation of the codebase (see 4.6).

Table 10. A FeatureCollection of two paths returned from the quiet path routing API.

```

Path_FC: {
  type: "FeatureCollection",
  features: [
    {
      geometry: { coordinates : [...], type: "LineString" },
      properties: {
        type: "short" ,
        id: "short" ,
        length: 5107.54,
        cost_coeff: 0,
        len_diff: null,
        len_diff_rat: null,
        missing_nosies: "false" ,
        mdb: 70.5,
        mdb_diff: null,
        nei: 3654.4,
        nei_norm: 0.72,
        nei_diff: null,
        nei_diff_rat: null,
        noises: { 45: 246.68, 50: 285.14, 55: 229.9, 60: 296.49,
                  65: 135.53, 70: 1782.62, 75: 2082.59 },
        noise_range_exps: {...},
        noise_pcts: {...},
        noises_diff: null,
        path_score: null
      type: "Feature"
    },
    {
      geometry: { coordinates : [...], type: "LineString" },
      properties: {
        type: "quiet" ,
        id: "q_0.2" ,
        length: 5189.25,
        cost_coeff: 0.2,
        len_diff: 81.7,
        len_diff_rat: 1.6,
        missing_nosies: "false" ,
        mdb: 61.3,
        mdb_diff: -9.2,
        nei: 2126.5,
        nei_norm: 0.41,
        nei_diff: -1527.9,
        nei_diff_rat: -41.8,
        noises: { 45: 1196.12, 50: 194.09, 55: 204.74, 60: 622.92,
                  65: 1081.62, 70: 1452.68, 75: 103.07 },
        noise_range_exps: {...},
        noise_pcts: {...},
        noises_diff: { 40: 0, 45: 949.44, 50: -91.05, 55: -25.16, 60: 326.43,
                      65: 946.09, 70: -329.94, 75: -1979.52 },
        path_score: 18.7
      type: "Feature"
    },
    {...}, {...}, ... ]
  }
}

```

4.4 Quiet path route planner

At the time of writing this, the interactive web map user interface (UI) of the quiet path route planner is accessible at: <https://green-paths.web.app/>. To facilitate testing and using the application in real-life (i.e. real-time) situations, namely on mobile phones, both Responsive Web Design (RWD) and mobile-first principle are applied in the design of the UI. Figure 32 represents a basic user story covering the typical sequence of actions for requesting, receiving and comparing route suggestions for one pathfinding problem. Since the main objective of the route planner application was to serve as a proof of concept of the quiet path routing method, only the most essential functionalities were implemented. Hence, for example, address geocoding functionality is not supported but the user can select the origin and destination only from the map. However, some minor features and functionalities are implemented in the UI to improve the overall user experience (Table 11).

To make the application more intuitive to use, most of the noise exposure indexes (see 3.5.4) are not shown in the UI as they would have required additional explanations. Instead, dynamic exposures to different traffic noise levels are visualized with dB-specific colors both on the map and in the list of paths. In the list, the ratios of the exposures to different traffic noise levels (%) are visualized as a colored bar chart. For quiet paths, the difference in traffic noise exposure index compared to the shortest path (EI_{diff}) is presented simply as reduction (%) in *noise*.

Figure 33 and Figure 34 represent the quiet path route planner in two practical situations. In the first figure, only two paths are shown for the OD pair. In the third picture of the first figure, a quiet path has been opened from the list and more detailed noise exposure information is shown for the path:

- 1) Exposures to different traffic noise levels (%) as colored bar charts for both the opened (quiet) path and the shortest path.
- 2) Durations of exposure to different traffic noise levels on the opened (quiet) path.

In Figure 34, routing was performed for a longer OD-distance, resulting more alternative quiet paths. To reduce the number of the displayed paths, user can select a maximum length for the paths via the filter button (third picture in Figure 34).

Table 11. Minor features and functionalities of the route planner UI that aim to improve the overall user experience of the application.

Trigger	Action
---------	--------

User clicks the “Find quiet paths” -button and routing is started	Map zooms automatically to fit both origin and destination in the view
User selects “Use current location” as origin	Map zooms automatically to user location
Routing results multiple quiet path alternatives of which some are calculated with high noise sensitivity coefficient	Longest quiet paths are filtered out by default if they were calculated with high noise sensitivity coefficient (user can show them by disabling filtering by length from the filter-button)
Routing results include quiet paths that are only slightly longer than the shortest path	The shortest quiet path is automatically selected if it is only slightly longer than the very shortest path
Path is selected from the map by clicking	The list of paths automatically “jumps” to display the selected path
An error occurred during routing	A descriptive error message is shown, e.g. “Error in routing”
User selects an origin or a destination outside the supported area	The UI prevents routing and shows an error message “Origin [or destination] is outside the supported area”
User is trying to select a path from the map on mobile device but does not click directly on the path	A small search radius is used when selecting paths from the map to ease selecting paths on mobile phones (i.e. without a mouse)
User changes the orientation of the mobile device (i.e. to landscape or portrait mode) or switches to a device of different size	The UI reacts to the dimensions of the screen in order to show practical layout on devices of any sizes (especially on mobile)
User triggers the “add to home screen” functionality of the web page in the browser of a mobile device	The web application is added to the “home screen” of the user’s phone. When opened from home screen, the application can be used similarly as installed apps: it runs in full screen mode without address and bookmark bars of the browser (see Figure 35) and avoids the need to be refreshed. This feature is enabled by specific HTML meta tags and a custom-made “app icon”.

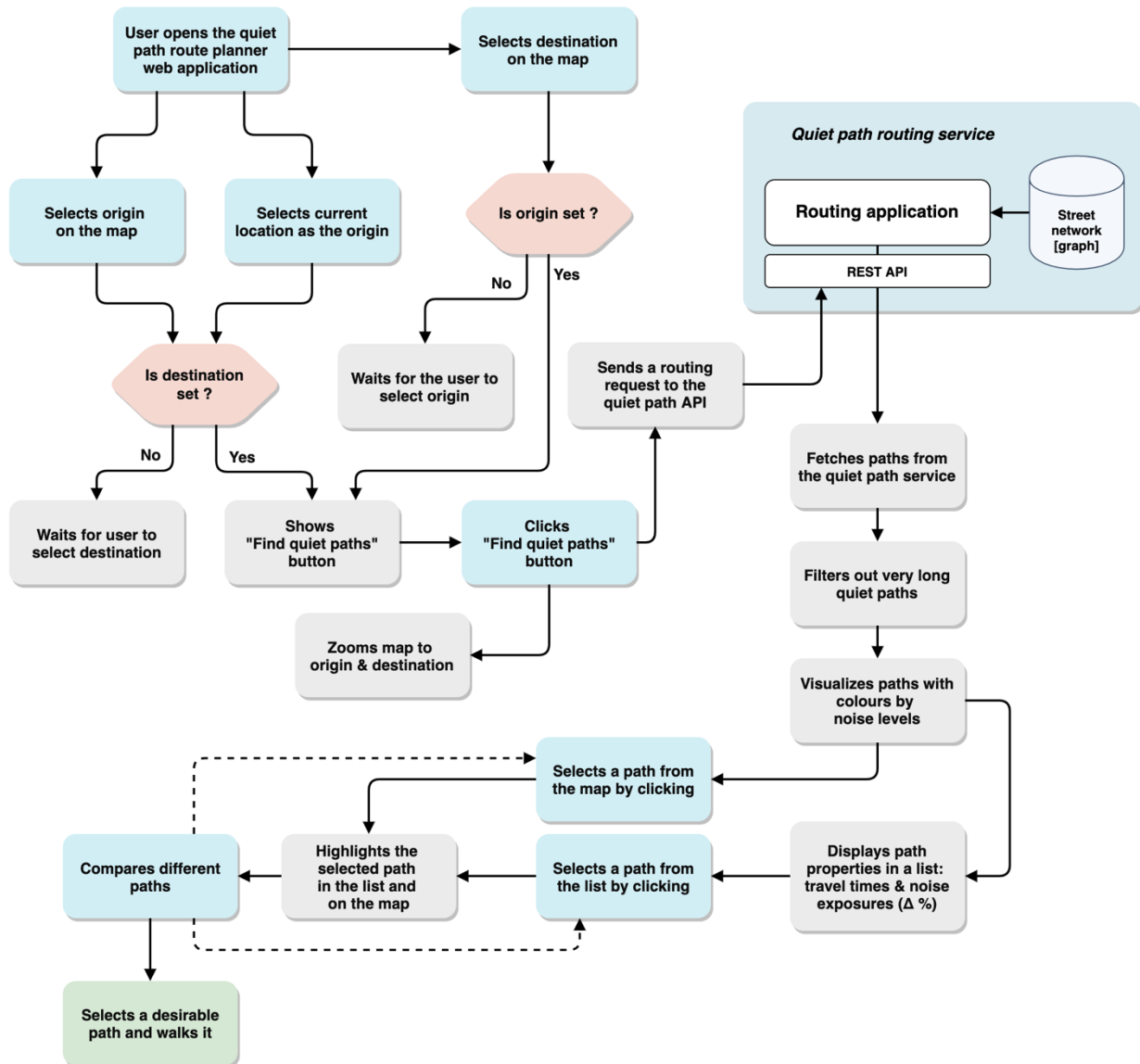


Figure 32. A typical sequence of actions included in solving one pathfinding problem from the perspective of the route planner application (grey) and user (blue).

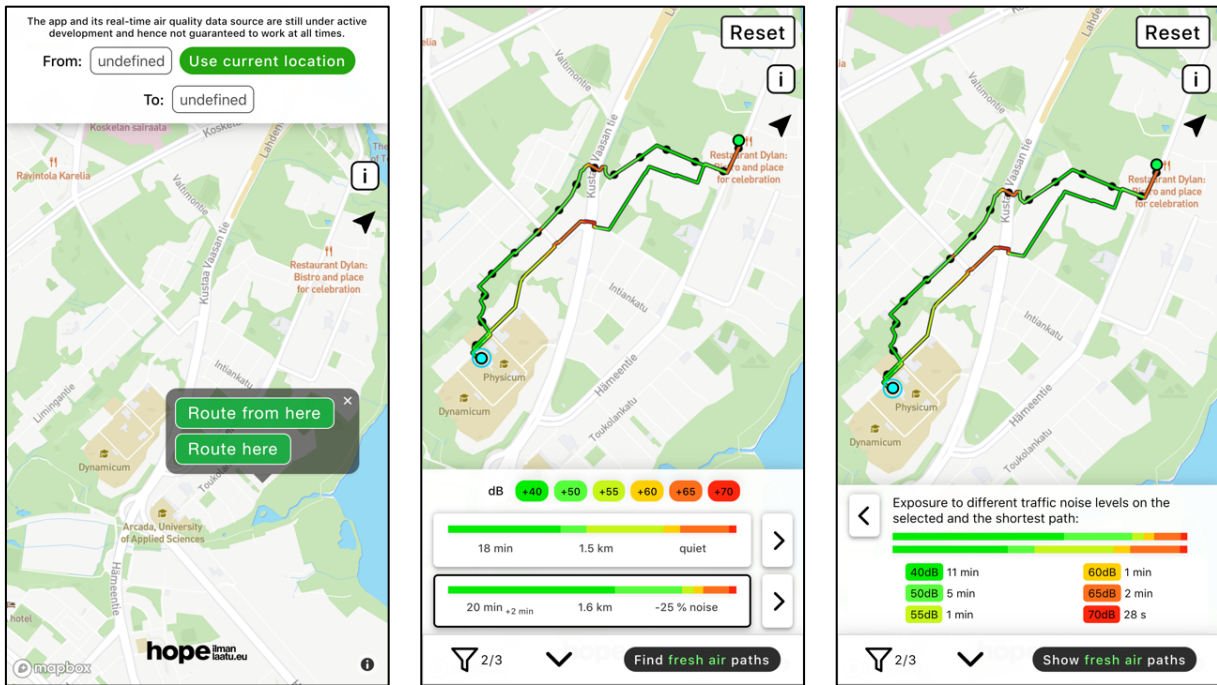


Figure 33. The user interface of the quiet path route planner when showing two alternative paths (one shortest path and one quiet path).

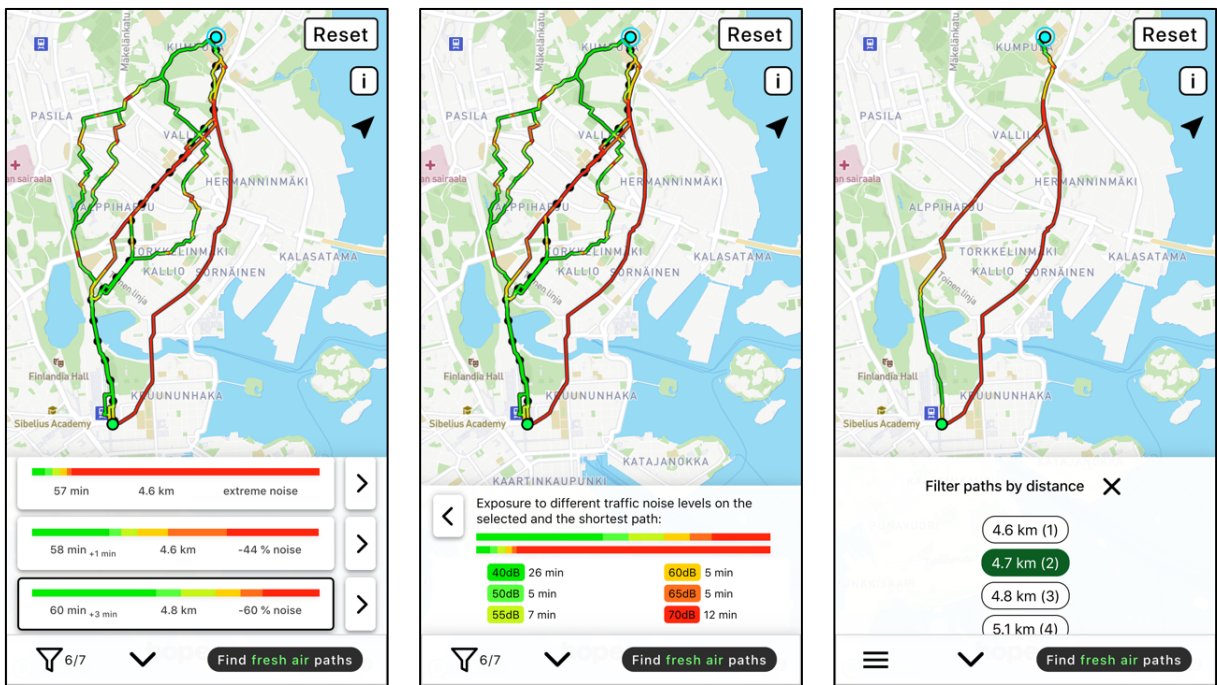


Figure 34. The user interface of the quiet path route planner when showing several alternative paths (one shortest path and six quiet paths). In the third picture, longest paths are being filtered by a user-defined length threshold.

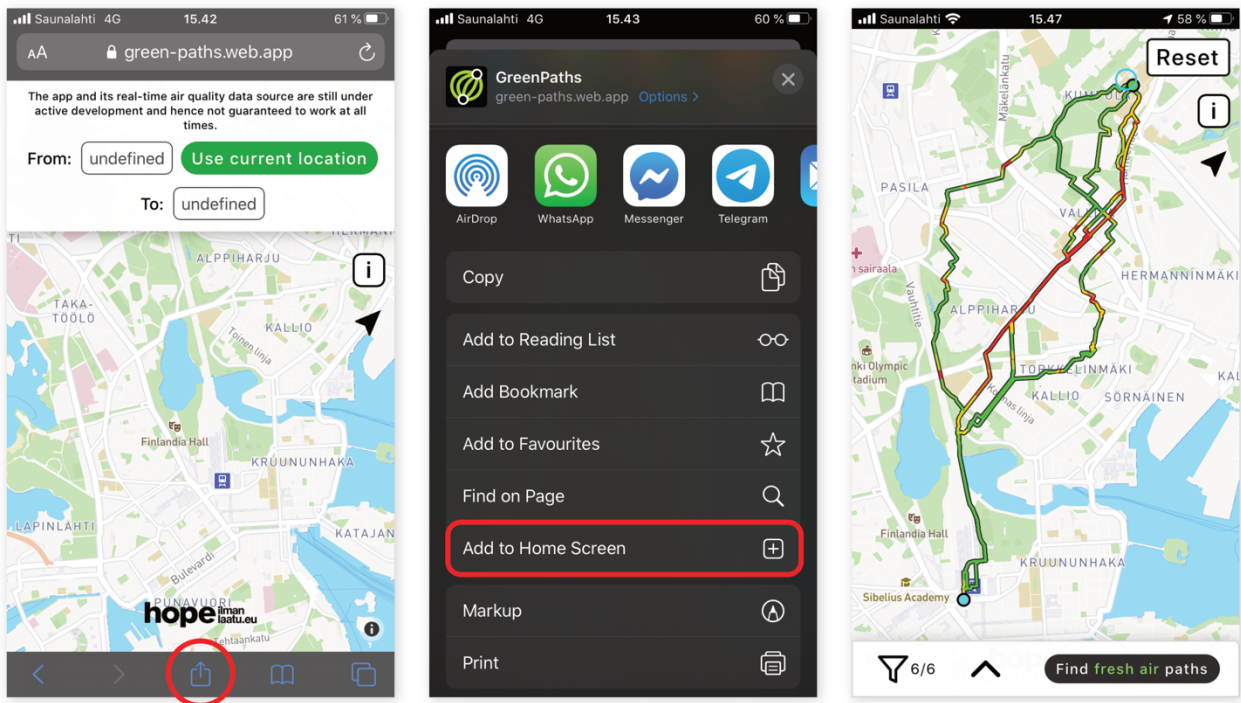


Figure 35. “Add to home screen” -functionality of the web application; the quiet path route planner can be “installed” on user’s phone to work similarly as installed apps (without web browser and address bar).

4.5 Achievable reductions in exposure to traffic noise

A statistical analysis was performed to assess the performance of the quiet path routing by achievable reductions in traffic noise exposures. Descriptive statistics of the reductions were calculated separately for two groups of paths: 1) short paths (length of the shortest path in the range of 300 to 600 m) and 2) long paths (length of the shortest path in the range of 700 to 1300 m). The achievable reductions were assessed by the following four noise exposure indexes (for definitions, see 3.5.4):

- 1) dB_{mean} (mean noise level on the path)
- 2) $\text{ER}_{+60\text{dB}}$ (percentage of exposure to noise levels higher than 60 dB)
- 3) $\text{ER}_{+65\text{dB}}$ (percentage of exposure to noise levels higher than 65 dB)
- 4) EI (noise exposure index)

In the following chapters, the term *initial noise exposure index* is used to refer to the noise exposure index of a shortest path of a given OD pair. Figure 36 represents scatterplots of achievable reductions in the noise exposure indexes and the initial noise exposure indexes for first subset of paths (short

paths). For each index, three scatterplots were created by the three length difference (addition) thresholds of the quiet paths (100, 200 and 300 m). In addition, the results of the simple linear regression analysis are shown in the figure for each scatterplot. Figure 37 represents the same set of scatterplots and metrics as Figure 36, but for the longer paths (700–1300 m). Three important observations can be made from the scatterplots and the results of the regression analysis:

- 1) Higher exposure to noise on the shortest path predicts higher achievable noise reduction (by quiet paths)
- 2) Greater additional length of the quiet path (compared to the length of the shortest path) seem to predict higher reduction in exposure to noise
- 3) The statistical relationships between reductions in noise exposure indexes and the initial noise exposure indexes are stronger for the longer paths (Figure 36 vs. Figure 37)

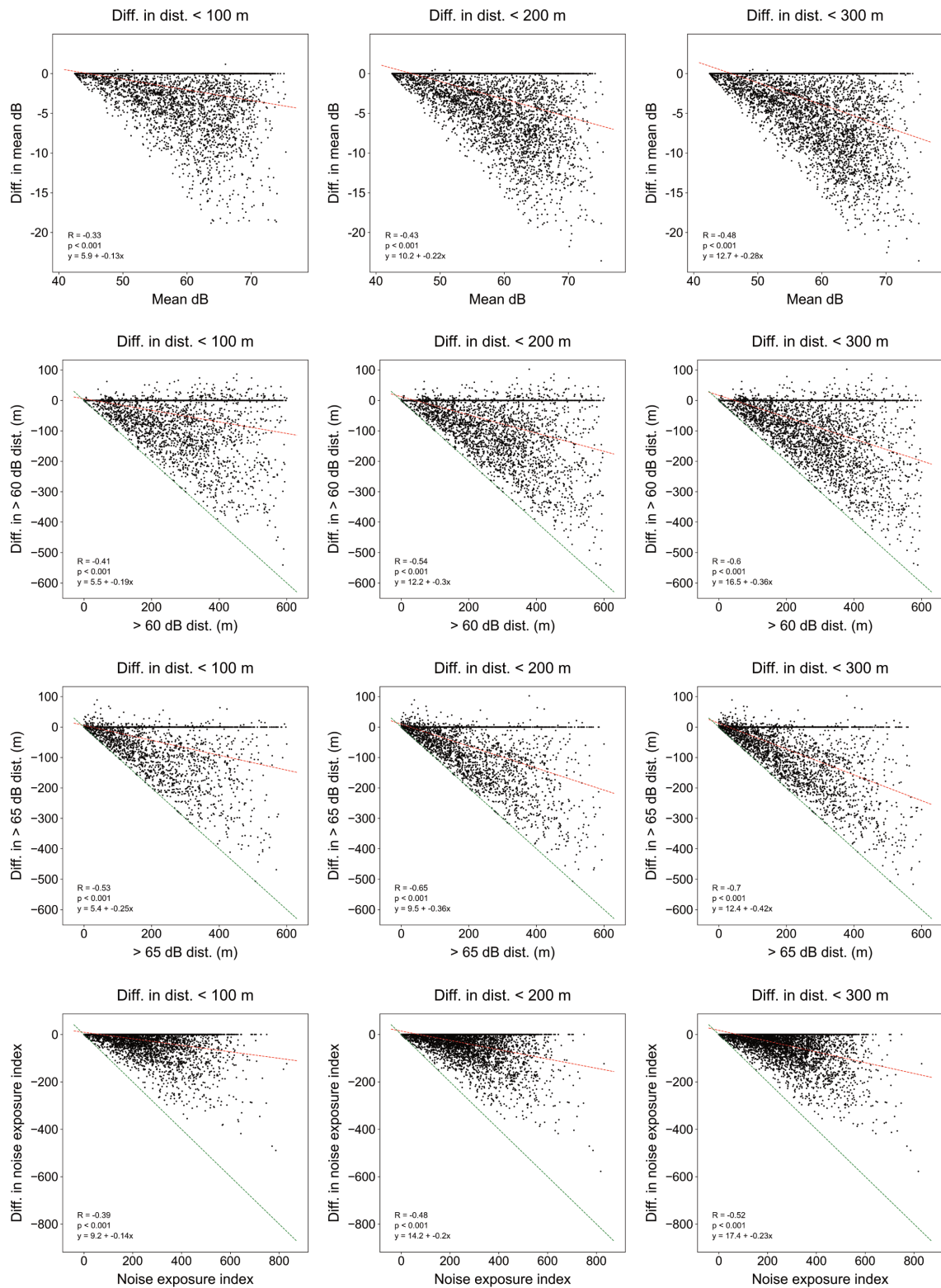


Figure 36. Regression analysis between the reductions in traffic noise exposures on quiet paths and the initial traffic noise indexes. The analysis covers shortest paths in the length range of 300 to 600 m and the respective quiet paths. The red lines represent the regression lines of the regression analysis and the green lines show the theoretical maximum reductions in the noise exposure indexes.

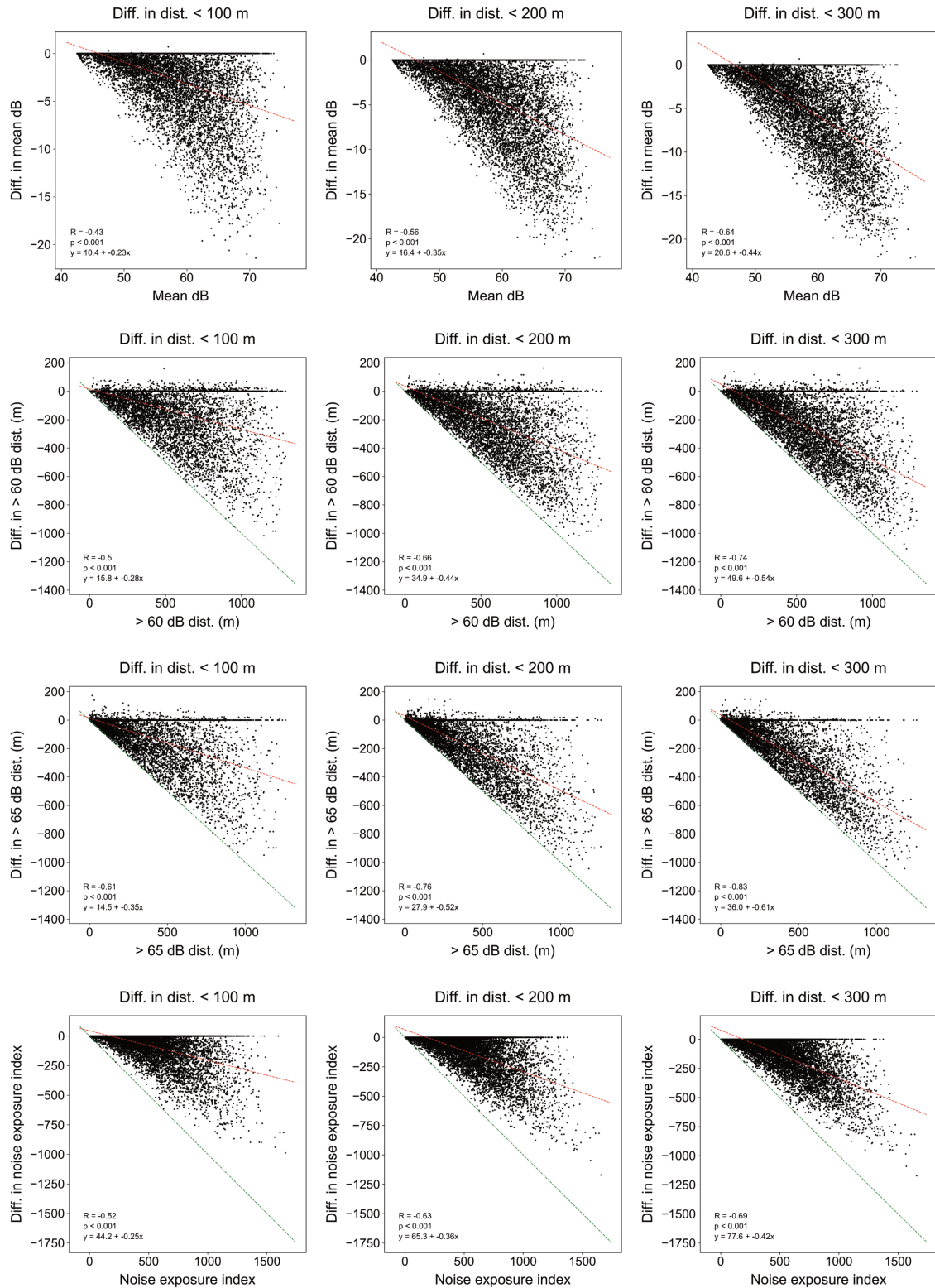


Figure 37. Regression analysis between the reductions in traffic noise exposures on quiet paths and the initial traffic noise indexes. The analysis covers shortest paths in the length range of 700 to 1300 m and the respective quiet paths. The red lines represent the regression lines of the regression analysis and the green lines show the theoretical maximum reductions in the noise exposure indexes.

Table 12 and Table 13 represent the descriptive statistics of the achievable reductions in traffic noise exposure indexes (ER_{+65dB} and dB_{mean}) for a set of path subsets. Since no quiet paths shorter than the maximum allowed length difference (100, 200 or 300 m) were found in many cases, the average length differences of the quiet paths were substantially lower than the allowed maximum length difference (threshold) in each group. For this reason, averages of the length differences of the quiet paths are also included in the table (“quiet path length difference”). At least five observations, partly overlapping with the previous ones, can be made by exploring the statistics:

- 1) Achievable reductions in traffic noise exposure seem to be higher for longer (shortest) paths
- 2) Initially higher noise exposures (on shortest paths) seem to predict also higher achievable reductions in them
- 3) Higher length addition of quiet paths seems to predict higher reduction in noise exposure
- 4) Higher mean and median length differences of quiet paths were found for longer shortest paths, indicating that more quiet paths are found for longer O-D distances
- 5) Accordingly, the low median length differences of the quiet paths for shorter paths indicate that in many cases no quiet paths are found for short O-D distances

The mean reductions in ER_{+65dB} are consistently and significantly higher for the longer paths (22–57 % vs. 12–38 %). Similarly, higher mean reductions in dB_{mean} were found for the longer paths (2.4–9.6 dB vs. 1.6–6.4 dB).

Table 12. Descriptive statistics of the achievable reductions in noise exposure index ER_{+65dB} on different subsets of the paths. The subsets were defined by 1) the length of the shortest path, 2) the length difference of the quiet path and 3) the initial ER_{+65dB} ($n_{300-600m} = 4338$, $n_{700-1300m} = 7842$).

Path length (m)	Quiet path length difference (m)	Subset of paths by ER_{+65dB}					
		10–40 %	40–70 %	70–100 %	Difference (%) in ER_{+65dB} (mean, median, SD)		
Range	Max	Mean	Median	SD			
300–600	< 100	18	0	28	-12, 0 (26)	-24, -0 (31)	-22, -0, (28)
300–600	< 200	41	6	56	-16, -0 (29)	-33, -29 (33)	-33, -30, (30)
300–600	< 300	60	17	81	-17, -0, (29)	-37, -36 (34)	-38, -40, (30)
700–1300	< 100	31	21	32	-22, 0 (30)	-35, -33 (32)	-32, -28, (30)
700–1300	< 200	74	64	64	-29, -20 (33)	-49, -53 (31)	-48, -54, (30)

700–1300	< 300	117	103	95	-32, -26, (33)	-56, -60 (28)	-57, -64, (27)
----------	-------	-----	-----	----	----------------	---------------	----------------

Table 13. Descriptive statistics of the achievable reductions in noise exposure index dB_{mean} on different subsets of the paths. The subsets were defined by 1) the length of the shortest path, 2) the length difference of the quiet path and 3) the initial dB_{mean} ($n_{300-600\text{m}} = 4103$, $n_{700-1300\text{m}} = 6925$).

Path length (m)	Quiet path length difference (m)	Subset of paths by dB_{mean}				
		55–60 dB_{mean}	60–65 dB_{mean}	65–80 dB_{mean}	Difference (dB) in dB_{mean} : mean, median (SD)	
Range	Max	Mean	Median	SD		
300–600	< 100	19	0	29	-1.6, -0.0 (2.7)	-2.6, -0.0 (4.0)
300–600	< 200	43	8	57	-2.3, -0.5 (3.2)	-4.1, -2.3 (4.7)
300–600	< 300	64	21	83	-2.7, -0.0, (3.4)	-4.9, -3.8 (5.0)
700–1300	< 100	32	22	33	-2.4, -1.4 (2.8)	-3.9, -2.8 (4.1)
700–1300	< 200	77	70	64	-3.6, -3.0 (3.2)	-5.9, -5.6 (4.5)
700–1300	< 300	122	113	94	-4.2, -3.9, (3.4)	-7.2, -7.3 (4.5)

4.6 Sharing of the methods and results

All content and methods developed in the thesis are shared with a permissive MIT license via a public GitHub repository: <https://github.com/hellej/quiet-paths-msc>. Unfortunately, many of the data sources consisted of too big files (e.g. graph data) or had restrictive license (e.g. YKR-commuting data) and hence couldn't be shared along with the source-code (for list of the used datasets, see Table 1). However, the complete method for downloading and processing OSM street network data for graph construction is included in the repository. Hence, a “noise-aware” walkable street network graph can be easily generated for any area of interest, as long as traffic noise data for the given area is available. After generating a graph for the area of interest, the quiet path routing application can be run on a personal computer (as opposed to a server-based setup).

During the study, the quiet path routing application was developed further within the HOPE project (Healthy Outdoor Premises for Everyone). A parallel version of the quiet path routing application was created by “forking” the source-code from: <https://github.com/hellej/quiet-paths-msc> to a new

repository under the GitHub community of the Digital Geography Lab: <https://github.com/DigitalGeographyLab/hope-green-path-server>. While developing the quiet path routing method further, the source code was also heavily refactored and documented. Also, to enable significantly faster routing analysis for longer O-D distances, the routing analysis was migrated to utilize the routing library igraph (Csardi & Nepusz, 2006) instead of NetworkX. The name of the application was changed from *quiet paths* to *green paths*. The source-code for the user interface application is accessible at: <https://github.com/DigitalGeographyLab/hope-green-path-ui>. Instructions for getting the application up and running locally are included in the README.md files at the root of both repositories (hope-green-path-server & hope-green-path-ui). Both repositories utilize GitHub releases, that enable creating snapshots of the repositories at a specific time. At the time of writing this, the latest release for the hope-green-path-server is v1.3 and for hope-green-path-ui: v1.2. New releases of both projects will be published as they are developed further.

V. DISCUSSION AND CONCLUSIONS

5.1 Technical assessment – quality of the paths

This study shows that a functional route planner for exposure-based routing can be built using exclusively open-source technologies and OpenStreetMap data. However, the true usability of the developed quiet path routing application would have remained uncertain if the quality of the paths was not assessed. Hence, along with the assessment of achievable reductions in exposure to traffic noise (by using the quiet path route planner), also the quality of the shortest path needed to be considered.

The components of the analysis enabled comparing lengths of the shortest paths and the reference paths calculated with the route planner service of Helsinki Region Transport (HRT). As per Table 14, the mean and median difference in shortest path distances were negative but minor, indicating that a typical (shortest) path calculated with the quiet path routing application was slightly shorter than the corresponding reference path. However, in respect of the high standard deviations of these length differences (16 % & 74.8 m), the paths calculated with the two routing tools were often significantly different in length. Yet, the 10th and 90th percentiles were still moderate, -58.2 m (-7.1 %) and 29 m (4.2 %), indicating that the differences in lengths were small for majority of the paths. Considering these numbers, it can be concluded that the quiet path routing application performed well in most situations.

Furthermore, the quality assessment of the paths facilitated improving the application by revealing problematic pathfinding results. Where higher differences in length were found, the paths were inspected in GIS software to debug possible faults in the routing application or in the street network graph. By this process, some critical, yet rare, bugs were discovered. Most of these were caused by the presence of unwanted street segments (e.g. underground service roads) in the graph. Since the few unwanted segments were not highly connected to the graph, majority of all paths were unaffected by them. The graph was fixed several times through an iterative process of 1) revising the graph construction script, 2) revising the application logic in routing 3) re-running the routing analysis and 4) assessing the quality of the shortest paths. Two key improvements were made to the application in this process: 1) functionality for filtering out service tunnels and validating topology of the graph were integrated in the graph construction script and 2) search radius and logic was improved in the function for finding and creating the origin and destination nodes.

Table 14. Differences in path lengths between the calculated shortest paths and the reference paths (n=31228).

Difference to reference length	meters	%
Mean	-7.8	-0.21
Median	-4.2	-0.55
SD	74.8	15.9
p10	-57.6	-7.1
p90	30.5	4.5

By comparing the shortest and the reference paths in GIS, three types of situations were identified where significant differences between the paths occurred, yet often acceptable:

- 1) The path takes a detour around a private area. In HRT's route planner, also the street segments tagged as private are allowed at the start and at the end of a walk but forbidden as shortcuts in the middle of a walk. In the quiet path routing app, all street segments tagged as private were filtered out in the graph construction to prevent pathfinding through private residential areas. This is a known, yet small, limitation of the application and will be fixed in the future. These cases constitute a subtype of the situations where different nearest edge was found for origin or destination (as described in the next chapter).
- 2) The path starts or ends at different street segment since different nearest edge to origin or destination was found. As per the descriptive statistics in Table 15, most of the offsets of origin and destination points (compared to the reference paths) were minor. However, the nearest edges were often different, leading to more or less divergent opportunities for pathfinding between the two route planners. Some of the differences could be traced back to the three-dimensional alignments of the edges. For example, in the case of Pasila, many sidewalks are located on top of each other. The lower lever typically features a more traditional layout of streets, sidewalks and intersections whereas the upper level features mainly exclusive walkways (raised above the cars). Where the nearest edge could be matched to two overlapping walkways at the same distance, differences between the paths from the two different route planners were likely to arise.
- 3) The path takes a detour around a walkable area. Some walkable OSM features have only polygon geometry. The graph construction method of the quiet path routing application does

not include creation of virtual street segments across walkable areas of OSM. However, pathfinding was affected by the missing walkable areas only in some restricted areas, such as by Helsinki Central Railway Station and other squares.

Table 15. Statistics of offsets (i.e. distances) between the origin and destination points of the paths and the origin and destination points of the reference paths.

Offset from reference paths'	origins (m)	destinations (m)
Mean	3.0	3.9
Median	0.5	1.3
SD	9.5	12.0
p5	0.0	0.1
p10	0.1	0.2
p90	4.4	8.5
p95	24.7	15.4

Also, the following common situations were identified by exploring the numerous minor differences in path lengths in GIS:

- The shortest path takes a shortcut through a forest (or other area featuring smaller paths) as opposed to the reference path that uses more conventional or major paths. It may be that the HRT's routing API incorporates so called turning costs that aim to restrict the amount of turns on the paths. On the other hand, the quiet path routing application finds the least cost path regardless of how many turns the path contains (by only considering the edge costs).
- The shortest path uses slightly different street segments (either the other side of the street or a parallel street) resulting in slightly shorter or longer path compared to the reference path.

5.2 Indirect assessment of pedestrians' dynamic exposures to traffic noise can reveal unequal distribution of exposures to high noise levels

As opposed to most of the previous studies where exposure to traffic noise has been assessed in a static manner (with respect to location), a dynamic exposure assessment was made in this study; exposure to traffic noise was addressed on modelled commuting-related walks. The results on dynamic (i.e. journey-time) exposures to noise were aggregated at origin-level and concepts *average*

local walk and *expected local walk* were introduced for interpreting the results. Drawing from the maps representing traffic noise exposure on average walks in Helsinki, dynamic traffic noise exposure seems to vary significantly between neighborhoods, indicating that opportunities for healthy walking are distributed unequally. Interestingly, some areas not directly exposed to high traffic noise levels seem to have highly exposed average walk.

One could argue that buildings usually manage to protect residents from harmful levels of traffic noise. Consequently, assessing residents' dynamic exposure to traffic noise *outside* the buildings becomes increasingly important component in assessing the total daily exposure. According to the review of (static) noise-annoyance studies by (Guski et al., 2017), all of the studied relationships between highly annoyed (%HA) residents and sound pressure level display considerable variance in the dependent variable. Considering this finding, dynamic exposure to traffic noise may well be one prominent, yet widely unstudied, explanatory variable for the unexplained differences in %HA.

5.3 Significant but varying reductions in traffic noise exposure can be achieved by quiet path routing

A quiet path routing method was developed in this thesis to address two objectives:

- 1) To assess achievable reductions in traffic noise exposure by route choices (in Helsinki).
- 2) To support a proof of concept quiet path route planner for finding healthier, exposure-based paths in Helsinki.

The achievable reductions in noise exposure were assessed for 12180 projected commuting related walks (OD pairs). Another way to assess the performance of the quiet path routing method would have been to calculate and compare shortest and quiet paths for a large number of random ODs. However, as a large number of commuting related walks (ODs) were already available from the dynamic noise exposure assessment of the study, using them provided presumably more realistic results on pedestrians' opportunities to reduce exposure to traffic noise in Helsinki. To summarize the main findings of the statistical analysis, the following factors seem to predict higher achievable reduction in traffic noise exposure:

- 1) Higher traffic noise exposure on the shortest path.
- 2) Longer distance between OD pair - i.e. longer shortest path.
- 3) Greater additional length of the quiet path compared to the shortest path.

The standard deviations of the average achievable reductions were of the same magnitude as the average reductions themselves, indicating high variability in opportunities for choosing quiet paths (in Helsinki); while in many cases a substantial share of the total noise exposure on the shortest path could be avoided by choosing a quiet path, in many cases no applicable quiet paths were found for the OD pair.

Despite the high variability in the achievable reductions, the averages can be interpreted as significant *expected* achievable reductions in traffic noise exposure (e.g. 12–57 % mean reduction in exposure to noise levels higher than 65 dB and 1.6–9.6 dB mean reduction in mean dB, depending on at least the three factors presented earlier in this chapter). The assessment confirmed that the quiet path routing method has the potential to calculate considerably quieter yet only slightly longer paths for many real-worlds situations. Therefore, it was worthwhile to build the web-based quiet path route planner to help citizens to find and utilize the opportunities for reducing journey time exposure to traffic noise in real-life situations.

5.4 The presence of alternative paths limits the accuracy of the indirect dynamic exposure assessment

In direct dynamic exposure assessments, the real paths of pedestrians are determined by e.g. GPS tracking. In this study, the dynamic exposure to traffic noise was assessed using modelled (commuting-related) walks assuming that pedestrians always take the shortest path. However, it is likely that often this is not the case, as discovered by e.g. (Buliung et al., 2013). Hence, the reliability of the dynamic exposure assessment may be limited for revealing the true exposures to traffic noise on local walks.

More accurate assessments on traffic noise exposures and opportunities for unexposed walking would require studying pedestrians' route choices in different noise environments; how long additional distances are pedestrians willing to walk in order to avoid exposure to noise (or other pollutants)? Then, a concept of “most probable path” would need to be established to model more realistic paths.

However, modelling route choices of pedestrians was left outside the scope of this study. Instead, the focus was on developing a conceptual and technical framework for assessing noise exposure and implementing an exposure-based least cost paths routing (“quiet path routing”) method. Despite calculating alternative quiet paths for each OD pair, no attempt was made to determine which of the paths is the best and thus most probable for a pedestrian to take.

Assumedly, in many cases the question of achievable reductions in traffic noise exposure is not only about assessing the quiet path alternatives at OD-level, but also assessing the alternative ODs for a walk. However, no attempt was made to assess opportunities for replacing the commuting-related walks with walks having different public transport hubs as destinations. The possibilities for such analysis were limited by the outsourced routing analysis for determining the local walks (by requesting planned itineraries from HRT's route planner for commutes) – in order to allow multi-destination least cost path analysis for the local walks, also the itinerary planning would have had to be involved in the quiet path routing analysis. The opportunities for integrating the quiet path routing method in a public transport route planner are discussed further in chapter 5.8.

In this thesis, no spatial analysis was conducted on the achievable reductions in exposure to traffic noise, but it was assessed statistically at a municipality-level. While some of the quiet paths were clearly outperforming the shortest paths (just slightly longer but considerably less noisy), the final decision on “choosing the path” was still left unanswered. One potential approach instead of using the shortest path in the exposure assessment would have been to define an index that measures both the presence of alternatives paths and the achievable reductions in traffic noise exposure on those paths. Then, comparing that index (aggregated at e.g. neighborhood-level) to the respective average traffic noise exposures (on the shortest paths), more applicable interpretations could be made on the likely exposures to traffic noise and opportunities for choosing quiet paths.

Given this uncertainty, more detailed assessments would be needed to validate the results on the dynamic traffic noise exposures. Presence and achievable reductions in noise exposure on the possible alternative quiet paths should be inspected at least for the areas with the highest average noise exposures. Then, those areas can be divided into two classes of which only the first contains unavoidably noisy and hence problematic walking conditions:

- 1) Local walks are exposed to high traffic noise levels and no quieter path alternatives are found.
- 2) Local walks are exposed to high traffic noise levels but for many of them alternative, only a little longer, quiet paths can be found.

However, when large-scale spatial analysis of the presence of quiet path alternatives on certain areas is not required, the web-based quiet path route planner allows quickly inspecting the availability of quiet paths in an area of interest. By using the quiet path route planner, a user can make his/her own interpretations regarding the exposure to traffic noise in certain area according to his/her willingness to walk additional distances to avoid exposure to noise. After all, the realized dynamic exposure to

traffic noise in a certain area is not a function of just the noise environment of the area but also of the route choices of the residents.

5.5 Alternative quiet paths need to be calculated to suit different situations and people with varying preferences

Since the environmental impedance function could not be formulated to accurately model the net health effect of a walk, the final decision on choosing the *best* path could not be implemented in the quiet path routing application. Likewise, no attempt was made to choose the *optimal* trade-off between reduction in noise exposure and addition in travel time with purely application logic, as sensitivity to noise and time-constraints depend on the person and the situation. Thus, one of the key features of the quiet path routing application is to calculate several alternative quiet paths for an OD pair to let the user make the final decision on the most desirable path.

The alternative quiet paths are calculated by gradually increasing the noise sensitivity coefficient in the environmental impedance function between parallel pathfinding calculations. The set of noise sensitivity coefficients was defined to range from 0.1 to 40, where the higher coefficients effectively override the effect of length in calculating the costs. Consequently, while many of the paths are almost identical with the shortest path, then others are typically significantly longer but also quieter. According to the results of the study (assessment of achievable reductions in exposure to traffic noise), the number of quiet paths seem to increase as OD-distance increases. When several paths have the same length and little variation in noise exposure, the importance of letting the user to choose the path increases. In these situations, the other aspects of walkability and pedestrians' personal preferences presumably start to play bigger role in the decision making.

5.6 Uncertainties in exposure-response relationships challenge the environmental impedance function

Exposure-based least cost path routing has been developed as a concept only in a few studies and the implementations, including the definition of the environmental impedance function, are often very case-specific and not perfectly explained (Lwin & Murayama, 2011; Quercia et al., 2014; Ribeiro & Mendes, 2011; Sharker et al., 2012; Su et al., 2010). The focus in these papers have been rather explaining the need and the technical and data-related methods of the proof of concept route planners for healthier routes.

Undoubtedly, the most challenging component of this study was defining and validating an environmental impedance function (EIF) for noise, as no well-established EIF for noise could be found from the prior studies. Ideally, the EIF should model the perceived annoyance from dynamic exposure to different noise levels. Hence, literature on sound pressure level – annoyance relationship was searched to guide defining the EIF. Since most of the papers where annoyance from traffic noise was assessed focus on static noise exposure (SPL vs. annoyance at in terms of home location), the scientific basis for defining an EIF for dynamic traffic noise exposure was limited.

Two alternative noise cost functions were defined and tested in quiet path routing: one power function and one linear function. The power function, that was selected for the quiet path routing application, is based on the (Stevens, 1960) power law's revision by (Parmanen, 2007), where sound intensity and sound pressure level (SPL) are assumed interchangeable and sound pressure level and loudness proportional. In this study, one more assumption was appended with the previous: sound intensity in Steven's power law can be replaced with A-weighted equivalent continuous sound level. It was left unclear how strong (or weak) this assumption is. According to Genuit (1999), Ouis (2001) and Parmanen (2007), even just the simple A-weighted SPL may be somewhat unreliable indicator of loudness and annoyance. Information of different tones and fluctuations of SPL in time, both presumably important qualities affecting the perceived loudness of traffic noise, is lost when using a heavily compressed (averaged) SPL metric such as L_{Aeq} . However, since the available traffic noise data featured only A-weighted equivalent continuous sound levels, the uncertainties in L_{Aeq} – loudness relationship were not investigated more deeply.

It can be argued that both (power and linear) functions presented in the study are likely to perform better than a non-continuous (threshold-based) cost function (e.g. Ribeiro & Mendes, 2013). The power function doubles the cost (loudness) at every 10-decibel increase, and may thus be slightly better match with the highly annoyed (HA %) - SPL curves (Figure 2) than a linear function. And as mentioned in chapter 3.5.1, the power function clearly meets the most important requirement for the EIF: it assigns radically higher costs to the very highest noise levels. The selection of the noise cost function was not further justified, since it seemed to perform well in practical situations but also due to the little differences in the quiet paths routing results between the two functions.

If the two noise cost functions were applied in a surface-based LCP analysis, more differences would probably arise between the quiet paths, as they would not be restricted by the limited number of connections in a street network graph. It is possible, that in many cases street network graphs do not provide enough alternative paths between an OD pair to allow the definition of the EIF affect the

resulting paths. The sensitivity coefficient defines the relative weights of both distance-based and exposure-based costs in calculating the composite cost. Therefore, the little differences in the quiet path routing results between the two functions suggest that the noise sensitivity coefficient is a critical variable in the EIF.

5.7 Exposure-based routing should be developed as a concept to consider multiple pollutants

In this study, the chosen traffic noise data included only vehicular traffic, leaving out noise from rail traffic, aircrafts and industrial sites. It can be argued that making separate assessments of dynamic noise exposure to different noise sources is important for the same reasons why separate assessments of static noise exposure are made: 1) it is likely that the health effects of different kinds of noise vary and 2) many of the mitigation actions for reducing citizens' exposure to noise vary between different noise sources (e.g. different kinds of noise barriers, speed limits, rerouting of trams or aircrafts). According to the review by (Guski et al., 2017): 35, different exposure-response relations (ERR) between highly annoyed residents (%HA) and sound pressure level have been discovered for different noise sources in many prior studies. Also, different thresholds for sound pressure levels causing "adverse health effects" were defined for different noise sources in the *Environmental noise guidelines for the European Region* by (Kephalaopoulos et al., 2012). Despite that these prior studies and guidelines consider only static noise exposure, it can be anticipated that ERRs of also dynamic exposures to different noise sources vary.

It can be said that the decision of assessing dynamic exposure to only traffic noise (from vehicular traffic) was appropriate for developing conceptual and technical framework for dynamic exposure assessment and exposure-based routing, but something that should be revisited when the quiet path route planner is developed further. According to the findings by (Guski et al., 2017), one promising way to incorporate many noise sources in one EIF would be to use the concept of dominant noise source: "...results point to the importance of the dominant source in terms of annoyance". Special attention should be paid on deciding whether different weightings should be used for different noise sources based on their different effects on annoyance. However, there seems to be lack of explicit information on ERRs of dynamic exposure to the different noise sources. Hence, the most appropriate way for determining the dominant noise source may be to use the maximum sound pressure level among the different noise sources. This would match the widely applied idea in determining composite air quality index value (AQI) by the maximum AQI value among its components (AQIs by different pollutants) (Plaia & Ruggieri, 2011). If using dominant SPL in quiet path routing, it

would be necessary to assess also the dominant noise source at each edge (street segment) and path, to allow comparing the results of quiet path routing with respect to the dominant noise sources.

While combining different noise sources together has its own challenges, then another level of complexity to exposure-based routing is introduced by considering exposures to also other pollutants or environmental conditions. A practical, yet naive, approach for integrating multiple environmental exposures in routing analysis has been adopted in many web-based route planner applications: user gets to decide the (singular) exposure to minimize per one pathfinding problem. Then, the user may have the option to re-calculate the routes with edited settings to minimize different exposure. However, an exciting possibility would be to combine two or more environmental exposure-based costs in one least cost path problem and hence enable calculating “composite green paths”. Perhaps the greatest challenge in this arises from the need to synchronize different EIFs for calculating initially equal weights for different exposure-based costs. For example, initial air and noise pollution-based costs should be possible to set equally important in the composite EIF. Normalized (i.e. equalized) impedances are needed to enable using relative weights for different pollutants in least cost path analysis (e.g. air pollution set to half as important as noise pollution). Normalizing EIFs of two completely different environmental exposures would require careful investigation of their exposure-response relationships. If it was challenging to model the relative increase in environmental impedance from increasing sound pressure level by 10 dB, it would be ever more challenging to determine the equivalent increase in quality index (by e.g. or PM₁₀ particles) that causes a similar increase in environmental impedance than the 10 dB increase in traffic noise level. Considering also personal differences in responses to different pollutants, defining a well-justified composite EIF for any set of pollutants is a very challenging, if not impossible, task. Nevertheless, a practical approach for normalizing the impedances from different exposures has been to use straightforward, yet rational, means. For example, (Ribeiro & Mendes, 2013) used average impedances by the separate EIFs in normalizing air and noise pollution based costs for composite “healthy routes”. Then Novack et al. (2018) normalized the relative weights of the different costs by dividing the costs by their maximum values observed at their test-site. This approach is somewhat similar than the one that was formed in this study for calculating the normalized noise exposure indexes.

If the ultimate goal for exposure-based routing is to minimize the net negative health effect from walking, deeper knowledge on both negative and positive health effects should be acquired. Also, it should be noted that minimizing the net negative health effect is not necessarily the same thing as maximizing the net positive health effects, as the latter would probably lead to routing considerably longer routes. The tricky question remains unanswered: in what situations do the negative health

effects from exposure to environmental pollutants override the positive health effects from the physical activity of the walk?

To find the healthiest paths, also several positive environmental exposures may be considered. For example, use of greenery (e.g. (Taleai & Yameqani, 2018), perceived security (Naharudin et al., 2017) and beauty (e.g. (Quercia et al., 2014)) in routing analysis have been demonstrated. When also positive exposures and exposures to conditions other than pollutants are incorporated in LCP analysis, the desired result of the path optimization problem is no longer just least-exposure path but rather the most walkable or healthiest path. Compared to exposure to typical environmental pollution (e.g. noise or air pollution), higher levels of subjectivity are associated with both quantifying the *other kinds of exposures* and assessing responses from the exposures to them. Consequently, while the number of exposures increases and also positive exposures are included in LCP analysis, using only exposure based EIF seem to become increasingly difficult. Thus, as opposed to the previously presented simple ways of calculating exposure-based impedances, a range of rather complex, but often fuzzy, statistical methods have been employed in calculating overall health or walkability scores. For example, (Taleai & Yameqani, 2018) demonstrated the use of analytical hierarchical process (AHP) for assigning relative weights for different criteria and (Sharker et al., 2012) used Bayesian belief network (BBN) in addressing the combined effect of possibly interrelated routing criteria. Despite utilizing advanced frameworks for multi-criteria analysis, subjective decision-making still plays a critical role in setting the relative weights for different criteria. Therefore, to meet varying personal preferences, it is increasingly important to take into account multiple scenarios for pathfinding when more criteria are considered.

5.8 Publishing a green path routing application online can facilitate citizens to choose healthier paths

While it could be reasoned that pedestrians (and cyclists) try to minimize their exposure to unhealthy environments, there is still a likely “exposure awareness gap” as demonstrated by (Ueberham et al., 2019); people (cyclists) are not necessarily aware of the pollutant exposure on their paths. According to a number of studies (e.g. Lwin & Murayama, 2011, 2013; Quercia, Schifanella, & Aiello, 2014; Ribeiro & Mendes, 2011), taking environmental factors into account in solving the routing problem seem to have the potential to generate healthier or in other ways more pleasant routes. Therefore, there is a motivation for developing accessible route planners to facilitate reducing pedestrians’ and cyclists’ journey-time exposure to pollutants.

In this study, a proof of concept of web-based quiet path route planner was developed to demonstrate the potential of the quiet path routing method in real-life situations. A number of test users were using the route planner during the project, but no structured survey was carried out to assess the users' experiences. However, the general feedback on the usage was consistent: the quiet path route planner facilitates comparing different paths with respect to noise exposure and thus choosing a quieter path. It was said that displaying the geometries of the paths with different colors based on the noise levels makes the route planner intuitive to use.

The application was developed as mobile friendly as possible, to facilitate real-time route planning especially on the move. Also, it was designed to be easy enough to use that no additional instructions are needed. Thus, no noise exposure indexes other than the self-explanatory ones are shown in the user interface. The difference in noise exposure index (between the shortest and a quiet path) is shown simply as a reduction in *noise (%)*, making it easier for the user to comprehend regardless of the underlying EIF for noise.

It is important to allow users to interactively select a path that suits their personal needs and circumstances at the time. An important feature, and possibly limitation, of the quiet path route planner are the fixed settings for routing: user does not get to decide the relative importance of noise exposure and walking distance before routing. Instead, the route planner calculates several alternative quiet paths (with different weightings) along with the shortest path for the user to choose from. This approach works well in an application that only minimizes one type of exposure, since it allows the user to decide the qualities of the best path only after comparing the alternative paths. However, a different approach is probably more suitable for route planners that take into account multiple exposures (or other factors) in routing. In the route planner developed by (Novack et al., 2018), user can set the relative importance of several factors (e.g. green areas, quietness and distance) using a set of slide-bars in the user interface. A weakness to functionality is posed by the uncertainties in the initial calibration of the weightings; when user sets multiple factors equally important, it is practically a decision of the software designer of what are the relative weights of the different factors. Therefore, deciding a set of weightings for different factors in advance may well be fuzzier for the user than selecting a desired path from a number of alternatives - provided that there is enough information on the alternative paths to base the decision on.

When the quiet path route planner is developed towards a general green path route planner, other (optional) environmental exposures need to be integrated in the routing analysis. If the route planner is developed even further, towards a route planner for overall healthier paths, a composite

environmental impedance function needs to be defined for calculating combined exposure-based impedances from different exposures. Finally, uncertainties in exposure-response relationships of different environmental exposures and the subjective nature of walkability should be acknowledged in designing the user interface. Thus, the user should always be given the final decision on choosing the *best* path to take.

VI. REFERENCES

- Agrawal, S., & Gupta, R. D. (2017). Web GIS and its architecture: A review. *Arabian Journal of Geosciences*, 10(23), 518.
- Ahuja, R. K., Mehlhorn, K., Orlin, J., & Tarjan, R. E. (1990). Faster algorithms for the shortest path problem. *Journal of the ACM (JACM)*, 37(2), 213–223. <https://doi.org/10.1145/77600.77615>
- Alam, M. S., Perugu, H., & McNabola, A. (2018). A comparison of route-choice navigation across air pollution exposure, CO₂ emission and traditional travel cost factors. *Transportation Research Part D: Transport and Environment*, 65, 82–100. <https://doi.org/10.1016/j.trd.2018.08.007>
- Apparicio, P., Carrier, M., Gelb, J., Séguin, A.-M., & Kingham, S. (2016). Cyclists' exposure to air pollution and road traffic noise in central city neighbourhoods of Montreal. *Journal of Transport Geography*, 57, 63–69.
- Babisch, W., Beule, B., Schust, M., Kersten, N., & Ising, H. (2005). Traffic noise and risk of myocardial infarction. *Epidemiology*, 33–40.
- Boeing, G. (2017). OSMnx: New methods for acquiring, constructing, analyzing, and visualizing complex street networks. *Computers, Environment and Urban Systems*, 65, 126–139.
- Boulos, M. N. K., Warren, J., Gong, J., & Yue, P. (2010). *Web GIS in practice VIII: HTML5 and the canvas element for interactive online mapping*. Springer.
- Brown, A. L., & Van Kamp, I. (2017). WHO environmental noise guidelines for the European region: A systematic review of transport noise interventions and their impacts on health. *International Journal of Environmental Research and Public Health*, 14(8), 873.
- Buliung, R. N., Larsen, K., Faulkner, G. E., & Stone, M. R. (2013). The “path” not taken: Exploring structural differences in mapped-versus shortest-network-path school travel routes. *American Journal of Public Health*, 103(9), 1589–1596.
- City of Helsinki. (2020). Liikennetutkimus Ja -Tilastot. <https://www.hel.fi/helsinki/fi/kartat-jaliikenne/kadut-ja-liikennesuunnittelu/tutkimus-ja-tilastot> (accessed on 4 April 2020)
- Cole-Hunter, T., Morawska, L., Stewart, I., Jayaratne, R., & Solomon, C. (2012). Inhaled particle counts on bicycle commute routes of low and high proximity to motorised traffic. *Atmospheric Environment*, 61, 197–203. <https://doi.org/10.1016/j.atmosenv.2012.06.041>
- Csardi, G., & Nepusz, T. (2006). The igraph software package for complex network research. *InterJournal, Complex Systems*, 1695(5), 1–9.
- Datakustik CadnaA 2017. (n.d.). <https://www.datakustik.com/products/cadnaa/cadnaa/> (accessed on 4 April 2020)

- Davies, G., & Whyatt, D. (2009). A least-cost approach to personal exposure reduction. *Transactions in GIS*, 13(2), 229–246.
- Directive 2002/49/EC of the European Parliament and of the Council of 25 June 2002 relating to the assessment and management of environmental noise—Declaration by the Commission in the Conciliation Committee on the Directive relating to the assessment and management of environmental noise.* (2002, July 18). <http://data.europa.eu/eli/dir/2002/49/oj/eng>
- Farkas, G. (2019). Hardware-Accelerating 2D Web Maps: A Case Study. *Cartographica: The International Journal for Geographic Information and Geovisualization*, 54(4), 245–260.
- Gaffuri, J. (2012). Toward web mapping with vector data. *International Conference on Geographic Information Science*, 87–101.
- Genuit, K. (1999). The use of psychoacoustic parameters combined with A-weighted SPL in noise description. *INTER-NOISE and NOISE-CON Congress and Conference Proceedings*, 1999, 1887–1892.
- Goldberg, A. V., & Harrelson, C. (2005). Computing the shortest path: A search meets graph theory. *Proceedings of the Sixteenth Annual ACM-SIAM Symposium on Discrete Algorithms*, 156–165.
- Gulliver, J., & Briggs, D. J. (2005). Time–space modeling of journey-time exposure to traffic-related air pollution using GIS. *Environmental Research*, 97(1), 10–25. <https://doi.org/10.1016/j.envres.2004.05.002>
- Guski, R., Schreckenberg, D., & Schuemer, R. (2017). WHO environmental noise guidelines for the European region: A systematic review on environmental noise and annoyance. *International Journal of Environmental Research and Public Health*, 14(12), 1539.
- Hasenfratz, D., Arn, T., de Concini, I., Saukh, O., & Thiele, L. (2015). Health-optimal routing in urban areas. *Proceedings of the 14th International Conference on Information Processing in Sensor Networks*, 398–399.
- Hatzopoulou, M., Weichenthal, S., Barreau, G., Goldberg, M., Farrell, W., Crouse, D., & Ross, N. (2013). A web-based route planning tool to reduce cyclists' exposures to traffic pollution: A case study in Montreal, Canada. *Environmental Research*, 123, 58–61.
- Helsingin kaupungin meluselvitys 2017.* (2017). <https://www.hel.fi/helsinki/fi/asuminen-jaymparisto/ymparistonsuojelu/ilmanlaatu-ja-melu/selvitys/>
- Hertel, O., Hvidberg, M., Ketzel, M., Storm, L., & Stausgaard, L. (2008). A proper choice of route significantly reduces air pollution exposure—A study on bicycle and bus trips in urban streets. *Science of the Total Environment*, 389(1), 58–70. <https://doi.org/10.1016/j.scitotenv.2007.08.058>

- International Standard ISO 226: 1987.* (n.d.). International Organization for Standardization, Geneva, Switzerland.
- Ising, H., Dienel, D., Günther, T., & Markert, B. (1980). Health effects of traffic noise. *International Archives of Occupational and Environmental Health*, 47(2), 179–190.
- Jäppinen, S., Toivonen, T., & Salonen, M. (2013). Modelling the potential effect of shared bicycles on public transport travel times in Greater Helsinki: An open data approach. *Applied Geography*, 43, 13–24. <https://doi.org/10.1016/j.apgeog.2013.05.010>
- Jarno Kokkonen, Kontkanen, O., & Maijala, P. (2016). CNOSSOS-EU Noise Model Implementation in Finland. *ResearchGate*, 38. https://www.researchgate.net/publication/307907554_CNOSSOS-EU_Noise_Model_Implementation_in_Finland
- Jasika, N., Alispahic, N., Elma, A., Ilvana, K., Elma, L., & Nosovic, N. (2012). Dijkstra's shortest path algorithm serial and parallel execution performance analysis. *2012 Proceedings of the 35th International Convention MIPRO*, 1811–1815.
- Jonasson, H. G., & Storeheier, S. (2001). *Nord 2000. New Nordic prediction method for road traffic noise*.
- Kephalopoulos, S., Paviotti, M., & Anfosso-Lédée, F. (2012). *Common noise assessment methods in Europe (CNOSSOS-EU)*.
- Leaflet*. (n.d.). <https://leafletjs.com/> (accessed on 23 February 2020)
- Lienert, C., Jenny, B., Schnabel, O., & Hurni, L. (2012). Current trends in vector-based Internet mapping: A technical review. In *Online maps with APIs and WebServices* (pp. 23–36). Springer.
- Lu, X. (2005). An investigation on service-oriented architecture for constructing distributed web gis application. *2005 IEEE International Conference on Services Computing (SCC'05) Vol-1*, 1, 191–197.
- Lwin, K. K., & Murayama, Y. (2011). Modelling of urban green space walkability: Eco-friendly walk score calculator. *Computers, Environment and Urban Systems*, 35(5), 408–420. <https://doi.org/10.1016/j.comenvurbsys.2011.05.002>
- Lwin, K. K., & Murayama, Y. (2013). Smart eco-path finder for mobile GIS users. *URISA Journal*, 25(2), 5–14.
- Maghelal, P. K., & Capp, C. J. (2011). Walkability: A Review of Existing Pedestrian Indices. *Journal of the Urban & Regional Information Systems Association*, 23(2).
- Mapbox GL JS*. (n.d.). <https://docs.mapbox.com/mapbox-gl-js/> (accessed on 4 April 2020)
- Meeker, M., & Wu, L. (2013). Internet trends. *Proc D11 Conference. Rancho Palos Verdes*.

- Meeker, M., & Wu, L. (2018). *Internet trends 2018*. Kleiner Perkins.
- Miedema, H. M., & Oudshoorn, C. G. (2001). Annoyance from transportation noise: Relationships with exposure metrics DNL and DENL and their confidence intervals. *Environmental Health Perspectives*, 109(4), 409–416.
- Naharudin, N., Ahamad, M., Sanusi, S., & Sadullah, A. F. M. (2017). OPTIMIZING PEDESTRIAN-FRIENDLY WALKING PATH FOR THE FIRST AND LAST MILE TRANSIT JOURNEY BY USING THE ANALYTICAL NETWORK PROCESS (ANP) DECISION MODEL AND GIS NETWORK ANALYSIS. *International Archives of the Photogrammetry, Remote Sensing & Spatial Information Sciences*, 42.
- Neis, P., & Zipf, A. (2017). OpenRouteService. *Dostupné z: Http://Www. Openrouteservice. Org.*
- Nielsen, H. L. (1997). *Road traffic noise: Nordic prediction method*. Nordic Council of Ministers.
- Noto, M., & Sato, H. (2000). A method for the shortest path search by extended Dijkstra algorithm. *Smc 2000 Conference Proceedings. 2000 Ieee International Conference on Systems, Man and Cybernetics. "cybernetics Evolving to Systems, Humans, Organizations, and Their Complex Interactions" (Cat. No.0, 3, 2316–2320 vol.3. https://doi.org/10.1109/ICSMC.2000.886462*
- Novack, T., Wang, Z., & Zipf, A. (2018). A system for generating customized pleasant pedestrian routes based on OpenStreetMap data. *Sensors*, 18(11), 3794.
- OpenLayers*. (n.d.). <https://openlayers.org/> (accessed on 23 February 2020)
- Ouis, D. (2001). ANNOYANCE FROM ROAD TRAFFIC NOISE: A REVIEW. *Journal of Environmental Psychology*, 21(1), 101–120. <https://doi.org/10.1006/jevp.2000.0187>
- Overpass API*. (2019). https://wiki.openstreetmap.org/wiki/Overpass_API (accessed on 10 April 2019)
- Parmanen, J. (2007). A-weighted sound pressure level as a loudness/annoyance indicator for environmental sounds – Could it be improved? *Applied Acoustics*, 68(1), 58–70. <https://doi.org/10.1016/j.apacoust.2006.02.004>
- Passchier-Vermeer W, & Passchier W F. (2000). Noise exposure and public health. *Environmental Health Perspectives*, 108(suppl 1), 123–131. <https://doi.org/10.1289/ehp.00108s1123>
- Plaia, A., & Ruggieri, M. (2011). Air quality indices: A review. *Reviews in Environmental Science and Bio/Technology*, 10(2), 165–179. <https://doi.org/10.1007/s11157-010-9227-2>
- PostGIS*. (n.d.). <https://postgis.net/> (accessed on 23 February 2020)
- Pucher, J., & Buehler, R. (2010). Walking and cycling for healthy cities. *Built Environment*, 36(4), 391–414.
- Qiu, G., & Chen, J. (2018). Web-based 3D map visualization using WebGL. *2018 13th IEEE Conference on Industrial Electronics and Applications (ICIEA)*, 759–763.

- Quercia, D. (2015). Chatty, Happy, and Smelly Maps. *Proceedings of the 24th International Conference on World Wide Web*, 741–741.
- Quercia, D., Schifanella, R., & Aiello, L. M. (2014). The shortest path to happiness: Recommending beautiful, quiet, and happy routes in the city. *Proceedings of the 25th ACM Conference on Hypertext and Social Media*, 116–125.
- Rabl, A., & de Nazelle, A. (2012). Benefits of shift from car to active transport. *Transport Policy*, 19(1), 121–131. <https://doi.org/10.1016/j.tranpol.2011.09.008>
- Recio, A., Linares, C., Banegas, J. R., & Díaz, J. (2016). Road traffic noise effects on cardiovascular, respiratory, and metabolic health: An integrative model of biological mechanisms. *Environmental Research*, 146, 359–370. <https://doi.org/10.1016/j.envres.2015.12.036>
- Reynolds, C., Winters, M., Ries, F., & Gouge, B. (2010). Active transportation in urban areas: Exploring health benefits and risks. *National Collaboration Centre for Environmental Health*, 2.
- Ribeiro, P., & Mendes, J. F. (2011). Route planning for soft modes of transport: Healthy routes. *WIT Transactions on The Built Environment*, 116, 677–688.
- Ribeiro, P., & Mendes, J. F. (2013). Healthy routes for active modes in school journeys. *International Journal of Sustainable Development and Planning*, 8(4), 591–602.
- Sharker, M. H., Karimi, H. A., & Zgibor, J. C. (2012). Health-optimal routing in pedestrian navigation services. *Proceedings of the First ACM SIGSPATIAL International Workshop on Use of GIS in Public Health*, 1–10.
- Sheng, N., & Tang, U. W. (2011). Spatial Analysis of Urban Form and Pedestrian Exposure to Traffic Noise. *International Journal of Environmental Research and Public Health*, 8(6), 1977–1990. <https://doi.org/10.3390/ijerph8061977>
- Statistics Finland*. (2020). Kuntien Avainluvut. <https://www.stat.fi/tup/alue/kuntienavainluvut.html> (accessed on 4 April 2020)
- Stevens, S. S. (1960). The psychophysics of sensory function. *American Scientist*, 48(2), 226–253.
- Su, J. G., Winters, M., Nunes, M., & Brauer, M. (2010). Designing a route planner to facilitate and promote cycling in Metro Vancouver, Canada. *Transportation Research Part A: Policy and Practice*, 44(7), 495–505. <https://doi.org/10.1016/j.tra.2010.03.015>
- Tainio, M., de Nazelle, A. J., Götschi, T., Kahlmeier, S., Rojas-Rueda, D., Nieuwenhuijsen, M. J., de Sá, T. H., Kelly, P., & Woodcock, J. (2016). Can air pollution negate the health benefits of cycling and walking? *Preventive Medicine*, 87, 233–236. <https://doi.org/10.1016/j.ypmed.2016.02.002>

- Taleai, M., & Yameqani, A. S. (2018). Integration of GIS, remote sensing and Multi-Criteria Evaluation tools in the search for healthy walking paths. *KSCE Journal of Civil Engineering*, 22(1), 279–291.
- Toivonen, T., Salonen, M., Tenkanen, H., Saarsalmi, P., Jaakkola, T., & Järvi, J. (2014). Joukkoliikenteellä, autolla ja kävelien: Avoin saavutettavuusaineisto pääkaupunkiseudulta. *Terra 126 (2014)*: 3.
- Torija, A. J., & Flindell, I. H. (2015). The subjective effect of low frequency content in road traffic noise. *The Journal of the Acoustical Society of America*, 137(1), 189–198. <https://doi.org/10.1121/1.4904542>
- Ueberham, M., Schlink, U., Dijst, M., & Weiland, U. (2019). Cyclists' Multiple Environmental Urban Exposures—Comparing Subjective and Objective Measurements. *Sustainability*, 11(5), 1412. <https://doi.org/10.3390/su11051412>
- Van Kempen, E., Casas, M., Pershagen, G., & Foraster, M. (2018). WHO environmental noise guidelines for the European region: A systematic review on environmental noise and cardiovascular and metabolic effects: a summary. *International Journal of Environmental Research and Public Health*, 15(2), 379.
- Veenendaal, B., Brovelli, M. A., & Li, S. (2017). Review of web mapping: Eras, trends and directions. *ISPRS International Journal of Geo-Information*, 6(10), 317.
- WHO Europe. (2018). *Environmental noise guidelines for the European Region*. http://www.euro.who.int/__data/assets/pdf_file/0008/383921/noise-guidelines-eng.pdf?ua=1
- Whyatt, J. D., Pooley, C., Coulton, P., Moser, M., Bamford, W., & Davies, G. (2007). Estimating personal exposure to air pollution on the journey to and from school using GPS, GIS and mobile phone technology. *11th International Conference on Harmonisation within Atmospheric Dispersion Modelling for Regulatory Purposes*, 1, 2–5.
- Zielstra, D., & Hochmair, H. H. (2011). Comparative study of pedestrian accessibility to transit stations using free and proprietary network data. *Transportation Research Record*, 2217(1), 145–152.
- Zielstra, D., & Hochmair, H. H. (2012). Using free and proprietary data to compare shortest-path lengths for effective pedestrian routing in street networks. *Transportation Research Record*, 2299(1), 41–47.

ACKNOWLEDGEMENTS

I would like to thank my supervisor Tuuli Toivonen for the fruitful conversations we had when planning the thesis and for seeing the value of the quiet path routing method in developing also other exposure-based routing applications. I am deeply grateful to Tuuli Toivonen and Age Poom for arranging excellent facilities for me to work on the thesis and the HOPE project, especially during the time of the corona crisis (COVID-19). I am very grateful to Henrikki Tenkanen for tips and support in setting up the server-based instance of the quiet path routing application (clearly some of the fundamentals of how internet works were still slightly unclear to me prior to this project). Also, I would like to thank Henrikki Tenkanen and all others who contributed in creating the course Automating GIS-processes – it was during that very course when I truly understood the seemingly unlimited possibilities in doing GIS by programming.

APPENDICES

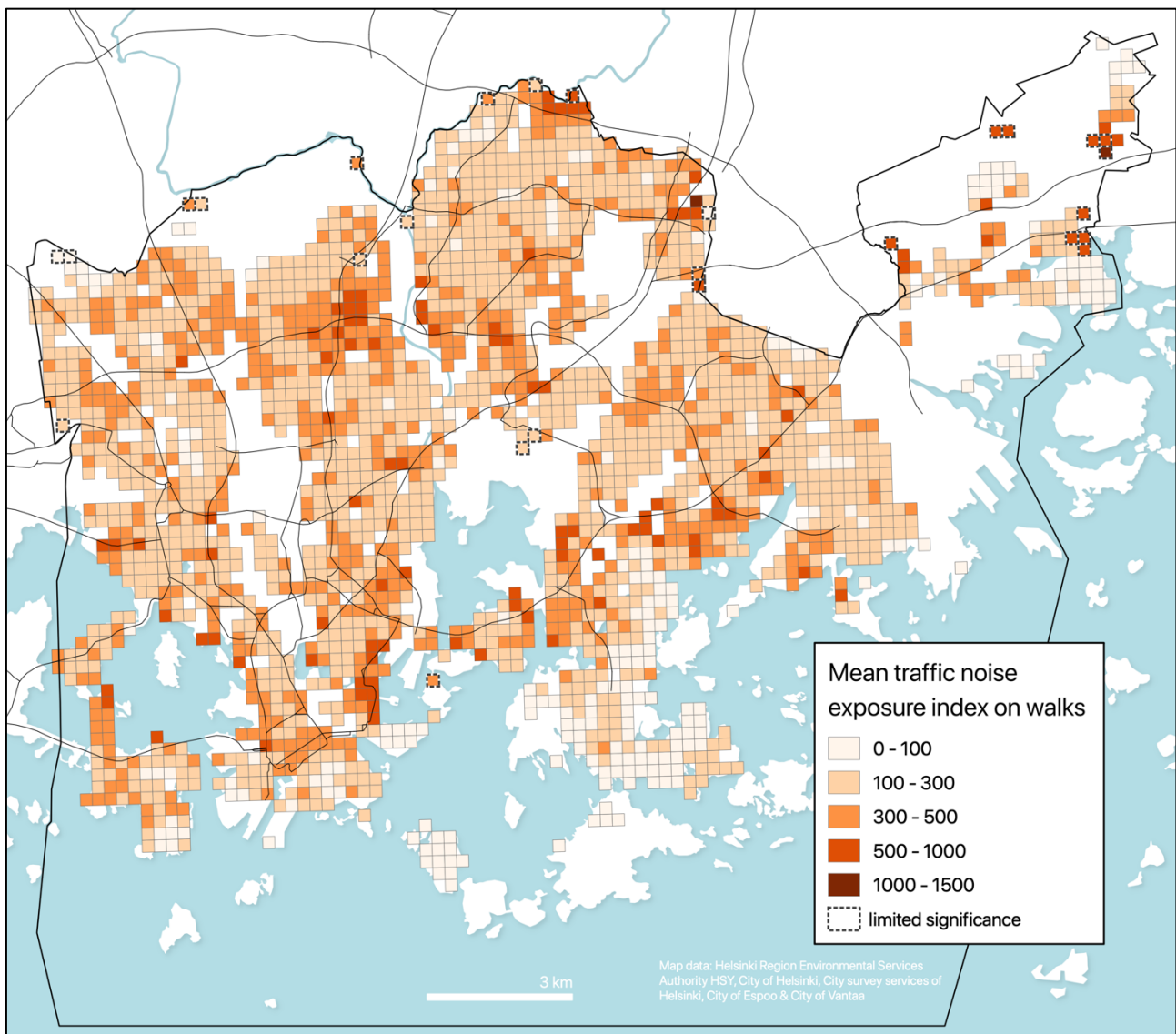
Appendix 1. The packages and libraries included in the Python development environment of the thesis (i.e. environment file). Conda package manager can create the environment simply by running: `conda env create -f env-gis-flask.yml`

where `env-gis-flask.yml` is the name of the environment file.

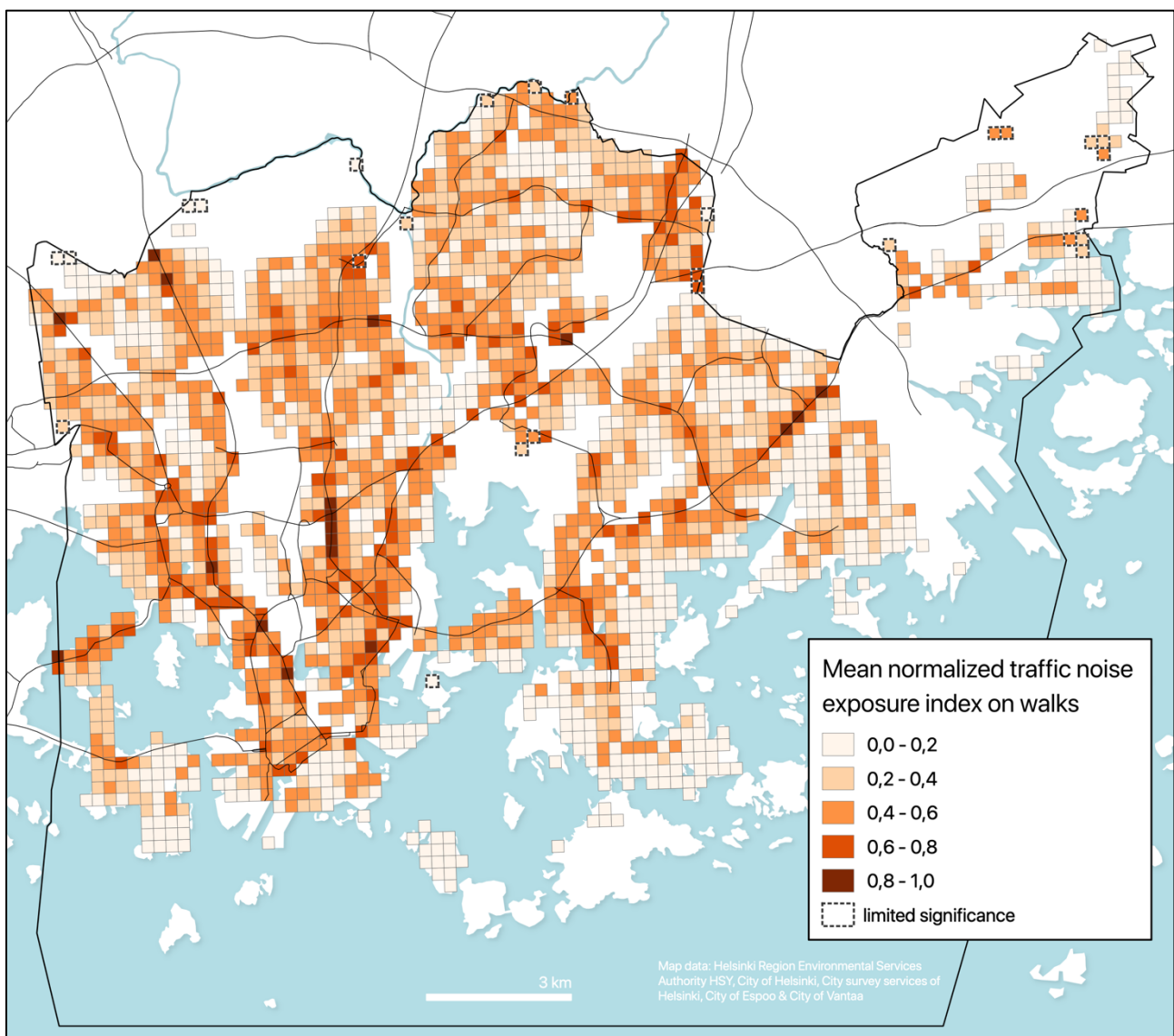
`https://github.com/hellej/quiet-paths-msc/blob/master/src/env-gis-flask.yml`

```
name: gis-flask
channels:
  - conda-forge
  - defaults
dependencies:
  - python=3.6
  - jupyterlab
  - pylint
  - pytest
  - geopandas
  - osmnx
  - gdal
  - geoplot
  - pysal
  - flask
  - flask-cors
  - flask-testing
  - gunicorn
  - requests
  - pip
  - pip:
    - pycrs
    - polyline
```

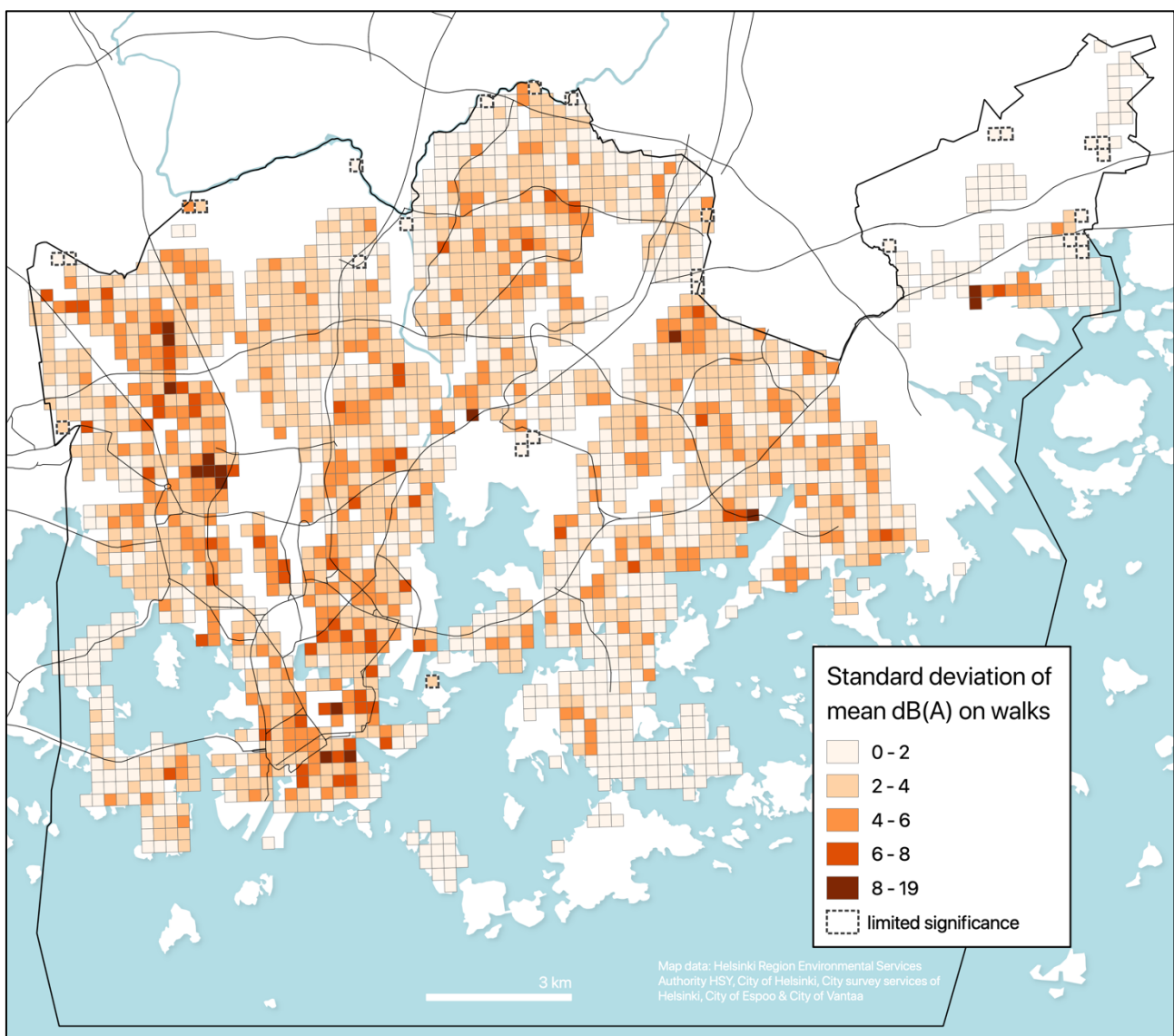
Appendix 2. Mean traffic noise exposure index (EI) on walks from homes to PT stops. The averages are weighted with the estimated utilization rates of the walks based on the total flow of commutes using each origin – PT stop pair.



Appendix 3. Mean normalized traffic noise exposure index (EI_n) on walks from homes to PT stops. The averages are weighted with the estimated utilization rates of the walks based on the total flow of commutes using each origin – PT stop pair.



Appendix 4. Standard deviations of the mean traffic noise levels (dB(A)) on walks from homes to PT stops.



Appendix 5. Highest total modelled utilization rates and mean traffic noise levels of street segments by 80th percentile. Only street segments with modelled utilization rates higher than 0 are included in the percentiles of both variables.

